ISBN 978-82-326-1032-7 (printed version)
ISBN 978-82-326-1033-4 (electronic version)
ISSN 1503-8181

Doctoral theses at NTNU, 2015:188

Anne Lalagüe

Use of Ground Penetrating Radar for Transportation Infrastructure Maintenance

NTNU
Norwegian University of
Science and Technology
Faculty of Engineering
Science and Technology
Department of Civil and Transport Engineering

NTNU – Trondheim
Norwegian University of
Science and Technology

Doctoral theses at NTNU, 2015:188

NTNU

NTNU – Trondheim
Norwegian University of
Science and Technology

Anne Lalagüe

Use of Ground Penetrating Radar for Transportation Infrastructure Maintenance

Thesis for the degree of Philosophiae Doctor

Trondheim, June 2015

Norwegian University of Science and Technology

NTNU – Trondheim
Norwegian University of
Science and Technology

NTNU
Norwegian University of Science and Technology

Thesis for the degree of Philosophiae Doctor

ISBN 978-82-326-1032-7 (printed version)
ISBN 978-82-326-1033-4 (electronic version)
ISSN 1503-8181

Doctoral theses at NTNU, 2015:188

Printed by Skipnes Kommunikasjon as

The committee for appraisal of this thesis was comprised of the following members:

Professor, Dr. Ing. Andreas Loizos
National Technical University of Athens, Greece

Chief engineer, Ph.D. Geir Berntsen
Norwegian Public Road Administration

Associate Professor, Ph.D. Alex Klein-Paste
Norwegian University of Science and Technology (Administrator)

The supervisors of this study have been:

Professor, Dr.Ing. Inge Hoff
Department of Civil and Transport Engineering
Norwegian University of Science and Technology

Associate Professor, Dr.Ing. Egil Eide
Department of Electronics and Telecommunications
Norwegian University of Science and Technology

ACKNOWLEDGEMENTS

This thesis is a result of six years of part-time study at SINTEF. It was financially supported by the Norwegian Public Road Administration, the Norwegian National Administration and Avinor whom I greatly thank for having made this work possible.

These six years were full of experiences of all kinds. My foremost gratitude and sincere thanks go to my main supervisor, Professor Inge Hoff, who has extensively contributed to the start-up of the GPR activity at NTNU/SINTEF. Thank you Inge, for your support, wisdom and for guiding the 22-year old girl that I once was. You gave me independence and freedom in my work, and allowed me numerous opportunities to improve my skills and challenge myself.

I extend my thanks to my co-supervisor Egil Eide, who made me familiar with Ground Penetrating Radar and field testing. I also appreciated the availability and reactivity of the 3d-Radar team regarding field surveys and equipment issues.

I had the privilege to spend 11 months at the research section of the Minnesota Department of Transportation. I am very grateful to the NPRA for arranging this stay, and to Maureen Jensen who ensured my stay took place in the best conditions possible. I felt incredibly welcome, and wish to warmly thank all MnDOT staff for their contribution to my work and taking so good care of me.

Many people have contributed in other ways to my years of doctoral study. I am especially thinking about my former colleagues at SINTEF/NTNU for their friendship and kind consideration for my personal life in Trondheim.

I also thank my family, and all my close friends – I am going to leave out the friend's list because I know I will forget someone and then I will be in trouble…!

Finally, a personal thought goes to my partner Nicolai, who has never doubted me even when I did.

Oslo, March 2015
Anne Lalagüe

SUMMARY

Routine inspection of transportation infrastructure is an essential component of maintenance and rehabilitation programs. However, it often necessitates a significant amount of work and resource allocation. In this study, the feasibility of the Ground Penetrating Radar (GPR) technology to assess and monitor the condition of infrastructure is investigated.

The thesis first introduces the basic principles of GPR, its advantages and limitations. The technology, based on the propagation of electromagnetic waves, has the ability to penetrate surfaces and see what is behind. The detection of hidden and underground objects depends on the contrast in the dielectric properties between the surveyed object and the traversed medium. In addition to being non-destructive, GPR has unique advantages such as the rapidity and continuity of measurements. However, traditional obstacles are conductive environments, the cost of data collection, and a relative complexity of data interpretation.

After a comprehensive background research, laboratory and field testing, the main conclusions of this thesis are:

The step-frequency GeoScope GPR, currently the only system available in Norway for infrastructure surveys, is a very accurate instrument. The error in GPR readings for pavement thicknesses is evaluated to 3,3 %, in line with other published studies. However, as for ground-coupled antennas, it requires more calibration effort with coring than air-coupled models that can calculate the dielectric permittivity continuously.

As a general rule, the accuracy of GPR systems is affected by the interpretation process of the collected data. Best results are obtained from manual interpretation. Semi-automatic layer tracking tools are time-saving but may increase inaccuracies in data analysis.

GPR is well-suited for geological inspections in tunnels, especially in remotely mapping the cavity behind concrete linings. The distance to the bedrock is very accurately determined since the thickness of the concrete walls is generally known and the dielectric permittivity of air is constant ($\varepsilon = 1$). Ground-coupled antennas are also found to be effective in detecting loose rocks that have fallen from the tunnel roof onto the concrete lining. Such surveys may help detect early signs of rock instability. Given the number of tunnels in Norway and type of construction, the use of GPR can ultimately result in improved tunnel evaluation and considerable cost savings.

In the light of the recent focus on environmental damages caused by salt, it is of interest to examine the ability of GPR to measure remaining salt on winter roads. Preliminary results are encouraging and indicate that the technology could have the potential to address this need. A research approach consists in establishing a relationship between GPR amplitudes and salt quantities. In that respect, the accuracy of the salt measurement device SOBO-20 and the water retention characteristics of pavements (not included in this thesis) are studied. However, further investigations of these issues are beyond the scope of this PhD thesis and are not researched.

Other applications of GPR in Norway are forensics studies related to frost heave of soils and pavements, and condition assessment of concrete airfields. The conclusion that emerges from this PhD thesis is that Ground Penetrating Radar can be used in various ways across many fields of engineering. Some applications have undergone great development worldwide, while others are innovative and relevant to Norwegian distinctive specificities. It is hoped that this PhD work will contribute to both research and implementation of the GPR technology in Norway.

TABLE OF CONTENTS

LIST OF FIGURES

LIST OF TABLES

NOMENCLATURE

Abbreviations

2WTT	Two-way travel time
3D	Three-dimensional
AC	Air-coupled
CMP	Common mid-point
CRIM	Complex refractive index model
DMI	Distance measuring instrument
DOT	Department of Transportation
EM	Electromagnetic
FHWA	Federal Highway Administration
FWD	Falling weight deflectometer
GC	Ground-coupled
GPR	Ground Penetrating Radar
GPS	Global positioning system
GSSI	Geophysical Survey Systems Inc.
HCP	Half-cell potential
HED	Horizontal electric dipole
HMA	Hot-mix asphalt
IE	Impact echo
IRT	Infrared thermography
MISW	Multiple impact of surface waves
NDE	Non-destructive evaluation
NDT	Non-destructive testing or non-destructive techniques
NPRA	Norwegian Public Road Administration
NTNU	Norwegian University of Science and Technology
PCC	Portland cement concrete
PCN	Pavement classification number
QA	Quality assurance

QC	Quality control
R	Coefficient of correlation
R&D	Research and development
SASW	Spectral analysis of surface waves
SD	Standard deviation
SF	Step-frequency
TDEM	Time-domain electromagnetic methods
TDR	Time domain reflectometry
TPAC	Total pavement acceptance device

Symbols

μ	Magnetic permeability
A	Amplitude of GPR waveform
c	Velocity of EM waves in free space
f	Frequency
G	Bulk specific gravities
δ	Skin depth
ε	Dielectric permittivity
σ	Electrical conductivity
υ	Fractional volume
λ	Wavelength

Chapter 1

Introduction

1.1. Background

1.1.1. Maintenance costs for the national transportation network

Transportation infrastructures are subject to strong impacts from traffic loads and adverse climate. In spite of this, it is necessary to keep them safe and maintain a high level of serviceability. In Norway, a large part of the road infrastructure was constructed between 1950 and 1970 and is now on (or beyond) the expected service life.

An extensive focus on further development of rehabilitation techniques is necessary. Due to an inadequate allocation of resources, the need for maintenance, repair and rehabilitation of Norwegian infrastructures has increased year by year. The Norwegian Public Road Administration (NPRA) has calculated the maintenance and rehabilitation costs for national roads to NOK 25 – 40 billions (Sund 2012). The costs to keep up with the deterioration of county and municipal roads come in addition.

Norway has a road network of about 94 000 km (CIA 2014), of which 10 400 km are national roads. Due to the varied and rugged Norwegian topography, the road network includes a significant number of tunnels and bridges that have to be regularly inspected, maintained and upgraded.

Delays in the repairs of such infrastructures (pavements, bridges, tunnels, drainage and sewer systems) can negatively impact the safety and accessibility of the transportation network, and lead to higher maintenance and rehabilitation costs. **Figure 1** shows the cost estimates for the rehabilitation of each type of infrastructure (Sund 2012).

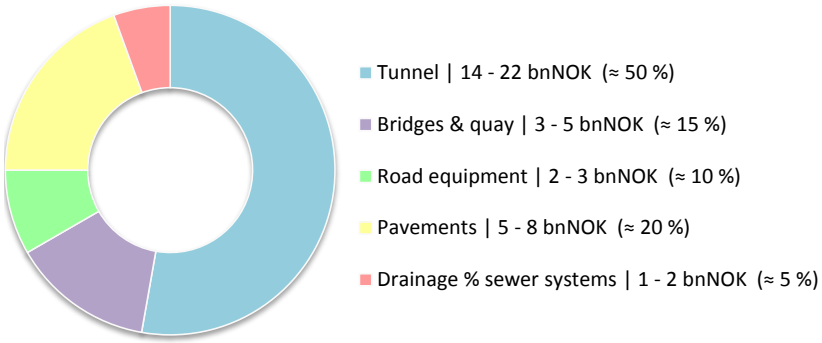

Figure 1 Financial need for the rehabilitation of Norwegian infrastructures

Established by the NPRA, this assessment is mainly based on up-to-date road condition data and current, conventional rehabilitation strategies.

In an attempt to limit costs, there is nowadays a will of the public authorities in Norway and other countries to better define maintenance priorities and hence, optimize the allocation of limited financial resources.

Based on the observation that:

- demolition and removal of the entire structure is often not necessary,
- information about the existing infrastructure condition is in many cases lacking,
- most distresses develop under the surface or inside the structure,

there is a need to rethink maintenance and rehabilitation strategies. Non-destructive techniques, because of their abilities, are now increasingly considered and incorporated in maintenance procedures.

In the light of the above considerations, serious attention has been directed in Norway to the development of innovative maintenance techniques and rehabilitation strategies. The research organization SINTEF conducted the strategic research program "Future Rehabilitation Strategies for Physical Infrastructure" (2008 – 2010). Other R&D programs have also been supported by the NPRA or the Norwegian Research Council to promote non-destructive techniques and improve rehabilitation strategies.

1.1.2. Use of Non-Destructive Testing in Transportation

Traditionally, inspection surveys of transportation infrastructure fall into two categories: the standard destructive methods (such as drilling and excavation) and the non-destructive evaluations techniques (also referred to as NDT).

Non-destructive geophysical investigations are increasingly used in transportation, as they have a significant advantage over traditional methods: they are non-destructive and do not require repair work. They are employed to assist engineers and technicians in infrastructure design, construction, maintenance and rehabilitation phases.

As opposed to conventional destructive methods, geophysical technologies use physical methods to indirectly measure the electrical and mechanical properties of a material. These physical methods can be seismic, electrical, magnetic, electromagnetic or gravitational.

Theories and practices of non-destructive geophysical techniques are largely described in literature (Wightman et al. 2003; Goel & Das 2008; Edwards & Mason 2011; Gucunski et al. 2012). **Table 1** summarizes common surface geophysical methods and some of their applications in transportation.

Most NDT benefits result from their non-destructive nature: they allow to "see the invisible" without damaging the structure. They also allow to collect continuous data at a relative fast rate. Provided that NDT are sufficiently reliable and accurate, this naturally leads to a reduction of cost compared to invasive techniques.

Table 1 Overview of common NDT used in transportation

NDT	Type	Applications (examples)
Pavement deflection testing	Force	Pavement stiffness, thickness
Seismic reflection/refraction	Seismic	Layer thickness, water table, fractures, depth of foundations
Impact Echo (IE)	Seismic	Voids, delamination, cracking, thickness
Ultrasonic tomographic imaging (MIRA)	Seismic	Voids, delamination, cracking, thickness
Spectral Analysis of Surface Waves (SASW)	Seismic	Layer thickness, material moduli
Resistivity	Electrical	Depth to bedrock, water table, voids, utility mapping, corrosion
Half-Cell Corrosion Potential	Electro chemical	Corrosion of steel in concrete
Non-nuclear electrical gauge	Electrical	Material density
Dielectric probe	Electrical	Material dielectric constant

Time-domain electromagnetic methods (TDEM)	Electromagnetic	Depth to bedrock, water table
Ground Penetrating Radar (GPR)	Electromagnetic	Utility mapping, layer thickness, depth to bedrock, moisture and air void contents
Metal detector	Electromagnetic	Utility mapping, buried tanks location
Nuclear gauge	Electromagnetic (Gamma rays)	Material density and moisture
Infrared thermography (IRT)	Electromagnetic (Infrared)	Voids, delamination, cracking, pavement density
Laser scanning	Electromagnetic (Laser)	Cracks, fissures, roughness, rutting on the surface

1.1.3. Norwegian experience

Among all non-destructive methods listed above, Ground Penetrating Radar (GPR) is recognised as one of the most advanced, versatile and promising non-destructive techniques. GPR is used in many countries, like Finland, Germany, Switzerland, Sweden, UK and Italy. 29 state agencies had experience with GPR in 2009 in USA (Maser & Pucinelli 2009), and 8 used it on an extensive or regular basis (Alaska, Florida, Indiana, Michigan, Minnesota, New Hampshire, Texas, and Wisconsin). GPR work is performed there by both state forces and contractors, and is used in a variety of applications.

In Norway, standard methods (visual inspections, sand patch test, rutting bar measurements, coring and drilling) are still predominant in pavement evaluations. However the benefits of non-destructive techniques have been acknowledged, and laser sensors and pavement deflection testing are currently in use (Thodesen et al. 2012). Seismic measurements, covermeters, rebound hammers, half-cell potentials are other approved NDT for geotechnical surveys and the testing of concrete structures (NPRA 1997).

The value of GPR has also been recognized in Norway. In 2006, SINTEF acquired a GPR system in cooperation with the NTNU and with the financial support of the NPRA. It was, and still is, the only system available in Norway for the testing of transportation infrastructure. The purpose of the investment was to supplement traditional methods for the identification of weak zones prior to rehabilitation (Hoff et al. 2008). Besides, funding was allocated to the research on the feasibility, practicality and areas of applications of this novel field technology. This PhD work was carried out within the framework of this strategic research programme.

1.2. Research objective and Scope

The main goal of this PhD study was to investigate the **feasibility** and **practicability** of the GPR technology in **innovative areas of application**, relevant to engineers and scientists who work in the field of transportation engineering. The specific objectives were to:

- Review the literature, reporting research and implementation projects in the field of GPR
- Evaluate the accuracy and reliability of the newly purchased GPR system
- Study the feasibility of GPR in some innovative civil engineering applications, with the requirements that results are rapidly implementable and satisfy necessities of the Norwegian infrastructure.

In contrast with traditional research approaches, GPR was not uniquely considered as a resource used to validate a hypothesis. It was rather seen as a promising technology whose potential benefits to the Norwegian infrastructure had to be studied and documented. GPR in the context of transportation infrastructure is the core of this research and this approach was decided from the start of the project.

Along with the PhD work, a significant period of time was also dedicated to the learning and mastery of software products. The interpretation of GPR is not a straight-forward process and requires considerable expert skills.

This lack of software expertise among civil engineers could in all likelihood explain partly the scarcity of GPR implementation in Norwegian routine inspection procedures. By gaining knowledge in a variety of areas, the intent of this cross-disciplinary PhD work is finally to assist road administrations in the evaluation of the infrastructure condition and promote cost-effective maintenance strategies.

However, the improvement of the GPR system and interpreting software as well as non-transportation related applications (although interesting or necessary) fall outside the scope of this study.

1.3. Research methodology

1. Literature review
2. Identification of existing GPR applications
3. Prioritization and formulation of the research objectives
4. Assessment of the validity and reliability of the 3d-Geoscope GPR
5. Selection of case studies, in accordance with the research objective
6. Feasibility study for each case study:
    - Ground information

- Expected target's depth, size and material
- Environmental conditions (weather, de-icing)
- Vehicle accessibility
- Choice of antenna and operating frequency
- Traffic management and traffic safety
- Resource planning

7. Data collection
    - Road, tunnels and airfields surveys
8. Displaying and interpreting data
    - Choice of software
    - Processing
    - Data interpretation
    - Editing and reporting
9. Further testing and analysis

During the course of the PhD period, more than 450 journal and conference papers, reports, thesis, standards and technical notes related to transportation engineering have been reviewed.

Classes taken at the NTNU as part of the PhD programme include: Pavement Design; Operation & Maintenance of roads; Mineral, Engineering and Environmental Geophysics. Specific trainings in GPR technology were given by manufacturers (3d-Radar) and software developers (Roadscanners). Valuable knowledge was also gained through participation in meetings, conferences, groups networks (EuroGPR), and European project (Mara Nord).

In addition, an academic stay abroad of 11 months at the Department of transportation of Minnesota has contributed to the sharing of experience, good practice and mutual assistance.

1.4. Structure of the thesis

This thesis consists of five chapters and seven papers.

- Chapter 1 describes the background, context in which this work takes place and the research objectives.
- Chapter 2 introduces the Ground Penetrating Radar technology, its abilities and limitations.
- Chapter 3 reviews the state-of-art and state-of-the-practice over the recent years, in the relevant field work.
- Chapter 4 describes the equipment and the experiments, and summarizes the findings of the papers.

- Conclusions are given in Chapter 5.

The author of this thesis has been the main author of all the papers, except for **Paper V** where the first and second author have equally contributed to the experimental design of the project, data analysis and writing.

Five papers were presented at international conferences, one is published in a scientific journal and one is submitted to a scientific journal.

Table 2 Overview of conference and journal papers

Paper no.	Authors, title, place and date of publishing
I	**Lalagüe, Anne and Hoff, Inge** *Use of Ground Penetrating Radar for detection of salt concentration on Norwegian winter roads.* Presented at the 8th International Conference on the Bearing capacity of Roads, Railways and Airfields.
II	**Lalagüe, Anne and Hoff, Inge** *Accuracy of Ground Penetrating Radar in Bituminous Pavement Thickness Evaluation.* Presented at the 5th Transport Research Arena, 2010.
III	**Lalagüe, Anne and Hoff, Inge** *Determination of space behind precast concrete elements in tunnels using GPR.* Presented at the 13th International Conference on GPR, 2010.
IV	**Lalagüe, Anne; Gryteselv, Dagfin and Hoff, Inge** *Bearing capacity of airfield pavements – In situ survey, measurements and calculations using GPR and FWD.* Presented at the 9th International Conference on the Bearing capacity of Roads, Railways and Airfields.
V	**Lysbakken, Kai Rune and Lalagüe, Anne** *Accuracy of SOBO-20 in the measurement of salt on winter pavements.* Published in the Journal of the Transportation Research Board, issue 2329, 2013.
VI	**Lalagüe, Anne; Lebens, Matthew A. and Hoff, Inge** *Accuracy of Ground Penetrating Radar in Pavement Thickness Evaluation – Impact of Interpretation Errors.* Presented at the 7th Transport Research Arena, 2014.
VII	**Lalagüe, Anne; Lebens, Matthew A.; Hoff, Inge; Grøv, Eivind** *Detection of Rock Fragments on Tunnel Concrete Lining with Ground Penetrating Radar (GPR).* Submitted to Rock Mechanics and Rock Engineering.

Appendix A (Extract from draft paper, unpublished):
Lalagüe, Anne; Lebens, Matthew A. and Hoff, Inge
Use of Ground Penetrating Radar in quality assurance of new asphalt pavements.

Chapter 2

Ground Penetrating Radar (GPR)

2.1. Basic principle

A GPR antenna is typically composed of a transmitter and a receiver. The transmitter sends electromagnetic (EM) energy into the medium to be surveyed. The EM waves propagate into the ground at a speed determined mainly by electrical properties of the medium. When a change in the latter occurs (at an interface between two adjacent materials for example), a portion of the energy is reflected back and captured by the antenna's receiver.

For each outgoing wave, the GPR system records the amplitude and the time taken by the wave to travel from the antenna's transmitter to the reflector and back to the antenna's receiver ("two-way travel time").

Pulses are transmitted at regular, defined time intervals. To construct a GPR profile, the antenna is moved along the survey line. GPR scans are plotted and stacked (**Figure 2**).

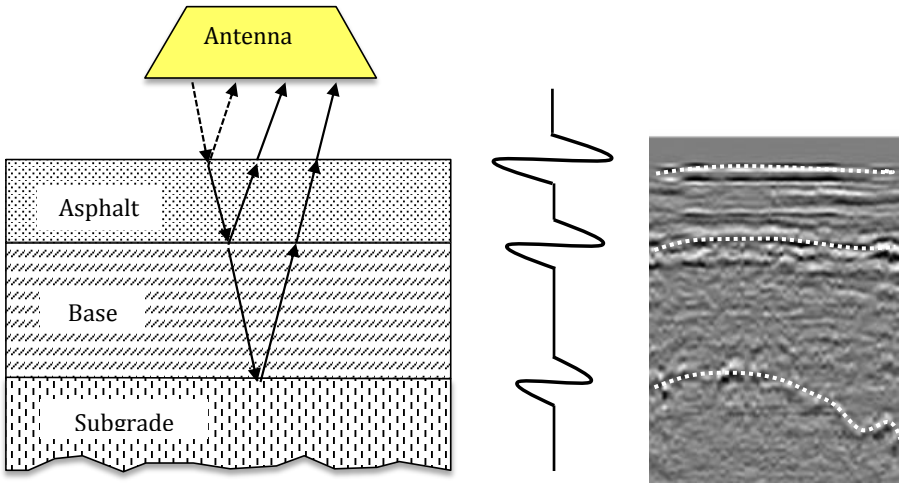

Figure 2 Generation of a GPR profile

2.2. Parameters of importance

The theory of the propagation of electromagnetic waves is largely described in the literature (Daniels 2004; Jol 2008) and will not be covered in details here. However, some parameters play a significant role in the performance of GPR and are briefly introduced in this section.

2.2.1. The electrical properties

The dielectric permittivity (ε), the electrical conductivity (σ) and the magnetic permeability (μ) are the key material properties that control the propagation and attenuation of electromagnetic waves. They are interrelated with each other.

Engineering materials are often described as dielectrics. Theoretically, dielectrics are perfect isolators and do not conduct electricity. In reality all geological materials attenuate to some degree the electromagnetic energy by turning it into heat. These materials are better referred as "low-loss dielectrics" instead of "dielectrics".

2.2.1.1. The conductivity (σ)

The conductivity (σ) of a material refers to its ability to conduct an electric current. When an electric current is applied, charges will move from place to place and this attenuates the electromagnetic energy.

In low-loss conditions, the attenuation is approximated to (**Eq. 1)**:

$$\alpha \approx \frac{\sigma}{2}\sqrt{\frac{\mu}{\varepsilon_r}} \qquad (Eq.1)$$

Where:
α is the attenuation (Np/m)
σ is the conductivity (S/m)
ε_r is relative dielectric permittivity (real part), dimensionless
μ is the magnetic permeability, μ = 1 for most geological materials

As can be seen, the higher the conductivity the greater the attenuation of EM waves. This is why GPR is ineffective in saline and clayey environments.

2.2.1.2. The relative dielectric permittivity (ε_r)

The dielectric permittivity ε_r is the second physical property of importance. It refers to the ability of a low-loss dielectric to store charge when an electric field is applied. It is the ratio of the absolute permittivity of a substance (ε) to that of free space or vacuum (ε_0), and is dimensionless:

$$\varepsilon_r(\omega) = \frac{\varepsilon(\omega)}{\varepsilon_0(\omega)} \qquad (Eq.2)$$

The relative dielectric permittivity is actually a complex function with real (storage) and imaginary (loss) components, both being frequency-dependent:

$$\varepsilon_r^*(\omega) = \varepsilon_r'(\omega) - i\varepsilon_r''(\omega) \qquad (Eq.3)$$

Where:
$\varepsilon_r^*(\omega)$ is the complex relative dielectric permittivity
$\varepsilon_r'(\omega)$ is the real part of the complex relative dielectric permittivity (storage)
$\varepsilon_r''(\omega)$ is the imaginary part of the complex relative dielectric permittivity (loss factor)

The imaginary part ε_r' is called the "loss factor" and describes the polarization that is not reversible after an electric field was applied. It is considered as negligible for most engineering materials that have low conductivities.

For the sake of simplicity, the relative permittivity of a subsurface material is reduced to its real component ε_r, measured at low frequencies. It is related to the material composition, moisture and void content, and is often referred as to the relative dielectric constant.

Pulses travel faster through a low dielectric permittivity material than a material with a higher ε_r. Typical values of ε_r for common engineering materials can be found in **Appendix B**.

2.2.1.3. The magnetic permeability (μ)

The magnetic permeability (μ) refers to the ability of a material to become magnetized when an electromagnetic field is applied upon it. Such as electrical conductivity, an increased magnetic permeability attenuates the EM waves, and renders GPR ineffective. However, most soils and engineering materials do not contain a significant amount of magnetite minerals such as iron oxide. The effect of the magnetic permeability on the EM energy is therefore assumed to be negligible ($\mu = 1$).

2.2.2. The GPR operating frequency (ω)

Electromagnetic waves are characterized by the frequency at which they oscillate. Low frequencies produce long waves, while high frequencies generate shorter waves:

$$\lambda = \frac{c}{f} \qquad (Eq. 4)$$

Where:
λ is the wavelength (m)
c is the velocity of the propagating EM waves in free space ($\approx 3 \times 10^8$ m/s)
f is the frequency (1/s)

The wavelength is in turn related to the depth of penetration of the wave and the vertical resolution of the data. Longer waves penetrate deeper in the medium but shorter waves offer a better resolution.

Because the electrical properties ε and σ of the ground are frequency-dependent, the frequency at which pulses are generated has a direct impact on their velocity and attenuation. The higher the antenna frequency, the better the resolution is. However high frequencies waves do not penetrate deeply in the ground and attenuate very quickly.

Table 3 Effect of parameters on the propagation of electromagnetic waves

Parameter	Action	Input for the calculation of
Relative dielectric permittivity ε_r	Describes how fast radar waves travel through a material	Velocity Layer thickness Density
	Water content ↗, ε_r ↗, velocity ↘ Water content ↘, ε_r ↘, velocity ↗	
Conductivity σ	Describes how deep we can see	Attenuation factor Skin depth
	σ ↗, attenuation ↗, exploration depth ↘ σ ↘, attenuation ↘, exploration depth ↗	
Frequency f	Describes how deep and clear we can see	Wavelength Vertical resolution
	f ↗, attenuation ↗, exploration depth ↘, resolution ↗ f ↘, attenuation ↘, exploration depth ↗, resolution ↘	
Magnetic permeability	Negligible for most engineering materials	

2.3. GPR equipment

2.3.1. GPR systems

GPR systems typically fall into two categories: impulse radars, and step-frequency radars. Impulse systems are the most common. The working principle is as described in section 2.1., i.e. data is registered in the time-domain. Conversely, step-frequency radars collect data in the frequency-domain. They emit a series of waves at a certain frequency that increases in increments. The radar then measures the phase and amplitude of the reflected waves and converts these data into the time-domain to build a GPR profile.

When using impulse radars, a trade-off must be found between resolution and depth of exploration. However, no compromise is needed for step-frequency radars since multiple frequencies are used.

Figure 3 Impulse GPR, air-coupled antenna

2.3.2. Antennas

Antennas can either be suspended above the ground (*air-coupled*), or in direct contact with the ground surface (*ground-coupled*). Ground-coupled antennas usually give an accurate image of the subsurface and especially concrete, while air-coupled antennas allow high-speed measurements and the estimation of density. Arrays are sets of several antennas; they are particularly suited for the measurements of large areas and allow common-midpoint data acquisition. On that matter, Leng et al. (2009) published comprehensive guidelines for the selection of antenna type and frequency for pavement surveys.

Figure 4 Antenna array (left) and ground-coupled antenna (right)

2.3.3. Other components

Data are typically acquired using a control unit, a laptop for data visualization, a GPS and a Distance Measurement Instrument (DMI). After acquisition, data are processed and filtered to correct location errors, remove interferences and unwanted background data, or enhance any particular features.

GPR systems are increasingly associated with other instruments and technologies to maximize the information obtained about the infrastructure. Digital cameras provide additional information about the aspect of the structure, and help the analyst in the interpretation of GPR data. Laser scanners can be mounted on GPR vehicles and record surface characteristics such as roughness and cracks while GPR detects subsurface features. An example of such multi-function vans is the Total Pavement Acceptance Device (TPAC), developed by the Texas department of Transportation (Stokoe et al. 2013). In addition to GPR, GPS, DMI and video, it includes a rolling dynamic deflectometer that is able to produce deflection profiling at a continuous speed of 1,6 – 4,8 km/h. Other examples of GPR data combined with non-destructive techniques (Infrared thermography and Falling Weight Deflectometer) are presented in Chapter 3.

2.4. Benefits and limitations

Using GPR to obtain information of the roadbed condition offers many advantages. Primarily, GPR is a non-destructive technique. This means that no massive excavations are needed, apart from calibration purposes. In this regard, GPR can be seen as more cost-effective than coring, that requires traffic control, a water source and repairs, and only provides limited information about the subsurface. In addition, some GPR systems (air-coupled) can collect data at normal vehicle speeds leading to minimum interference with the traffic. With multiple antennas or multichannel arrays it is even possible to record the data crosswise, which allows a significant gain of time. They can easily be used on a network-level basis and are particularly suited to utility mapping surveys.

As every geophysical method, the GPR technology has also some limitations. These are principally related to the environment. GPR is not able to distinguish materials with similar dielectric properties. It is very sensitive to water content and conductivity, and performs poorly in clayey, organic or saline medium.

2.5. Areas of applications

The GPR technology is relatively well-established and is used in a variety of fields, from geological and archaeological investigations to landmine detection. In transportation infrastructure inspections, GPR is increasingly being used to image the subsurface profile of road- and railways, detect and locate buried objects and structures, assess the condition of bridge decks, tunnel linings, airfields and ballasts. The technology has also the potential to be used as a QA/QC tool in thickness and material density measurements. An overview of the current state-of-the-art is presented in the next chapter.

Chapter 3

State of the Art and the Practice in Transportation Infrastructure

This state of the art does not intend to replace literature searches and books already published on the subject, but it is hoped to give the reader a synthesis of current GPR practice and background on the different analysis methods.

3.1. Roadway

3.1.1. Pavement layer thickness

The GPR's main application is probably the determination of pavement thickness. Accurate layer thickness is an important input in Pavement Management databases, for design, rehabilitation and QA/QC purposes.

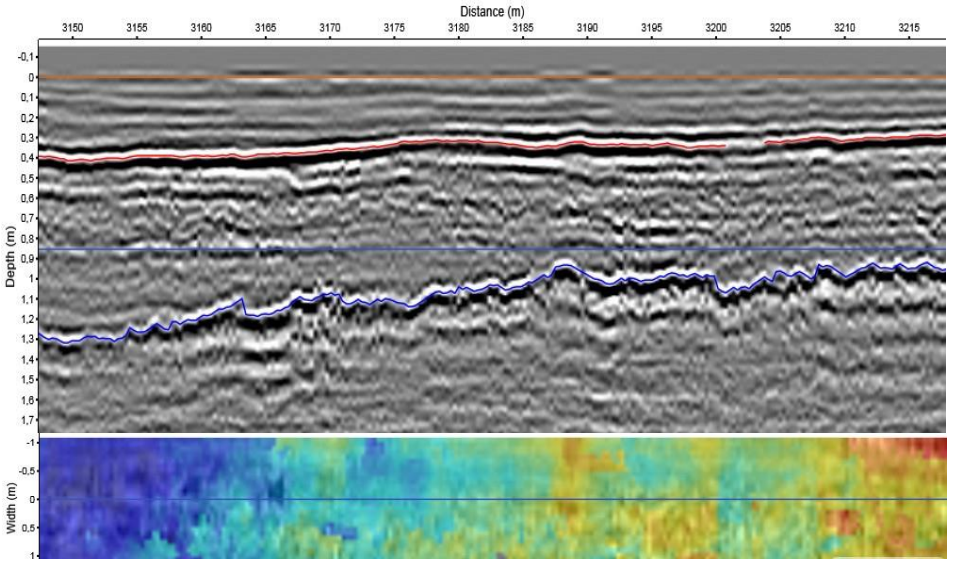

Figure 5 Road profile mapping

The accuracy at which GPR systems are able to measure a layer thickness has been extensively investigated. The studies presented in this section (and summarized in **Table 4**) illustrate the different calculation methods of pavement thickness. This list is not exhaustive and detailed literature reviews can be found in Maser (1996), Gordon et al. (1998), Goel & Das (2008), Saarenketo (2008) and Maser & Pucinelli (2009).

3.1.1.1. Calculation methods

The calculation of the pavement thickness is based on the reflection of electromagnetic waves when a change in electrical properties occurs. The relative dielectric permittivity ε_r controls the velocity at which the waves travel through a material. For non-magnetic materials and assuming ε_r is the real part of the dielectric permittivity, the velocity is given by:

$$v\ (m/s) = \frac{c}{\sqrt{\varepsilon_r}} \qquad (Eq.\ 5)$$

Where:
v is the velocity of the propagating EM waves in the material
c is the velocity of the propagating EM waves in free space ($\approx 3 \times 10^8$ m.s^{-1})
ε_r is the relative dielectric permittivity (real part)

The layer thickness d is calculated as the product of the two-way travel time Δt of reflected pulses, and the wave velocity v inside the layer:

$$d = v \times \frac{\Delta t}{2} \qquad (Eq. 6)$$

$$d = \frac{c \times \Delta t}{2\sqrt{\varepsilon_r}} \qquad (Eq. 7)$$

The calculation of d requires the estimate of the relative dielectric permittivity ε_r. In other words, the accuracy at which the thickness is measured depends on how well the parameter ε_r is assessed.

Several methods exist to obtain the value of ε_r and they are briefly described in the section below. As can be seen in **Figure 6**, assigning a value of 6 instead of 5 to ε_r ($\Delta\varepsilon_r = 1$) leads to an error of 8,7 % in the layer thickness calculation. Likewise, using a value of 9 when the dielectric constant of the ground is in reality 7 ($\Delta\varepsilon_r = 2$) underestimates the layer thickness by almost 12 %.

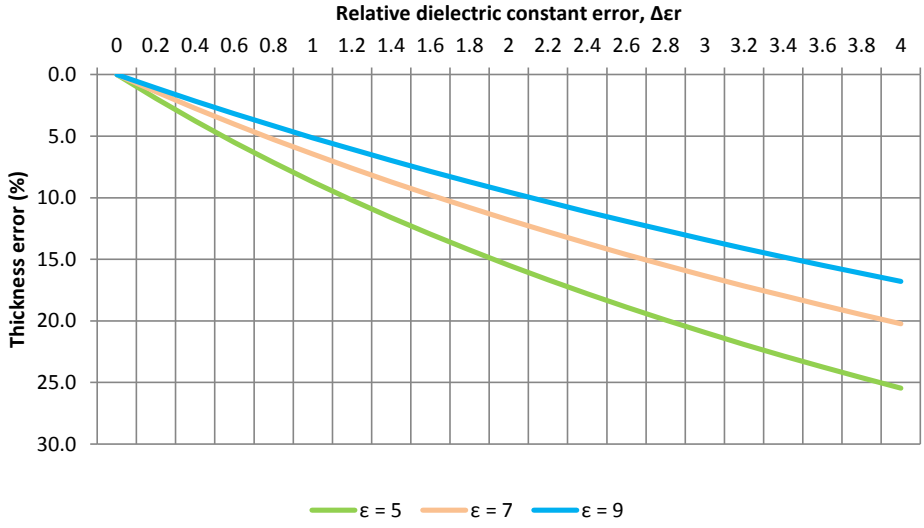

Figure 6 Relative thickness error versus error in dielectric permittivity (Lahouar 2003)

Therefore it is important to choose the best calculation method: the more accurate the value of ε_r is, the more reliable the layer thickness will be.

- Educated guess

The easiest way to obtain the value of ε_r is to search in the literature. The dielectric permittivity of most engineering materials has been extensively measured in laboratory and reported (**Appendix B**). For a qualitative overview of the road profile or for a rough estimate of the layer thickness, "guessing" the value of ε_r from experience and standard data might be sufficient. However, since the dielectric permittivity varies from site to site, this method may lead to significant deviations and should be avoided if quantitative and accurate measurements are needed.

- Curve fitting method

As an antenna approaches a detectable target in the ground (like a pipe), the two-way travel time (2WTT) of the reflected wave decreases until the antenna is placed right over the target. When the antenna is dragged away, the 2WTT increases again. This builds up a hyperbola curve whose apex represents the location of the target (**Figure 7**). The parabolic shape is specific to each environment and depends on the wave velocity in the layer:

$$t = \frac{2}{v}\sqrt{x^2 + d^2} \qquad (Eq. 8)$$

Where:
t is the two-way travel time
v is the velocity of the propagating EM waves in the layer
x is the distance between the antenna and the target
d is the depth of the target

When a hyperbola is visible on a radargram, it is possible to calculate the velocity and ε_r from the slope of its asymptote (**Eq. 5** and **8**). This technique is theoretically relatively accurate if the layer is homogeneous and hyperbolas are well-shaped. However, this is not always the case and only discrete, point measurements are possible with this technique. The variations in dielectric permittivity along the section are overlooked.

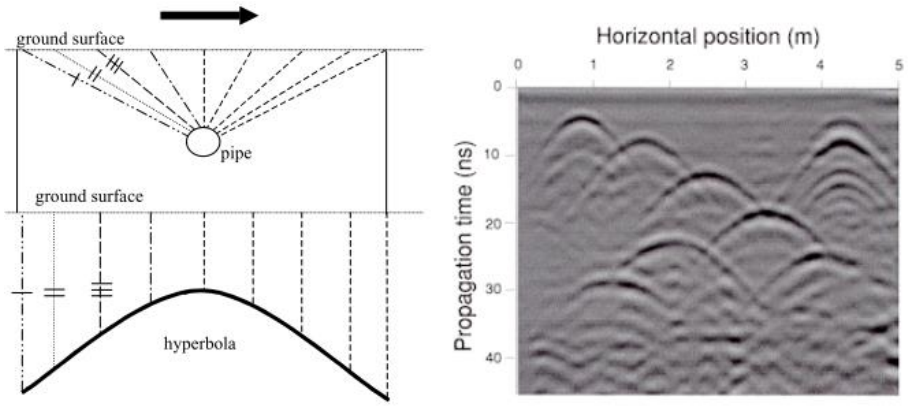

Figure 7 Hyperbola formation (Ruthenberg 1998)

- Calibration from a core thickness

Calibration consists of taking a core and recalculates the layer thickness with the new value of ε_r. ε_r can be obtained from the equation below, derived from **Eq. 7**. Several studies confirmed the accuracy of this method (Loizos & Plati 2007b; Morcous & Erdogmus 2010). However, it is again assumed that the dielectric permittivity remains constant all over the road section. If it is not the case, the calibration on a single core may result in relative high errors (Edwards & Mason 2011).

$$\varepsilon_r = \left(\frac{c \times \Delta t}{2 \times d}\right)^2 \qquad (Eq. 9)$$

- Percometer

Percometer is an easy-to-use instrument that measures the conductivity and the dielectric permittivity of a material. It consists of a control unit and a coaxial probe. The device emits an electric signal that is reflected when a change in capacitance occurs which is directly related to the dielectric permittivity of the specimen. Percometer is convenient to use, but the main pitfall with this method is the coaxial probe that is not suited to rough surfaces (**Figure 8**) and the void between the probe and the pavement interferes with the measurements. A solution proposed by Loizos & Plati (2007) is to saw the core in the middle and measure ε_r on the flat surface. This also has the advantage to measure ε_r in the middle of the layer and not only in the top part. The authors observed a drop in the measurement error from 26 % to 7 %. However samples get wet from coring and sawing, and have to be dried before measurement.

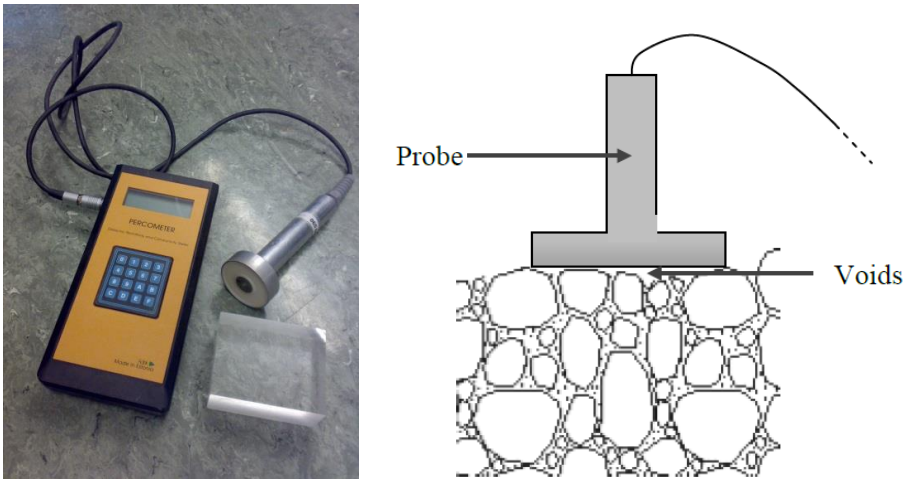

Figure 8 Percometer (left), Measurement errors on rough surfaces (right)

- Reflection amplitudes method

When the GPR survey is carried out with an air-coupled horn antenna, one of the most accurate ways to obtain the value of ε_r is to use the reflection amplitudes method. The dielectric permittivity ε_1 of a layer is calculated as:

$$\sqrt{\varepsilon_1} = \frac{1 + \frac{A_0}{A_m}}{1 - \frac{A_0}{A_m}} \qquad (Eq. 10)$$

Likewise, the dielectric permittivity ε_2 of the layer below is calculated as:

$$\sqrt{\varepsilon_2} = \sqrt{\varepsilon_1} \times \frac{1 - \left(\frac{A_0}{A_m}\right)^2 + \frac{A_1}{A_m}}{1 - \left(\frac{A_0}{A_m}\right)^2 - \frac{A_1}{A_m}} \qquad (Eq. 11)$$

Where:
A_0 is the amplitude of the GPR waveform from the pavement surface
A_1 is the amplitude of the GPR waveform from the asphalt/base interface
A_m is the amplitude of the GPR waveform from a metal plate

The reflection amplitudes method allows the continuous estimation of ε, which makes it a very accurate method for layer thickness calculation. Most studies report errors between 2 % and 10 % (**Table 4**). Although reliable, the method still benefits from calibration on core(s). However depending on the project's purpose, the

improvement in results can be considered as marginal. Edwards & Mason (2011) concluded in a large-scale survey that when using air-coupled horn antennas "calibration could be eliminated, if necessary".

- Common Mid-Point (CMP)

Ground-coupled antennas are directly in contact with the ground. So the waves do not travel through air and there is no surface reflection. Because of this, the dielectric permittivity cannot be calculated using the reflection amplitudes method. However it is still possible to calculate ε_r continuously using the Common Mid-Point (CMP) technique. The method requires two ground-coupled antennas that are moved in opposite directions, both remaining at equal distance from the mid-point P (**Figure 9**).

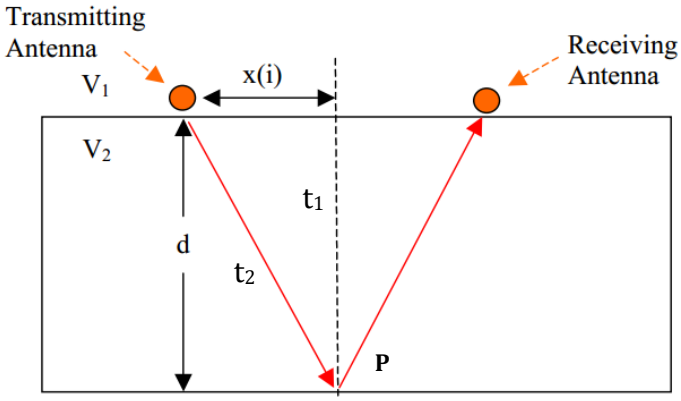

Figure 9 Common midpoint geometry using ground-coupled antennas (Infrasense 2003)

According to the Pythagorean Theorem,

$$(x)^2 + d^2 = \left(v.\frac{t_2}{2}\right)^2 \qquad (Eq.12)$$

$$v.t_2 = 2.\sqrt{d^2 + (x)^2} \qquad (Eq.13)$$

And,

$$v.t_1 = 2.d \qquad (Eq.14)$$

Where:
t_1 is the two-way travel time when the two antennas are adjacent
t_2 is the two-way travel time when the two antennas move in opposite directions
x is the distance between the two ground-coupled antennas

Combining Eq. 13 and 14, we eliminate *d* and we obtain the following relation:

$$v = \frac{2x}{\sqrt{{t_2}^2 - {t_1}^2}} \qquad (Eq. 15)$$

Finally,

$$d = \frac{x.t_1}{2\sqrt{{t_2}^2 - {t_1}^2}} \qquad (Eq. 16)$$

Unlike the reflection amplitudes method, the CMP technique calculates the dielectric permittivity from the reflection at the bottom of the layer, and not at the top. This makes it a theoretically very accurate method to assess the pavement thickness since it takes into account the variations of ε_r within the layer. Several studies reported good results (Lahouar et al. 2002; Lahouar 2003).

- Other techniques

New methods and advanced data processing techniques are regularly tested to maximize the accuracy of GPR. Cao (2011) developed a forward model that simulates the electromagnetic wave propagation for a wide range of pavement profiles. Since information about the dielectric permittivity and conductivity is included in the reflection amplitudes, it is possible to "back-analyze" the GPR waveform and find the best match among the thousands of simulated scans. This innovative method has been successfully applied, with an average error of 2,3 % between GPR thicknesses and ground-truth data.

Thick asphalt pavements are typically composed of several intermediate layers, applied year after year. Although similar, the mix design of these thin layers varies slightly and so do the dielectric properties. However the contrast in dielectric permittivity is generally low and reflections are masked by stronger ones. To account for changes in asphalt properties, Lahouar (2003) applied the deconvolution filter the reflection amplitudes method to "clean" the waveform, reveal the hidden reflections and separate the individual asphalt layers. They obtained during field validation an average error in overall layer thickness of 3,1 %, compared to 12 % for the reflection amplitudes method alone.

Maser et al. (2012) introduced an "error checking procedure" based on FWD data. The E-modulus of a pavement is back-calculated from surface reflections and thicknesses. At locations where the asphalt modulus is out of range (above 2500 ksi), the data has to be re-interpreted. Using this method reduced the error from 10,3 % to 7,6 %.

3.1.1.2. Effect of surface water on GPR measurements

A study conducted at the Kentucky Transportation Center (Willett & Rister 2002) researched the effect of surface water on GPR data. Water was sprayed on an asphalt pavement during 20 minutes until the surface became wet but not saturated. A series of measurements was then carried out on dry, wet and half wet/half dry surfaces using a 1 GHz air-coupled antenna. The difference in GPR thickness (1,2 mm at most) was not found to be significant.
However the effect of water is far more noticeable at high frequencies. In a recent study using a 2 GHz air-coupled antenna, compaction monitoring was found to be impacted by the water sprayed by roller (Shangguan et al. 2013). At frequencies lower than 1 Ghz, the effect of water was again found to be negligible.

3.1.1.3. Significance of calibration cores

As stated earlier it is often necessary to calibrate the GPR data with ground-truth. The improvement in accuracy is often significant (**Table 4**). In the previously cited study (Willett & Rister 2002), researchers examined how the number of calibration cores improves the level of accuracy of GPR data. When no calibration is made (i.e. the value of ε_r is a blind estimate), the error in thickness is about 65 %. It should be noted that the tested pavement is a thin asphalt (less than 5 cm thick), so misinterpretation in the GPR data often results in highly magnified percent error. When the data are calibrated on one core, the mean error is reduced to 17 %. When multiple cores are used, the error drops to 5,3 %. More about the significance of calibration cores on GPR results can be found in Chapter 4.

3.1.1.4. Repeatability of measurements

A few studies have been conducted to verify the repeatability of GPR measurements. Al-Qadi et al. (2002) collected three data sets on different dates and reported thickness errors from 5,9 % to 12 %. The different moisture conditions of the test sections could explain the disparity of the results. More recently, Holzschuher et al. (2007) observed a good repeatability of the measurements done the same day. In addition, the speed of survey does not seem to significantly impact the performance of GPR. The thickness error was found to be 6,7 % for stationary measurements, 7,9 % at low speed and 8,3 % at high speed. However, the authors

recommend using more markers when collecting data at highway speed to avoid offset and errors in site chainage.

3.1.1.5. Sources of inaccuracies

As discussed above, the accurate estimation of the dielectric permittivity is important to GPR performance. It is, though, worth mentioning that numerous other factors may influence the GPR results. Some of them are listed here:

- The calibration considerably improves the GPR performance in measuring pavement thickness. However calibration with core sampling often comes with its share of shortcomings. It is indeed not always easy to take cores at the same exact locations where GPR measurements were made, and offsets may lead to erroneous calculation of ε_r. In addition, cores may be broken which makes the reading of the thickness difficult.
- Layers may be difficult to separate when the contrast in the dielectric permittivity is low. It is often the case of intermediate asphalt layers which have very similar dielectric properties. For rigid pavements, the interface concrete/base layer might be very weak as well. It can be tempting to analyze the data even if the contrast is low, but the risk to make interpretation errors is high. Results from accuracy studies in **Table 4** suggest that, when the interface concrete/base layer is clearly visible, GPR is reliable in pavement thickness (2%, Al-Qadi et al. 2005).
- Of considerable significance are the skills of the analyst. Sufficient experience is necessary to accurately interpret GPR data.
- The dielectric permittivity is generally assumed to be real, although losses in materials occur. The loss part of the dielectric constant should be included in any GPR modeling to assure accurate results (Loulizi 2001).

Table 4 Overview of GPR accuracy studies

Author	Year	Type antenna	Data analysis technique	Pavement type	Thickness (mm)	Error	Comment
Lahouar et al.	2002	1 GHz air-coupled horn and 900 MHz ground-coupled antennas	CMP	Flexible	267 - 375	6,8 %	Modified CMP configuration
Al-Qadi et al.	2003	1 GHz air-coupled horn antenna	Reflection amplitudes	Flexible	100 - 250	2.9 %	
Lahouar	2003	1 GHz air-coupled horn antenna	Reflection amplitudes	Flexible	195 - 355	12 %	
			Deconvolution + Reflection amplitudes			3,1 %	Deconvolution is used to separate individual HMA layers
		900 MHz ground-coupled antenna	CMP			3,9 %	Modified GPR system
Al-Qadi et al. (DOT Virginia)	2005	1 GHz air-coupled horn antenna	Reflection amplitudes	Rigid	≈ 300	2 %	
Flintsch et al. (DOT Virginia)	2005	1 GHz air-coupled horn antenna	-	Flexible	≈ 240 - 370	5,7 %	
Loizos et al.	2007	1 GHz air-coupled horn antenna	Reflection amplitudes	Flexible	≈ 90 - 340	≈ 9,5 %	Median values
			Ɛ determined from calibration core			≈ 5 %	
			Percometer (top)			≈ 26 %	
			Percometer (sub-core)			≈ 7 %	
Holzschuher et al. (DOT Florida)	2007	2 GHz air-coupled horn antenna	Reflection amplitudes	Flexible	≈ 71 - 328	8 %	No calibration

Author	Year	Type antenna	Data analysis technique	Pavement type	Thickness (mm)	Error	Comment
						4,9 %	Calibrated
				Rigid	≈ 15 - 20	8,8 %	No calibration
						5 %	Calibrated
Loizos & Plati	2007	2 GHz air-coupled horn antenna	Reflection amplitudes	Flexible	< 50	2,7 %	Wearing course
Lahouar & Al-Qadi	2008	1 GHz air-coupled horn antenna	Reflection amplitudes + multiple reflections model	Flexible	195 - 355	2,5 %	Aims at revealing the masked weak reflections from the individual asphalt layers
Morcous & Sekpe	2010	1,5 GHz ground-coupled antenna	Ɛ determined from calibration core	Rigid	≈ 327 - 336	1,5 %	
Cao	2011	1 GHz air-coupled HED (bowtie modified) antenna	Full waveform simulation	Flexible	89 - 127	2,3 %	
Edwards & Mason (U.S. Army Engineer Research and Development Center)	2011	1 GHz Horn antenna	Reflection amplitudes	Flexible	≈ 65 - 316	4,5 %	Calibrated
						7 %	Non calibrated
				Rigid	≈ 192 - 284	6,1 %	Calibrated 42 % of the test locations measured
						9,7 %	Non calibrated 42 % of the test locations measured
		2 GHz Ground-coupled antenna	Ɛ determined from calibration core	Flexible	≈ 65 - 316	15 %	
				Rigid	≈ 120 - 634	25,4 %	100 % of the test locations measured

Author	Year	Type antenna	Data analysis technique	Pavement type	Thickness (mm)	Error	Comment
		1,5 GHz ground-coupled antenna	Ɛ determined from calibration core	Flexible	≈ 65 - 316	10 %	
				Rigid	≈ 120 - 285	20 %	63 % of the test locations measured
			CMP	Flexible	≈ 65 - 316	22 %	Non calibrated
						13,5 %	Calibrated
				Rigid	≈ 191 - 634	18,4 %	Non calibrated 63 % of the test locations measured
						15 %	Calibrated 58 % of the test locations measured
		Step-frequency 140 MHz – 3 GHz	Ɛ determined from calibration core	Flexible	≈ 65 - 316	3,9 %	
				Rigid	≈ 120 - 634	28,5 %	42 % of the test locations measured
Maser et al. (DOT Montana)	2012	2 GHz air-coupled horn antenna	Reflection amplitudes	Flexible	≈ 60 - 278	10,3 %	
			Reflection amplitudes + check with FWD data			7,6 %	GPR thicknesses are used for backcalculation. If asphalt moduli exceed thresholds, the GPR data are re-interpreted.

3.1.2. Pavement density and segregation

The density of asphalt pavement is conventionally measured using nuclear gauges or core samples. For safety and economic reasons, NDT such as non-nuclear density gauges, infrared thermography and seismic pavement analyzer have recently been introduced and tested. A number of descriptions of their use is currently available in the literature (Rao et al. 2007; Popik et al. 2009; Schmitt et al. 2012).

GPR has also the capacity to evaluate the pavement density and can be used as a quality assurance tool. As for pavement thickness determination, the main benefits of GPR are the speed of measurement and the significant reduction of coring. Several methods exist to calculate the void content or asphalt density, such as regression analyses and mixture models.

3.1.2.1. Exponential regression analysis

The method has been first developed by (among others) Finnish researchers (Saarenketo & Scullion 2000) and is commonly used in Finland for quality control surveys (Saarenketo 2012). It is based on the relationship between the dielectric properties of asphalt and the void content. Since the dielectric permittivity of air is 1, the more the void content the less the total dielectric value of asphalt. The relationship is exponential and based on statistical regression:

$$\%Void = 272.93 \times e^{-1{,}3012.k.\varepsilon} \qquad (Eq.\ 17)$$

Where:
ε is the total dielectric permittivity of asphalt
k is a calibration coefficient

The method requires at least one calibration core to obtain the value of the factor k. The void content is measured in laboratory in accordance with national standards. The dielectric permittivity is determined during the data collection using the reflection amplitudes method (air-coupled antennas are required).

A Finnish study found the method to be ± 0.9 % accurate (Sebesta et al. 2012). This result of this study conducted in 1998 is in Finnish but appears in the Finnish specifications PANK 4122: Air void content of asphalt pavement, Ground Penetrating Radar method. Although the details of the experiment are not known, it is assumed that the testing was done in a controlled environment to achieve such a high accuracy.

In 2003, the exponential method was employed to detect segregation in three asphalt overlays (Sebesta & Scullion 2003). The variable and mixture-dependent

parameters of **Eq. 17** were determined for each section using calibration cores, and the degree of correlation between surface dielectric permittivity and laboratory measurements of air voids was obtained. For all the sections, the correlation is very high (from 0,80 to 0,99). Thus areas of "coarse" gradation (low binder content and pavement density) may potentially be uncovered.

Two other studies (Popik et al, 2009) conducted on 26 and 18 asphalt sections also obtained a good correlation between the GPR-measured dielectric values and laboratory-measured air voids, with a correlation index R^2 of 0,73 and 0,80 respectively. Comparable results were found in a SHRP 2 research project for 3 out of 4 tested sections, with R^2 varying from 0,76 to 0,81 (Sebesta et al. 2012), and in another study from 2012 using a similar exponential formula (Kassem et al. 2012).

3.1.2.2. Linear regression analysis

In order to simplify the assessment of the void content, Loizos & Plati (2011) established a linear regression relationship between the dielectric properties and void content of 20 asphalt specimens:

$$\%\, Void = 49{,}81 - 7{,}6.\varepsilon \qquad (Eq.\ 18)$$

The dielectric values were measured in laboratory with Percometer. The data correlate well, with a coefficient of correlation R^2 of 0,92.

3.1.2.3. Density models

Asphalt is composed of aggregates, binder and air. The dielectric permittivity of asphalt depends on the dielectric permittivity of its components and their fractional volume. Several mixing laws have been proposed to characterize the dielectric properties of a composite material. The Complex Refractive Index Model (CRIM) is by far the most widespread one and is given by the following expression:

$$\sqrt{\varepsilon_{asphalt}} = v_{agg}\sqrt{\varepsilon_{agg}} + v_{binder}\sqrt{\varepsilon_{binder}} + v_{air}\sqrt{\varepsilon_{air}} \qquad (Eq.\ 19)$$

With,

$\sqrt{\varepsilon_{air}} = 1$ and $v_{agg} + v_{binder} + v_{air} = 1$,

The bulk specific gravity of asphalt ($G_{asphalt}$, numerically equivalent to density) is then calculated as follows:

$$G_{asphalt} = \frac{\sqrt{\varepsilon_{asphalt}} - 1}{\frac{P_{binder}}{G_{binder}} \times \sqrt{\varepsilon_{binder}} + \frac{1-P_{binder}}{G_{agg}} \times \sqrt{\varepsilon_{agg}} - \frac{1}{G_{mm}}} \quad (Eq.\ 20)$$

G_{binder} and G_{agg} are the bulk specific gravities of binder and aggregates, respectively. G_{mm} is the maximum specific gravity of asphalt and P_{binder} the binder content. All four material parameters are known from the mix design. The value of the dielectric permittivity of aggregates ε_{agg} and ε_{binder} is assumed.

Beside the CRIM mixture theory, Al-Qadi et al. (2010) tested two others density models: the Rayleigh and the Böttcher mixing models. After a comparative study, the Rayleigh model seems to perform the best in density prediction with an average relative error of only 0,4 % (after calibration with a field core). The models were further developed and tested on a full-scale test site (ALL model). The average errors vary between 0,5 % and 2,8 % (Leng et al. 2011; Leng & Shangguan 2012). Other tested mixture models gave errors of the same order of magnitude (Mardeni et al. 2010).

3.1.3. Moisture

Excessive moisture is responsible for the weakening of the pavement structure and numerous pavement distresses, such as potholes, cracking, rutting, and stripping. Several approaches exist to detect and measure the moisture content in pavements layers. The studies described in this section consider both bituminous, concrete and unbound pavements layers.

Time Domain Reflectometry (TDR) and nuclear/non-nuclear gauges are traditional non-destructive devices employed to measure the water content in pavement layers. Although reliable, they only provide points measurements. To address this limitation, several attempts have been made to assess the moisture condition with Ground Penetrating Radar.

Several methodologies exist for measuring the soil water content with GPR. They have been comprehensively reviewed by Huisman et al. (2003). One of the most common method is to use a polynomial function proposed by Topp et al. (1980):

$$\theta = -0{,}053 + 0{,}0293\varepsilon - 0{,}00055\varepsilon^2 + 0{,}0000043\varepsilon^3$$

Where:
θ is the water content, in m^3/m^3
ε is the dielectric permittivity

To prove the accuracy of GPR, the data is usually compared to TDR or gravimetric results. In a study by Stoffregen et al. (2002), GPR data collected with a 1 GHz air-

coupled antenna could measure the amount of water in a cubic meter of sand with an accuracy of 0,01 m^3. The data was calibrated and compared with lysimeters. These devices consist of cylinders placed in the soil on a platform scale. They are habitually used in soil hydrology to measure the evaporation and transpiration of plants and trees by measuring the weight difference between the received precipitation and the amount of lost moisture. The dielectric permittivity of the sand was determined from the reflection at the bottom of the lysimeter, and the water content estimated using Topp's equation. Likewise, another study (Grote et al. 2005) using a similar experimental approach obtained a difference of 0,02 m^3/m^3 between GPR and gravimetric measurements.

Al-Qadi et al. (2004) used a development of the CRIM mixture model and nuclear gauges to calculate and calibrate the moisture content of granular base layers. A linear relationship was found between the moisture content and the dielectric permittivity, with a R^2 of 0,88.

On asphalt and concrete pavements both prediction models can be employed (Laurens et al. 2005; Li et al. 2010), although they require the determination of the dielectric permittivity. To avoid any calibration step, the Rayleigh theory (reflection/diffraction of EM waves by objects much smaller) can be used to estimate the moisture content of a soil without knowing the dielectric permittivity. This has be analyzed by Benedetto (2010), who observed that the Rayleigh scattering produced a non-linear frequency modulation of the signal related to the water content. The correlation between the shift of the frequency spectrum of the radar signal and the moisture content was established in laboratory on five different types of soil. The Rayleigh theory should not be confounded with the scattering attenuation that occurs when the particles size are close to the wavelength (section 3.4.4.2).

3.1.4. Stripping and delamination

Excessive water content in asphalt pavements may further lead to "stripping", which pertains to the loss of bond between the binder and the aggregates.

Rmeili & Scullion (1997) investigated in Texas the feasibility of GPR in detecting stripping. A large-scale study was conducted using a 1 GHz air-coupled antenna. On GPR return waveforms (**Figure 10**), reflections A and B represent the top and bottom of the asphalt layer. However in some areas, a negative peak C of low amplitude is visible. This peak is thought to reveal the presence of stripping within the layer. After comparison with cores, it was found that the depth of stripping was "reasonably" estimated but that the severity of stripping (thickness of the stripped

layer) was more difficult to measure. Results may be improved using a higher frequency GPR antenna that produce shorter wavelengths.

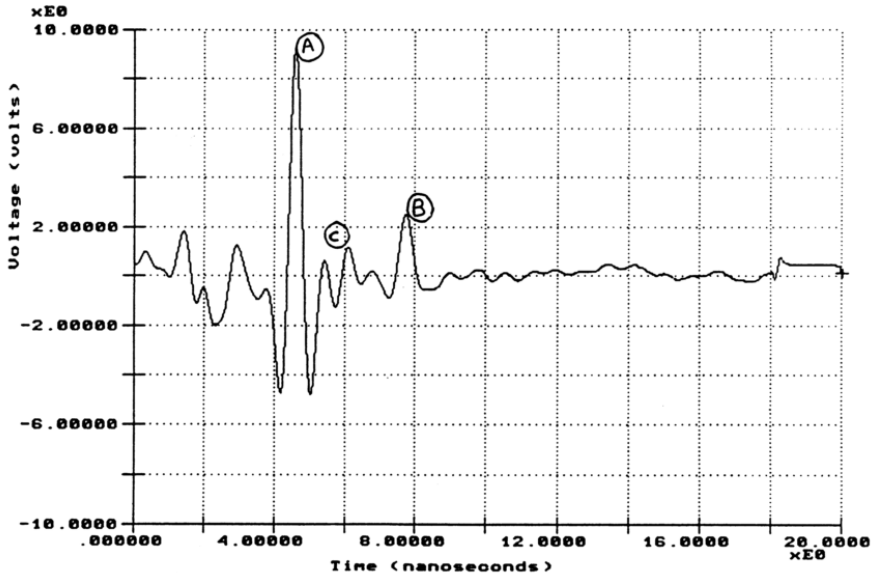

Figure 10 GPR waveform of a stripped asphalt layer (Rmeili & Scullion 1997)

In 2006, Hammons et al. attempted to detect stripping in asphalt layers using several non-destructive methods. Among the tested techniques, only the GPR and seismic responses were impacted by subsurface anomalies. The stiffness, calculated from FWD, and surface temperatures did not prove to be affected by the presence of stripping. However, as shown in previously mentioned studies, the GPR reflection amplitudes were found to be sensitive to the level of overall damage. Additional testing such as seismic surveys may further help distinguish sound from damaged materials, but the differentiation between stripping and excessive moisture may be hard to establish using reflection amplitude analysis only.

Heitzman et al. (2012) also tested the feasibility of NDT to detect the extent and severity of another form of de-bonding: delamination, which relates to the loss of bond between two surface layers on top of each other.

In this study the tested technologies are again Ground Penetrating Radar, infrared thermography, Falling Weight Deflectometer and mechanical wave-based techniques. All of these methods are susceptible to detect some form of change or discontinuation in the investigated material, since delamination typically results in:

- An increase in the void content, moisture content, surface deflection and temperature
- A decrease in density and stiffness.

Similarly to the study by Hammons et al., infrared thermography and FWD did not succeed in detecting delaminated areas. GPR, impact echo and SASW were the ones that performed the best. Particularly, GPR was able to estimate the depth of delamination and some degree of severity. However the identified shortcomings are that only moisture related delamination can be detected (as opposed to no bound due to inadequate tack coat) and it requires significant manual data analysis.

These findings were reported by Liu et al. (2008), who tested ground-coupled GPR on reinforced concrete. With further data analysis and development, delaminated areas can be detected.

3.1.5. Structural damages

Several studies reported a good performance of GPR in structural damage diagnoses. Vertical cracks have a relatively good detectability, especially when water infiltration occurs. GPR may also be effective at detecting cracks on concrete layers with asphalt overlays. Numerical modelling may sharpen the GPR response and facilitate the interpretation (Diamanti & Redman 2010).

Settlements are also relatively easily detected. As can be seen in **Figure 11** below, the extent of subsurface defects can sometimes be important. In the present case, it is an old pavement that has sunk due to a compressible peat subgrade.

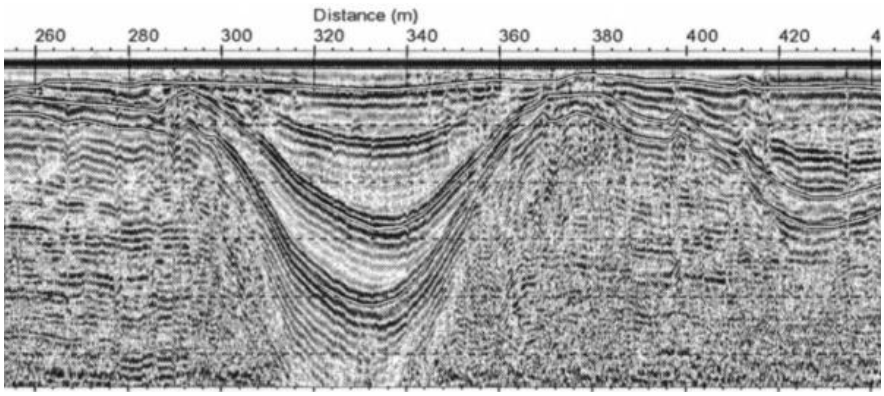

Figure 11 Example of settlement (Saarenketo & Scullion 2000)

In line with settlement issues, some studies have attempted to identify the causes of rutting. Surface deflections often originate from deeper layers, but rehabilitation strategies depend on whether the deformations are a result of inadequate base

materials, a weak subgrade (**Figure 12**) or asphalt mix instability. The GPR method has been applied on test sections with 10 mm or more rutting by the TxDOT which actually found out that deformations only occurred in the top asphalt layer (Chen et al. 2003). Such resolution can solely be achieved with a high-frequency antenna and the authors concede that the "exact contribution to rutting by layer [was] difficult to determine". However, the type of GPR system used in this study is not mentioned.

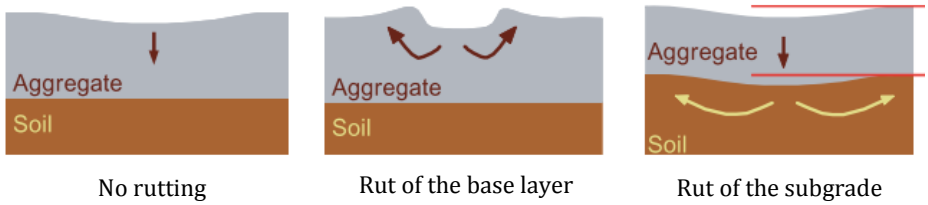

Figure 12 Mechanism of rutting (Dawson et al. 2007)

The detection of voids under pavements is also of interest and relatively easy to achieve given the contrast in dielectric permittivity between air and the surrounding material. As for rutting evaluation, the size of the voids must be significantly larger than the wavelengths in order to be detected. An example of a successful survey is a study conducted in Texas where a 30,6 m^3 cavity was identified by a GC GPR under a concrete pavement (Chen and Wimsatt 2010). It is believed that the void could have led to serious hazard if not discovered in time.

3.1.6. Utility mapping

Ground Penetrating Radar is attracting more and more attention in the field of utility mapping. The lack of accurate information about buried facilities is often pinpointed as a major cause of delays in transportation projects (Sterling et al. 2009; Quiroga et al. 2011). With GPR mapping, disruptions and damages to utility installations can be avoided.

As described in section 3.1.1, a crossing pipe has a shape of a hyperbola on a radargram. The two-way travel times becomes smaller and smaller as the antenna approaches the top of the pipe. The propagation time is maximal when the antenna is situated right above the pipe and then decreases when the antenna draws away.

In contrast with other pipe and cable locators, GPR has the potential to detect leakages and utilities of various materials and several studies have been published on the subject (Roackaway & Rivard 2010; Ariaratnam & Guercio 2006; Seung-veup et al. 2003). Cast iron has invariably the best detectability level, while concrete and PVC conduits may sometimes be disguised by the surrounding medium. The size and depth of the targeted pipe must be foreseen as much as it can be, as well as the road

structure which is often complex in an urban environment. Successive rehabilitation operations can lead to highly variable ground conditions and render the detection of buried utilities more challenging. In that respect, it can be an advantage to use arrays over single antennas because they cover at least half of the lane and generate cross-profiles. They allow to differentiate pipes from other buried structure and hidden defect.

However a major problem using GPR (and most other methods) is the difficulty to find 100 % of utilities in an urban area. Even if as much as 90 % is found the missing 10 % is likely to cause costly surprises and unsatisfied clients.

3.1.7. Frozen grounds

In cold regions, frost is a major cause of pavement deterioration which cannot be ignored. Repetitive freeze-thaw cycles lead to:

- Frost heave and cracking in winter,
- Rutting and weakening of the road structure during the thawing period.

A detailed description of the cause and mechanism of frost heave is available in the literature (Schaus & Popik 2011; Aho & Saarenketo 2006). Estimating the frost depth allows to select the best rehabilitation and strengthening method, which can be for example the use of geotextiles, steel reinforcement or the removal of frost susceptible soil. The thickness of the frozen ground is typically measured by frost depth meters embedded in the soil, but it can also be assessed on a larger scale with GPR. Frost depth meters are usually cumbersome to install, and expensive/laboriously to extract the readings.

Japanese researchers (Nakano & Sakai 2008) confirmed the ability of GPR to easily detect the frost line. The study compared the results of GPR and electrical sounding with ground truth, obtained from frost depth meters. Both techniques located the frost line at a depth of 0,5 – 1m, in agreement with frost tubes data. However the GPR method is considered as superior than electrical sounding because of the practicability and repeatability it offers.

In another study conducted in Greenland (Jørgensen & Andreasen 2007), GPR was used to identify the cause of deep airfield pavement deflections. Three test areas were painted in white in order to reduce the pavement temperature and prevent further settlement. GPR measurements revealed that the permafrost layer was significantly thinner beneath the painted areas than beneath the normal black asphalt. It shows that the white paint can act an insulation, and prevent the frost penetration in the ground. The dark areas were exposed to the sun in a greater extent, resulting to the melting of the permafrost surface and the weakening of the top layers.

3.1.8. Resulting new practice and rehabilitation strategies

The ability of GPR to provide accurate data about the infrastructure condition can be expanded to a wider range of applications. When conducted on a large scale, GPR measurements can aid decision makers with resource allocation, data inventory and prioritization of section for repairs. The benefits and added value of GPR at the network level have been largely documented by transportation agencies (Noureldin et al. 2003; Williams et al. 2006).

Particularly, GPR data can be incorporated to pavement managements systems (PMS) together with roughness index, rut depth, pavement quality index, and skid resistance. New practices for pavement monitoring, data integration and pavement structure segmentation are regularly proposed and/or implemented (Kohler et al. 2006; Loizos et al. 2011; Zhao et al. 2011; Plati & Loizos 2012).

GPR thicknesses can also be used for the backcalculation of layer moduli from FWD data. FWD deflection bowl only provides information for the overall structure, but not for the different layers. From the pavement profile obtained with GPR, the layers stiffness can be backcalculated (Gucunski et al. 2004; Wu et al. 2013).

The question of the economic efficiency of GPR surveys is regularly addressed, particularly by transportation agencies. Costs related to deployment (equipment, data collection and storage, lane closure, coring etc.) are relatively easy to measure, while costs associated with data processing times have a greater uncertainty. Two cost-effectiveness studies conducted for the states of South Dakota and Mississippi (Infrasence 2006; Uddin 2006) showed high benefit/cost ratios of using GPR for pavement and bridge evaluations. The gain is the most pronounced in quality assurance of new pavements, with a benefit/cost ratio reaching 113. This analysis by Infrasense is based on the relationship between variations in thickness and reduction of the pavement life. Numerous other studies confirm the performance of GPR to accurately measure the layer thickness, and thus verify that contractors laid asphalt at the prescribed thickness (Maser et al. 2003; Al-Qadi et al. 2003; George & Erdogmus 2009; Saarenketo et al. 2011; Rajagopal 2011; Poikajärvi et al. 2012). These studies are evidently multifactorial and only valid at the time and place of testing.

3.2. Bridge decks

3.2.1. Concrete deck thickness

Similarly to flexible pavements, Ground Penetrating Radar can be applied to bridge decks to determine reinforced pavement thickness, concrete moisture and damages, and locate tendons and reinforcement bars. Such information is still

obtained from the reflection amplitudes of the detected targets and the value of the dielectric properties of the concrete deck (Loulizi 2001).

The bridge deck thickness is generally accurately measured, although reinforcement may significantly disturb the propagation of the electromagnetic waves through the layer. It seems that when the interface concrete/base layer is sufficiently distinct, the average error of rigid pavement thickness can be as low as 1,5 – 6 %. The best results are obtained after calibration and when using air-coupled antennas (**Table 4**).

More specifically about bridge deck thickness, Hugenschmidt (2004) reported a mean difference of 5 mm between GPR and ground-truth data, for a total deck thickness of about 100 mm.

Likewise, rebar cover depths can successfully be measured. Hugenschmidt (2004) again obtained a mean difference of 17 mm for a concrete cover of ≈ 40 – 150 mm. Analogously, an analysis approach developed by Al-Qadi & Lahouar (2005) combining image-processing techniques with a theoretical reflection model resulted in a an error of 2,6 % between GPR data and ground-truth cores.

3.2.2. Deterioration of bridge decks

There are several forms of bridge deck deterioration. The most serious ones are delamination, corrosion of rebars, vertical cracking and concrete degradation. Recently, a wide range of non-destructive methods has been tested by Gucunski et al. (2012) for the quality control of concrete. The results of their large-scale evaluation suggest that GPR is more suited for the detection of delamination and corrosion of rebars. For the most part, the assessment of the deck condition is based on the attenuation of the reflected waves and is primarily qualitative.

3.2.3. Rebar corrosion

There is a very close relationship between the GPR reflection amplitudes and the chloride content in concrete, which contribute to the corrosion of steel reinforcements. As shown by Hugenschmidt & Loser (2007), the higher the chloride content, the lower the signal amplitudes. The correlation was corroborated by Kalogeropoulos (2012), who also developed empiric relationships between electromagnetic parameters and chloride content.

In a aforementioned study (Gucunski et al. 2012), several GPR systems were tested on a 24 cm thick reinforced bridge deck. Compared to ground-truth, the method gave satisfactory results in detecting corroded elements. They especially ranked high for the repeatability, speed of measurement and cost criteria. However GPR could detect the presence of corrosion but could not measure the degree of it.

3.2.4. Delamination

Delamination in concrete occurs when reinforcements corrode to the point that they expand, creating a horizontal crack. Most corrosion processes are chloride-induced, i.e. caused by the infiltration of water and salt.

Delamination in bridge decks is traditionally detected using hammer sounding, impact echo (IE), half-cell corrosion potential (HCP), or chain dragging. They are all seismic waves-based techniques, except the half-cell potential method which monitors corrosion activity through electrical potential (voltage) measurements. They are well-established methods, although most of them may be time-consuming.

Several studies have been conducted to assess the feasibility of GPR in detecting delamination damage. The analysis often consists in comparing the extent of the attenuation of the GPR response with HCP or chain-dragged results.

In a comparative study on the three methods (Barnes & Trottier 2004), GPR provided better results than HCP with 57 % of deteriorated concrete that was detected. Chain dragging, often considered as the method of reference, gave equivalent results. However the GPR surveys were unsuccessful on concrete decks containing less than 10 % or more than 50 % of delamination.

In another study GPR was able to identify 77 % of the deteriorated areas and the depth of cracking was measured with an accuracy above 80 % (Yehia et al. 2008). This time only 23 % of damaged areas were correctly identified with chain dragging. It should be noting that unlike the previous study, the tested deck was not covered with an asphalt overlay which may explain the deviation in the chain dragging results.

Other research also observed a correlation between GPR amplitudes and corrosion-induced delamination (Pailes et al. 2013). Maser et al. (2012) obtained a correlation of 90,2 % between GPR and HCP, and 79,3 % between GPR and impact-echo. Since the two methods have different purposes (the detection of corrosion for HCP, and cracking for impact-echo), it is suggested that GPR is in reality more capable to locate corrosion than delamination. This assumption is in agreement with the electromagnetic principles that interact with conductivity.

Generally speaking, delamination is usually the cause of an attenuated GPR response. However, the reverse is not always true: weak amplitudes may indicate delamination but also variations in moisture content, or surface distresses. The variety of physical and environmental factors that may dampen the GPR response has been well detailed by Barnes & Trottier (2002).

Moreover, GPR can only detect corrosion-induced delamination, not cracking due to traffic overloading. As in road surveys, the best results are obtained when GPR is complemented by ground-truth and other NDT. These can be half-cell potential or

impact echo in the case of bridge deck condition characterization. The combined use of GPR and Infrared Thermography has also shown to maximize the accuracy of the detection of the deteriorated areas (Maser 2009). The survey approach is the same as for asphalt pavement assessment. The main benefit of GPR is evidently the speed and the continuity of measurements but as pointed out by Gucunski et al. (2010), the emphasis should not be on the comparison of non-destructive methods but rather "on the recognition of the benefits of their complementary use".

3.3. Airfields

Most GPR applications in airfield surveys are similar to road and bridge pavement diagnostics; namely:

- The measurement of airfield pavement thickness
- The detection of subsurface voids and pipes.

Few papers found in this literature search specifically address the topic of airfields. Most of them report the use of GPR together with complementary non-destructive techniques, such as heavy weight deflectometer and road surface profiler.

In 2002, the airport of Athens in Greece was investigated using GPR and infrared thermography (Moropoulou et al. 2002). The purpose of the survey was to detect the presence of defects in asphalt and crushed rock pavements.
The infrared thermography was used to locate cracks and other anomalies based on temperature variations, while GPR was found to be capable of determining the depth and thickness of those defects.

Field testing was also conducted in Canada, at the Meadow Lake airfield (Berthelot et al. 2009). Both the thickness and dielectric permittivity of the structure layers were measured with GPR, with the dielectric permittivity being related to water infiltration. Data were then used to develop a Surface Layer Quality index, which was in turn employed to assess the value of rehabilitation and preservation treatments.

Other literature reports applications of GPR in void detection (Malvar 2010) and utility mapping (Eide et al. 2005).

3.4. Railway

Keeping a good track quality is important for the safety, durability of granular layers and track components, and comfort of passenger trains. The monitoring of the ballast layer is of special importance as this layer takes the toughest loads, and is also subject to the very costly maintenance of ballast cleaning. To use GPR to pinpoint the sections where ballast drainage or ballast cleaning is needed could

optimize cleaning intervals and lead to great functional and economic benefits to the railway system. For the substructure, accumulation of moisture and fines may also cause problems – frost heave and stability issues are some obvious examples of this.

A number of GPR applications can be identified. The most important being the following:

- Identifying the sub-ballast layering and the depth to bedrock
- Assessing the depths to buried objects like culverts, pipes, cables, concrete structures etc.
- Detect fouled and wet ballast. Fouling of the reinforcement layer (sub-ballast layer) and the frost protection layer may also be detected.

3.4.1. Dielectric permittivity measurements

Several studies have been conducted to determine the relative permittivity of ballast materials (**Table 5**). As detailed in section 3.1.1, the value of ε is a prerequisite for the calculation of the ballast thickness. The measurement of ε can also be used to assess the ballast grading and relative moisture content.

In 2001, Clark et al. conducted laboratory experiments to assess the dielectric permittivity of both clean and spent granite ballasts. In this study it was found that ε of the spent ballast was 39 % higher than that of the clean ballast. Likewise, in other studies, the dielectric permittivity of the dry ballasts is lower than that of the wet/saturated ballasts. It is explained by the presence of fouling material in spent ballasts that fills the void space and retain moisture.

Table 5 Published relative dielectric permittivity of ballasts

Ballast material	Dielectric permittivity ε			
	Clark et al. 2001	Sussmann 1999	Leng & Al-Qadi 2009	Gobel Ž.et al. 1994
Dry clean	3	3,6	3,25 (granite) 3,96 (limestone)	2 – 6,25
Moist clean (5 %)	3,5	4		
Saturated clean	26,9			
Dry spent	4,3*	3,7	3,77** (granite) 4,84** (limestone)	6,25 - 14
Moist spent (5 %)	7,8 *	5,1		
Saturated spent	38,5*			

*The spent ballast used in these experiments was at the end of its usable life. The amount of fines has usually reached 10 % of the total mass of the ballast.
**50 % level of fouling, which corresponds to 50 % of air volume that is filled with dry clay

3.4.2. Ballast thickness

The determination of the ballast thickness is based on the reflection of electromagnetic waves, described in section 3.1.1. In comparison with road surveys, relatively fewer studies have investigated the accuracy of GPR in ballast thickness evaluation.

In a study conducted in Switzerland (Hugenschmidt 2000), the authors used a constant pulse velocity of $1{,}4.10^8$ m/s, corresponding to a constant dielectric permittivity of about 4,6. The velocity was calibrated on site and kept constant for economic reasons. The GPR service providers Rail Radar found for its part a layer thickness measurement accuracy of 5 % (Keogh et al. 2006).

An issue that is encountered in ballast thickness determination is the poor quality of the ballast/subgrade interface. As time goes by, the reflection of the top subgrade layer tends to weaken and become shallower. This is partly due to the migration of fines and clay from the subgrade that makes the interface blurred and not easily detected. To remedy this, Carpenter et al. (2004) developed a special geotextile called Terram PW5 that contains stripes of conductive materials. The main benefit of these conductive capsules is to remotely confirm the presence of the geotextile after construction. It is also utilized to ease and improve the measurement of the

depth to the subgrade, at any time after the construction. Under laboratory conditions, the error in depth measurement was found to be less than 1 %.

Table 6 Reported ballast thickness accuracy in the literature

	Antenna	Frequency	Technique	Accuracy
Keogh et al. 2006	Rail Radar ™, ground-coupled multi-channel array	Unknown	Common Mid-Point (CMP)	5 %
Carpenter et al. 2004	PulseEKKO 1000 bi-static	900 MHz and 1.2 GHz	Curve fitting + geotextile	1 %
Hugenschmidt 2000	GSSI air-coupled horn antenna	900 MHz	Standard value of ε	4 cm*

*The total ballast bed thickness is unknown.

3.4.3. Object identification

One of the most straightforward GPR applications is the detection of subsurface objects. Features in the ground create a disruption in the GPR signal that is interpreted by the analyst. The identification of the detected objects is primarily based on experience and comparison with ground-truth data. Some examples of detected features in railway ballasts are shown below.

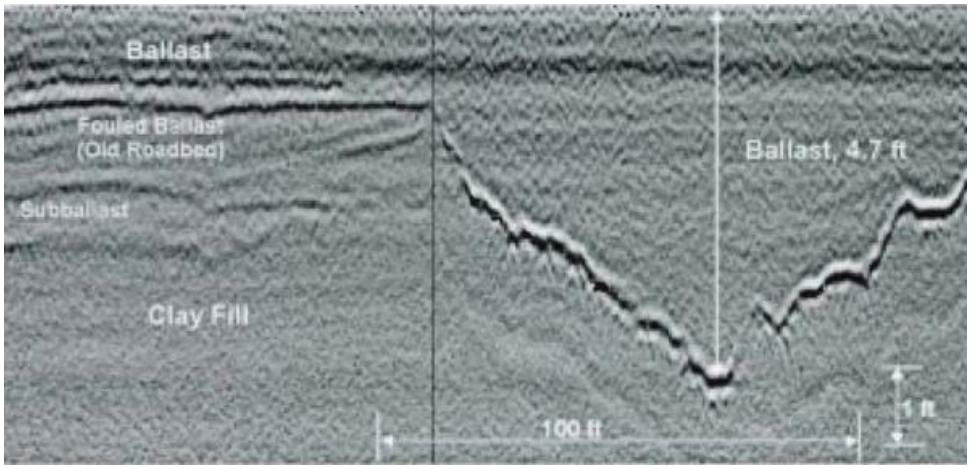

Figure 13 Deep V-Shaped Ballast Trench (Hyslig et al. 2005)

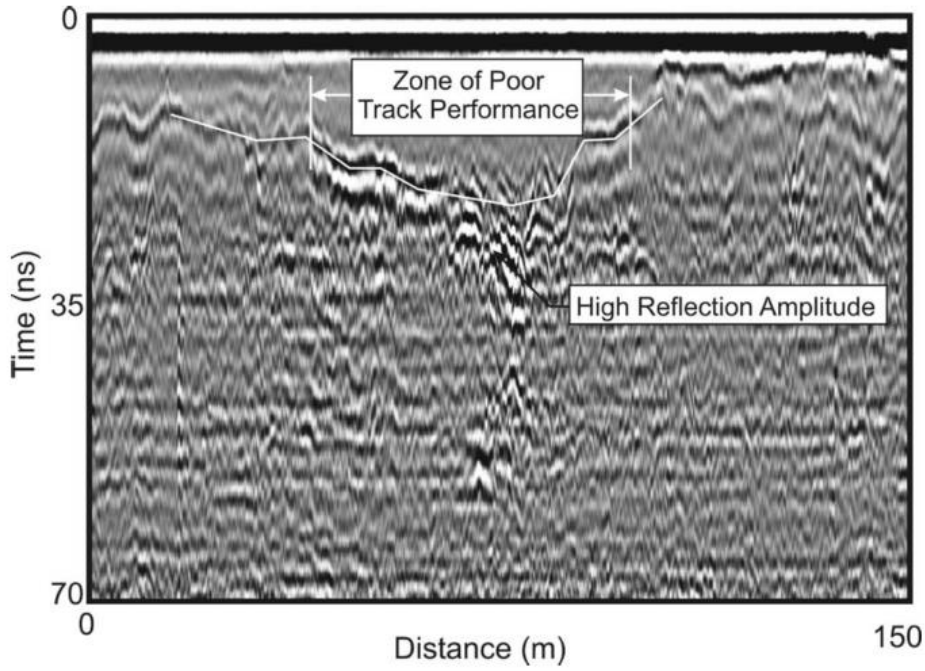

Figure 14 Track settlement (Sussmann et al. 2003)

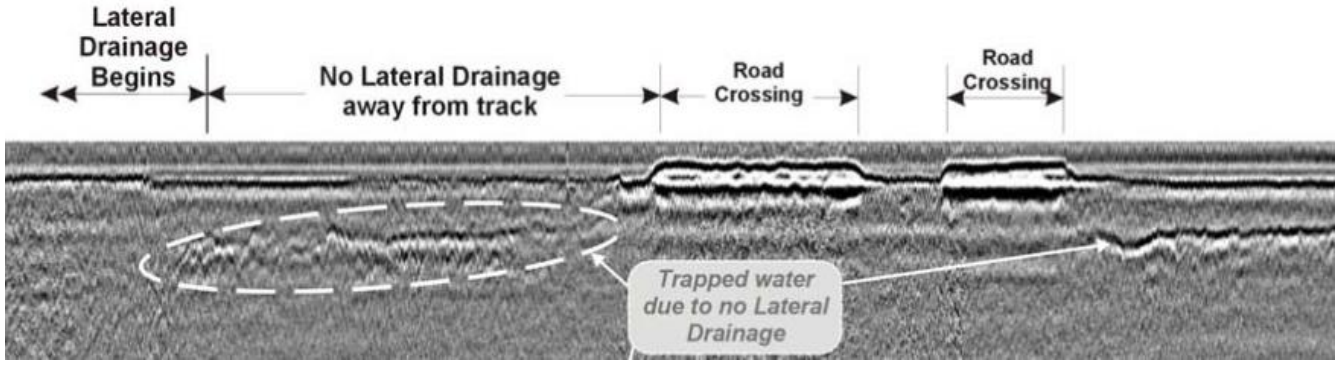

Figure 15 Detection of trapped water (Hyslig et al. 2005)

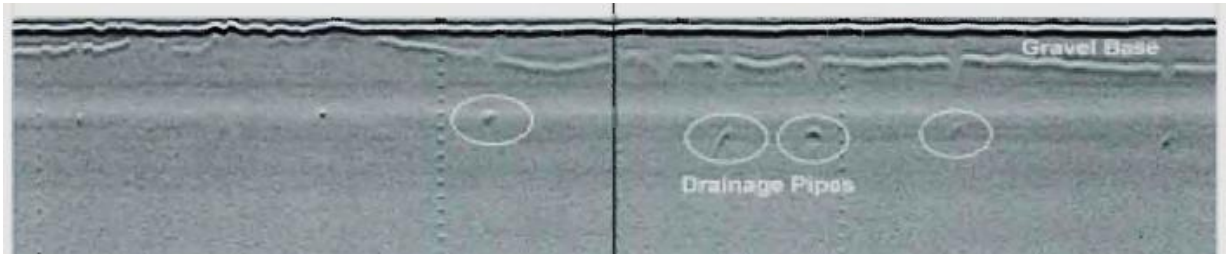

Figure 16 Detection of utilities (Hyslig et al. 2005)

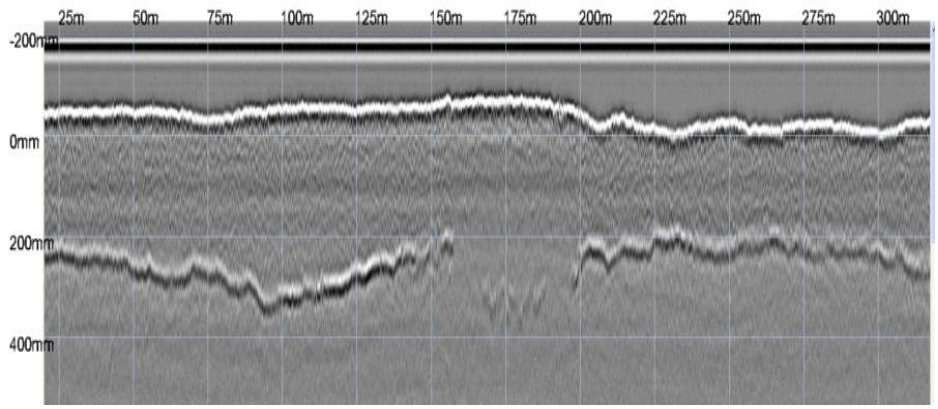

Figure 17 Anomalous track-bed profile (Q. Zhang et al. 2010)

3.4.4. Ballast fouling

GPR has successfully been used in ballast condition assessment. Over time, the ballast is fouled by the deterioration of aggregates under rail traffic loads and maintenance action. Air voids are progressively filled with fines and crushed aggregates. The difference between clean and spent ballasts can often be seen on a radar profile, as illustrated in **Figure 18**. Typically spent layers have a more heterogeneous texture (space between top and base of ballast) than clean ballast. However, advanced techniques are necessary to quantitatively estimate the ballast condition.

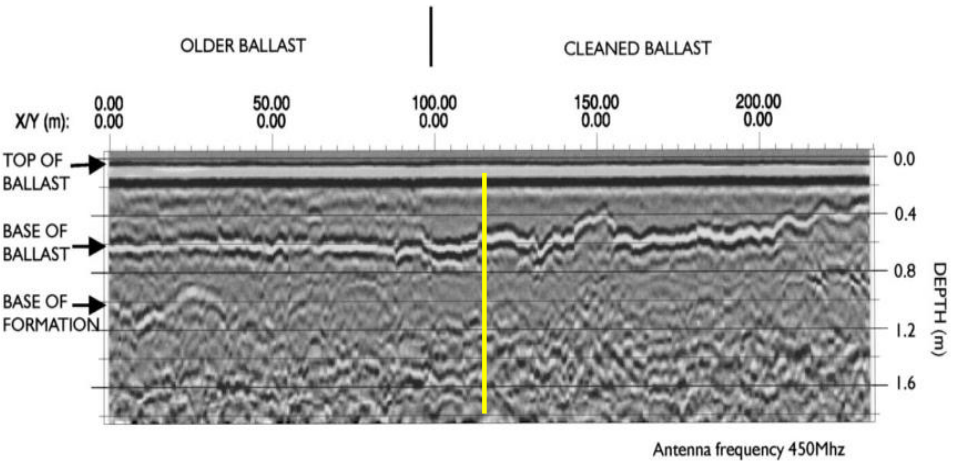

Figure 18 GPR profile of a spent/clean ballast (Jack & Jackson 1999)

3.4.4.1. Wave velocity method

One non-destructive evaluation technique to assess ballast contamination is to establish a relationship between the dielectric permittivity of the ballast, and the degree of fouling. Indeed, the dielectric permittivity of a composite material (aggregate, void and water in the case of ballast) can be seen as the sum of the dielectric permittivity of each constituent (**Eq. 17**):

$$\varepsilon_r = \sum (V_n . \varepsilon_n) \qquad (Eq. 17)$$

Where:
ε_r is the dielectric permittivity of the ballast
ε_n is the dielectric permittivity of each constituent (aggregate, water, void)
V_n is the volumetric ratio of each constituent

Thus a decrease in the void space (the ballast changes from a clean to a fouled condition) results in an increase in the dielectric permittivity and a decrease in the wave velocity. The dielectric properties are then correlated to ballast samples sieve analysis and charts can be established.

This technique requires using a GPR system that is able to provide accurate and continuous material properties. This is the case of the Rail Radar ™ (Keogh et al. 2006), a multi-channel ground-coupled antenna that collects data using the CMP method (section 3.1.1.1). In cooperation with the Canadian National Railway, Rail Radar ™ claims to successfully establish ballast assessments and ballast condition overlay plan maps based on velocity thresholds. However, the speed of survey is limited to 40 km/h.

3.4.4.2. Scattering information of void space

Another approach is to consider the scattering of the EM waves from the voids in ballast. As explained by Al-Qadi et al. (2008), aggregates and air voids are much larger in ballasts than in asphalt pavements, and ballasts cannot be considered as homogenous. When using high-frequency antennas, the wavelengths approach the size of the voids (**Eq. 4**). The scattering response then becomes predominant and is indicative of the degree of contamination: the scattering is strong in clean ballasts with large voids, while it is barely noticeable in fouled ballast (filled voids). On radargrams, this corresponds respectively to a "rough" and smooth scattering texture.

The scattering response and its use seem to be optimal at a frequency of 2 GHz. Below, the wavelengths are too long and the void scattering is not discernable (Roberts et al. 2006); above, the depth of penetration is too superficial. De Bold et

al. (2009) reported contradictory results, with high scattering response for low frequency antennas. However, the type of antenna was different from the ones used in the studies cited above.

Roberts et al. (2009) further developed the method and assigned threshold levels to the scattering amplitude envelops, corresponding to different degrees of fouling (**Figure 19**). The technique has successfully been tested on more than 614 km of track in Colorado, Wyoming and Alaska. GPR generally showed a very good correlation with ground-truth data.

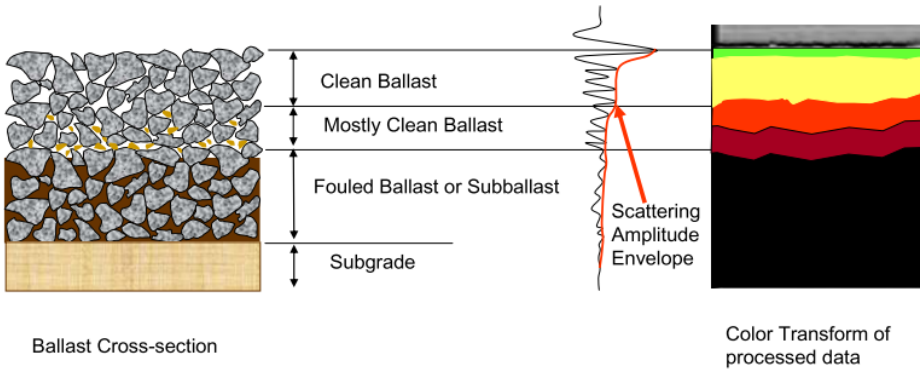

Figure 19 Construction of scattering amplitude envelops from GPR data (Roberts et al. 2009)

3.4.4.3. Others approaches

The scattering method described above has some shortcomings: threshold levels are empirically determined, and do not take into account that fouling may gradually vary with depth. To overcome these limitations, other signal processing techniques can be used, such as the Short-Term Fourier Transform (Al-Qadi et al. 2010) and continuous wavelet transforms (Shangguan et al. 2012). These approaches need further studies to be more accurate, but they have the great advantage to estimate the fouling condition gradually over depth, i.e. without a clear interface between clean and fouled ballasts.

Shangguan et al. performed a wavelet analysis and calculated the standard deviation of the signal fluctuation. As the same locations, field samples were collected and sieved in laboratory. The fouling index was calculated as follows:

$$F_1 = P_4 + P_{200}$$

Where:
F_1 is the fouling index
P_4 is the weight percentage of particles passing the 4,75 mm (no. 4) sieve
P200 is the percentage of fine particles passing the 0.075-mm (No. 200) sieve

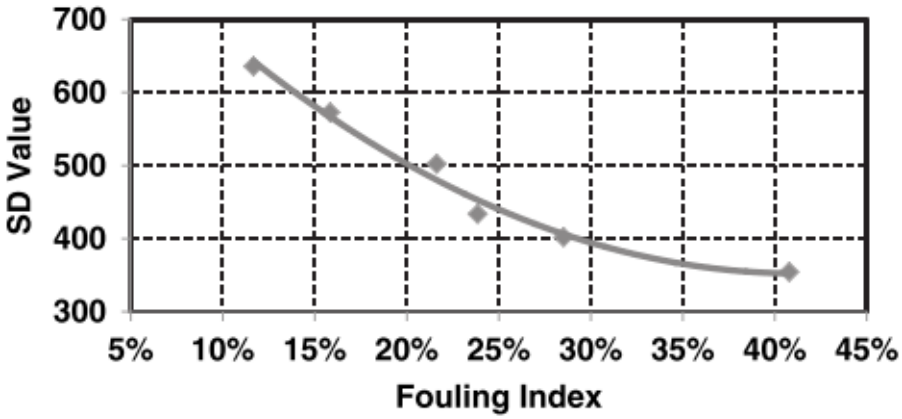

Figure 20 Standard deviations values for different fouling indices (Shangguan et al. 2012)

The calculated standard deviation (SD) of the GPR signal fluctuation was plotted against the Fouling Index determined from field sampling and field analysis. As can be seen in **Figure 20** the standard deviation value decreases when the fouling index increases, i.e. when the scattering effect diminishes due to less void space. From these results the following regression relation was determined:

$$F_1 = 3{,}043 \times 10^{-6} \times SD^2 - 3{,}924 \times 10^{-3} \times SD + 1{,}394$$

The coefficient of correlation R^2 is 0,95 and the standard error of estimation is 0,02, which means there is a good correlation between the fouling index and the calculated standard deviation of the signal fluctuation. These results show a great potential of the wavelet technique to assess ballast fouling levels.

3.4.5. Maximum speed of measurement

Ideally GPR surveys should be conducted at a high speed (around 80 km/h) to be time saving and cost-effective. Ground-coupled antennas, which are in direct contact with the ground, must be dragged along the surface at a walking pace. However, high-speed monitoring of railway track-bed is possible with air-coupled antennas (20 – 50 cm above the surface).

The speed at which a GPR survey can be conducted depends on several factors (Clark et al. 2004):

- The rate at which GPR emits pulses
- The number of channels/antennas
- The number of voltage samples per scan
- The type of Distance Measurement Instrument (DMI) that is used.

The number of scans per meter (scans/m) that a GPR system is able to produce determines the maximum speed of measurement. This rate of sending radar pulses can be controlled in two different ways:

1. In free-wheel measurements (no DMI), the radar system emits pulses as selected in the settings. GPR are typically able to produce from 2 to 400 scans per second (scans/s). The number of scans per meter (scans/m) depends therefore on the velocity of survey:

$$Scans/m = \frac{Scans/s}{Speed\ of\ survey\ (m/s)}$$

   The problem with this method is that it does not consider changes in the speed of survey, in case of obstacle on the track-bed for example. The number of scans/m is not constant but depends on how fast the survey is conducted.

2. It is recommended to use a survey wheel in order to obtain a uniform horizontal scale. When measuring with a DMI, the number of scans/m selected in the settings is kept constant. That means that the radar produces pulses only depending on the speed of survey. It does not emit signal when at a standstill. In that case the number of scans per m is defines as:

$$Scans/m = \frac{1}{t \times speed\ of\ survey}$$

   With,

   t = time to produce one scan

$$= \left(\frac{1}{\text{Transmit rate}} \times \text{Samples per scan}\right) \times \text{Nb. of antennas}$$

In their study, Clark et al. (2004) determined the speed of survey at which two radar systems (SIR-10H and SIR-20) could still emit a pulse every 14 cm. Both the free wheel and the DMI methods were considered.

From the settings listed in **Table 7**, it was found out that the maximum survey speed is 80 km/h for the SIR-10H and 250 km/h for the SIR-20.

Table 7 GPR systems settings

GPR Model (GSSI)	Transmit rate	Samples/scan	Scans/s	Max. survey speed (km/h)
SIR-10H	200 kHz	512	160	80
SIR-20	500 kHz	512	500	250

3.4.6. Track modulus measurements

The track modulus is an important parameter that describes the bearing capacity of the track-bed. The standard track modulus measurements (e.g. Falling Weight Deflectomer test) are typically labor intensive and time consuming, and it was investigated whether the track modulus could be obtained from GPR data.

In 1995 Saarenketo & Scullion identified a possible relationship between the dielectric permittivity, the conductivity and the CBR value. The materials tested were base course aggregates. Based on this strong correlation between the dielectric properties and the strength of the track, Narayanan et al. developed in 2004 a multivariate linear regression model. This model aims to correlate the GPR signal voltage to ground-truth measurements. Preliminary results showed that the model was able to predict low track modulus within 3,4 MPa, after correction (**Figure 21**). The method is presented as time-saving and non-invasive. However, the authors underline that it is still dependent on a significant number of ground-truth measurements.

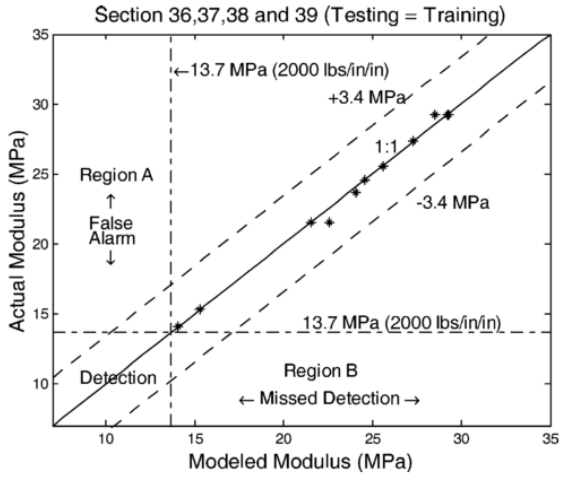

Figure 21 Comparison of modelled and measured track modulus (Narayanan et al. 2004)

3.4.7. Norwegian studies

In 2001, a pilot study was conducted by SINTEF/NTNU to assess the feasibility of GPR to determine the ballast layer thickness (Eide et al. 2001). An antenna array operating in the frequency range 100 MHz – 1 GHz/1,6 GHz was mounted on a Robel (**Figure 22**).

Figure 22 Antenna array mounted on a Robel

Four locations were tested in the vicinity of Trondheim, with different subsurface conditions and types of sleepers (concrete or timber). Some measurements were especially made in a railway tunnel to study the effects of the tunnel's walls and roof. The GPR measurements gave satisfactory results. It was in most cases possible to detect the subgrade layer, even if the data were sometimes disturbed by timber sleepers. Indeed, timber sleepers produced much stronger reflections than concrete sleepers, even if these were reinforced. The hypothesis is that timber absorbs a significant amount of moisture, and has therefore a high dielectric permittivity. The study also concluded that the tunnel's walls and roof did not interfere with the GPR data.

3.5. Tunneling

Tunnels deteriorate mostly because of water leakages. The flow of water coming from the soil leads to cracks in the concrete lining, corrosion damage of steel reinforcement and concrete spalling. Although it is not always possible to directly locate the source and volume of water, leakages can be revealed by monitoring damages in concrete walls. The tunnel environment being dark, confined and busy, the inspection procedure has to be quick. In that context, there is naturally a particular focus on non-destructive technologies.

The most sensitive structure is the concrete lining, which ensures the water tightness and which may also acts as a rock support. As for bridge decks surveys, impact echo, impulse response, infrared thermography are some examples of NDT that are typically used for the assessment of the concrete condition. A review of their applications can be found in Delatte et al. (2003) and Wimsatt et al. (2012).

With regards to GPR, most papers found in the literature review relate to the thickness and quality of:

- The inner lining
- The backfill grouting

3.5.1. Inner lining

The thickness of the concrete lining is generally known, as it is usually made of prefabricated elements. However it is sometimes so deteriorated that the thickness is not constant anymore, and the mechanical strength is compromised. This situation was encountered in the Mont-Blanc tunnel, after the deadly fire that occurred in 1999 (Abraham & Dérobert 2003). To evaluate the extent of the damages, cores were taken from the inner lining and it was discovered that the fire had significantly decreased the elastic and shear moduli of the concrete. Seismic refraction and Ground Penetrating Radar measurements were then conducted to get

a larger picture of the condition of the lining, with no discontinuity. The GPR data revealed that the fire had created cracks, and changed the electromagnetic properties of the concrete. On radargrams the inner lining appears as heterogeneous instead on homogenous, and several intermediary layers are detected. The total concrete thickness varies from 0,4 to 0,6 m in heavily deteriorated zones, which is in agreement with the results obtained with the seismic method. The benefits of the NDT surveys are so compelling that is concluded in the paper that cores "may not be representative of a very wide vicinity and that any interpolation between them is definitely not valid".

Other studies were conducted to evaluate the condition of the concrete. Reinforcement mesh and other steel components are generally speaking the most easily detected elements and several studies reported positive results (White et al. 2013a; White et al. 2013b). Bosela et al. (2006) also checked the ability of GPR to locate steel reinforcement, but considered the data interpretation as somewhat subjective for the detection of delamination.

In a study performed under SHRP2, Wimsatt et al. (2012) obtained more favorable results. Several NDT technologies were tested for the identification of moisture, voids and corrosion of tunnel linings. GPR used in this research work were a 1 GHz air-coupled and a 900 MHz ground-coupled system.

On specimens with simulated delamination (concrete slabs), it was concluded that neither the air-coupled nor the ground-coupled antenna could efficiently detect delamination. It is supposed that the size of the voids and moisture area were not significant enough to be discernable. However in field testing, air-coupled horn antennas "provided good quality structural information" about the inner lining. The authors finally recommend conducting air-coupled GPR measurements to identify areas of low dielectric properties. Such areas can further be investigated using ground-coupled antennas, which allow for a better penetration.

More broadly, Parkinson & Ekes (2008) investigated the ability of GPR to detect, among others, concrete honeycomb, embedded wooden timbers, liner-rock contact, and voids empty or filled with water. They claim good results in all cases.

3.5.2. Backfill grouting

To reinforce the tunnel structure, grout mortar is commonly injected between the inner lining and the bedrock. Although the quantity and pressure of grout are regulated by standards, the quality of the injection is not always straightforward and some gaps may remain unfilled.

GPR has recently been used with the purpose to verify the homogeneity of the backfill grouting layer. Xie et al. (2007) tested the method in Shanghai, China. The measurements were conducted using a ground-coupled antenna with a frequency

of 200 MHZ to be able to see through the inner lining and reinforcement steels. Because the water content varies a lot during the curing time, the dielectric permittivity was deduced from a known point at the time of the measurements and no standard value from the literature was used. The survey appeared to be successful, as depicted on **Figure 23**.

Few years later the same authors expanded their research to 250 MHz, 500 MHz and 1 GHz frequencies. The tests also showed satisfactory results, with the 500 MHz GPR system giving the most promising results (Zhang et al. 2010). Further on this topic, Karlovšek et al. (2012) studied the feasibility of GPR to detect voids at 400 MHz, 1 GHz and 1,5 GHz frequencies, and also reported encouraging results.

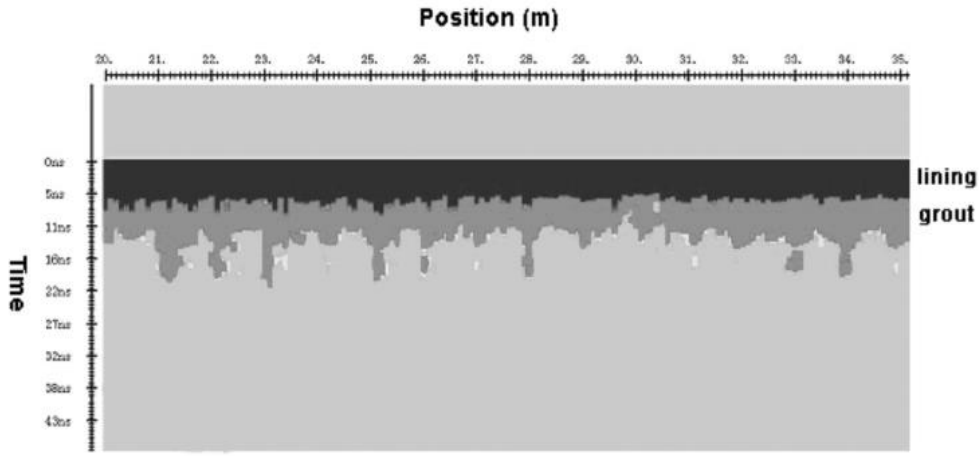

Figure 23 Grout behind concrete lining

Chapter 4

Experimental work and results

This chapter describes the field experiments conducted in this PhD study, and results that have been found. Detailed descriptions and discussions can also be found in the papers attached.

4.1. Data collection

4.1.1. Equipment

GPR data were collected at different sites in Norway and USA. Several types of GPR systems/antennas were used during the course of the research work (**Table 8**), all produced by either 3d-Radar AS or Geophysical Survey Systems Inc (GSSI).

3d-Radar is a Norwegian company established in 2001 in Trondheim. Their main products are the GeoScope GPR unit and the interpretation software Examiner. The system operates by transmitting stepped frequency waves at a frequency of 200 MHz - 3 GHz, to provide both good penetration and high resolution. The antennas used during the GPR surveys were mainly the V2429 and V0605 models, with the 2005 version GeoScope unit. More details about the technical specifications of the equipment can be provided on request by the manufacturer.

GSSI is an American company formed in 1970 and is one of the world leader in the development of Ground Penetrating Radars. They produce a wide range of devices, from horn to multi-channel antennas operating at a variety of frequencies. The devices used in the study were horn and ground-coupled antennas along with the SIR-20 unit. They also developed the RADAN interpretation software.

These GPR systems differ in their technology, benefits and limitations (section 2.3). However, when appropriately used and in good conditions, they have shown to be

similarly reliable and accurate. This was demonstrated in a comparative study conducted in Finland by Roadscanners, where several GPR systems (including the ones used in this doctoral study) were tested on the same road section (Maijala & Herronen 2011).

Table 8 List of equipment used in the doctoral work

<table>
<tr><th></th><th>Manufacturer</th><th>GPR units</th><th>Antenna</th><th>Frequency</th><th colspan="2">Software</th></tr>
<tr><td>1</td><td rowspan="3">3d-Radar AS</td><td rowspan="3">Step-frequency</td><td rowspan="2">Array 2,4 m</td><td>200 MHz – 2 GHz</td><td rowspan="3">Examiner</td><td rowspan="8">Road Doctor</td></tr>
<tr><td>2</td><td rowspan="2">200 MHz – 3 GHz</td></tr>
<tr><td>3</td><td>Array 0,6 m</td></tr>
<tr><td>4</td><td rowspan="5">GSSI</td><td rowspan="5">SIR-20</td><td rowspan="2">AC Horn</td><td>1 GHz</td><td rowspan="5">RADAN</td></tr>
<tr><td>5</td><td>2 GHz</td></tr>
<tr><td>6</td><td rowspan="3">GC</td><td>400 MHz</td></tr>
<tr><td>7</td><td>1,5 GHz</td></tr>
<tr><td>8</td><td>2,6 GHz</td></tr>
</table>

4.1.2. Test sites

Most GPR tests were performed in Norway on road sections and tunnels relevant to the given research questions (**Table 9**). The study of Paper I and V were conducted in laboratory, while the GPR testing of Paper VII was performed at a specially constructed concrete wall at the pavement test facility MnROAD, Minnesota, USA. More details about the field and laboratory studies can be found in the papers.

Table 9 Test locations

Paper	*Topic*	*Test location*
I	Salt	Laboratory
II, VI	Accuracy	Trøndelag, Norway
III	Tunnel	Trøndelag, Norway
IV	Airfields	Troms, Norway
V	Salt	Laboratory
VII	Tunnel	MnROAD
-	Frost heave	Trøndelag, Norway
-	Calibration	MnROAD

4.1.3. Methodology

Before any GPR survey, a feasibility study has to be conducted to assess whether the project is technically possible and to uncover any potential source of limitations.

This implies to gather as much information as possible regarding the target's depth, geometry and nature, the surrounding material and the complexity of the structure. Other parameters such as the accessibility of the test site, the amount of traffic, the time slot to conduct the survey, the weather or any possible interference with existing equipment must also be considered.

From there, the type of GPR system can be decided, as well as the operating frequency. The choice is made according to the advantages and weaknesses of each. When data have been collected (with location referencing – DMI, GPS), they can be processed using an interpretation software. The data is filtered (background removal, noise and interference filtering), the time-zero is set, the positioning corrected and the gain can be modified to increase the contrast at a certain depth. Finally, the wave travel time is converted to depth using a calculated (horn-antenna), measured (Percometer) or assessed dielectric permittivity.

The figure (**Figure 24**) below illustrates the effect of data processing on raw GPR data:

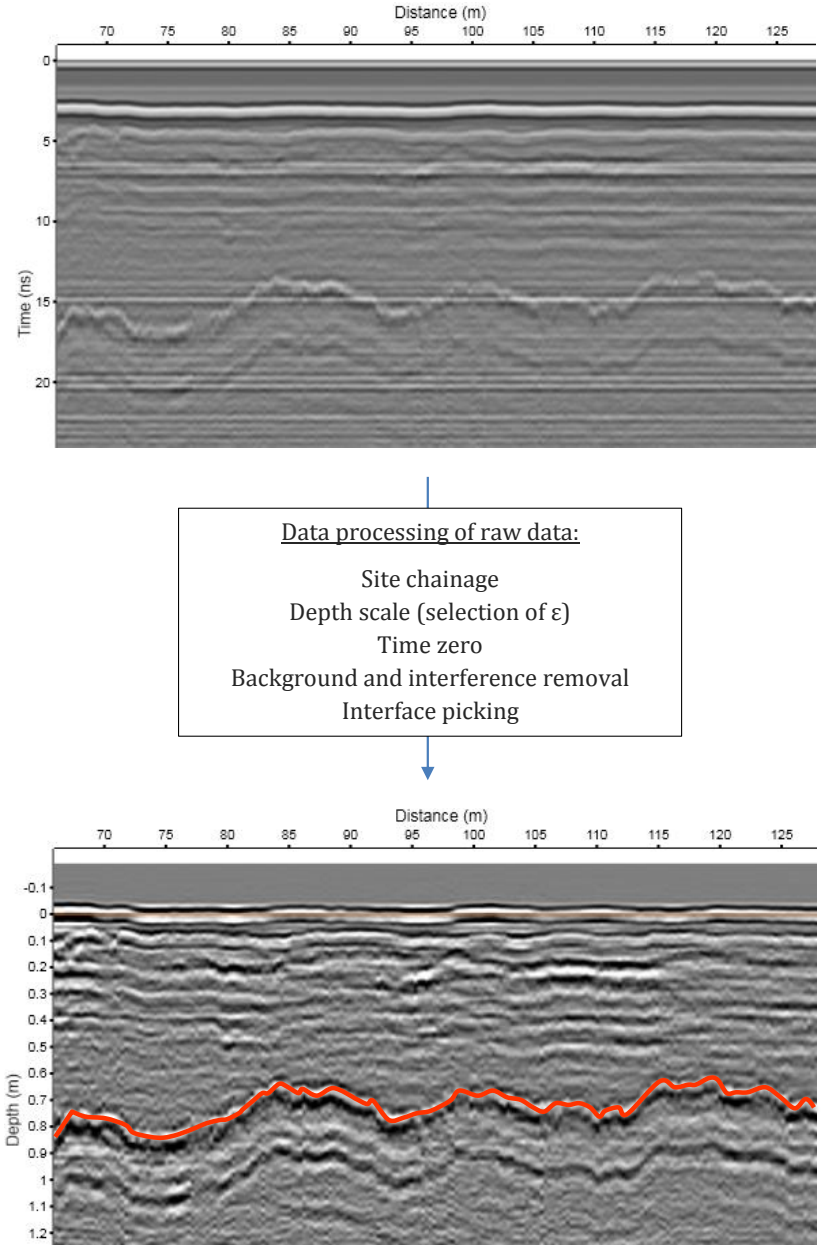

Figure 24 Data processing of raw data

4.2. Research results

4.2.1. Accuracy of the 3d-Geoscope GPR (Papers II and VI)

Much importance has been given throughout this PhD work to the accuracy of GPR systems. Regular discussions and questions from customers and NPRA personal have underlined the necessity to gauge the accuracy of the measurements and the value of the results. A high accuracy is obviously essential and has to be achieved, especially in QA/QC surveys and project-level analyses. A study conducted in 2009 (K. R. Maser & Pucinelli) on US states showed that most states verify GPR data with ground-truth and feel comfortable with an accuracy of 90 % and over. However, still a few states do not considerate the technology as accurate enough.

As described in section 3.1.1, significant effort has been devoted worldwide to determine the accuracy of GPR data for the pavement thickness evaluation. The GPR error usually varies between 2 and 10 % (**Table 4**), but very few studies were carried out using a step-frequency 3d-GeoScope system.

The first step was therefore to evaluate the accuracy of the 3d-GeoScope system, the main GPR available in Norway. The data collection took place in Trondheim, Norway. A road section was scanned using both the 200 MHz – 2 GHz and 200 MHz – 3 GHz antennas and cores were taken. After calibration on a single core, the GPR error were found to be 3,6 % for the 200 MHz – 2 GHz antenna, and 3,3 % for the antenna operating at 200 MHz – 3 GHz. Comparatively, a study conducted some years later by other researchers using the same type of GPR and calibration method, obtained an similar error of 3,9 % between GPR measurements and ground-truth (Edwards & Mason 2011). It was thus concluded from the Norwegian study that the 3d-GeoScope GPR could provide data of sufficient quality and accuracy.

It was then observed after regular use of GPR that the way to interpret the data could impact on the overall accuracy. Indeed, the interface that separates the pavement layers may be clear and sharp, or poorly defined and wide. In that case, picking the center of the interface is not easily done, be it manually or automatically. A study was conducted to attempt to evaluate the impact of semi-automatic layer tracking vs. manual interface selection on the accuracy of GPR data in pavement thickness assessment (**Paper VI**). It was found that even small deviation of the tracking from the middle of the interface could result in considerable GPR errors (almost 20 % in the studied case instead of 3,6 %). Whenever possible, manually tracking should be used.

4.2.2. Salt concentration on winter roads (Papers I and V)

Cold regions require specific winter maintenance activities to maintain the integrity and safety of the transportation infrastructure. Significant research has

been conducted the past years to further understand deicing mechanisms and improve serviceability under winter conditions (Thordarson 2002; Klein-Paste 2007; Ikiz 2008; Lysbakken 2013).

As in many other countries, salt is the most common deicer in Norway. Although it offers significant advantages (effectivity at a relatively low cost), it is also harmful to the environment and its use must be limited. In 2013, the NPRA started the research program Salt SMART to examine ways to optimize anti- and deicing strategies, and salt consumption (Sivertsen et al. 2012). In 2014, 188 000 tons of salt were spread on Norwegian roads against 238 000 tons in 2011 (Sivertsen & Ofstad 2014).

An approach to reduce salt consumption is to determine the amount of remaining salt from previous spreading. The device SOBO-20 is currently the main method available to achieve surface measurements. While convenient, the accuracy of the instrument had never been investigated before 2013 (**Paper V**) and only provides point measurements.

It was hypothesized at an early stage of the research work that GPR could be used as an assisting method to calculate the quantity of remaining salt on road surfaces. The first testing (**Paper I**) was conducted in laboratory, at NTNU. The objective was to determine if variations in amount of salt could reflect in GPR reflection amplitudes.

Both dry, pre-wetted and dissolved salt particles (saturated brine) were placed on an asphalt sample, and scanned with the SF GPR. Details about the experimental set-up can be found in **Paper I**. As expected, no variation in GPR amplitude was detected as the amount of dry salt increased. Dry salt, just as glass, does not have sufficient contrasts in dielectric properties with air. However, a strong correlation between GPR first amplitudes and the concentration of brine was found. The method could potentially lead to a promising, innovative solution for salt measurements. The inability of GPR to see through conductive materials could be used as an advantage.

These promising results initiated a number of field experiments around Norway, unfortunately all unsuccessful. Problems were encountered when converting salt concentration to salt quantity. Shortly after salt spreading, SOBO-20 measurements were conducted and the pavement was scanned with GPR. However, the two devices systematically gave contradictory results and no correlation could be found.

Several possible factors of influence were identified:

- The accuracy of SOBO-20 itself,
- The evaporation process, noticeable even at moderate temperatures (12 °C)
- The brine flowing off the road

In an attempt to go further with the field testing, the accuracy of SOBO-20 was investigated. The testing finally concluded that the device was very accurate (**Paper V**). After that possibility was eliminated, the subject of the water retention of pavements was addressed (report not included in this document). The project, conducted at MnROAD, showed that the pavement texture plays a significant role in water retention and consequently impacts SOBO-20 readings. Although trapped salt cannot be detected neither by SOBO-20 nor by GPR, flowing water represents an obstacle during field testing since GPR and SOBO-20 measurements cannot be conducted at the exact same time.

It was not possible to investigate further this topic since other parts of this PhD project had to be completed. Nevertheless, it is hoped that the research done on salt constitutes a good basis for further work. Many obstacles could be overcome by conducting the field testing on a pavement test track, free from traffic and shielded.

4.2.3. Tunnel safety (Papers III and VII)

The application of GPR in tunnel inspection was determined through considerable field investigations. The feasibility of six GPR systems were assessed in:

- Remotely mapping the cavity behind concrete linings
- Detecting rock instability and loose rocks that have fallen from the roof.

Results presented in **Paper III** show that it is possible to detect the free space between the concrete lining and the rock surface using the SF GPR. Measurements turned out to be relatively convenient to perform thanks to the system setup designed at NTNU/SINTEF. There are numerous objects along a tunnel's wall (extinguisher, emergency telephones, road signs) that must be avoided and the antenna can easily be lifted. However, measurements must be performed at night to not impede the traffic, and data collection is done at relatively slow speeds (≈ 5 – 7 km/h). Linings made of lightweight concrete with expanded clay aggregates also strongly attenuate and disperse the radar signal. Otherwise, the technique was implemented with success in several tunnels of Norway.

Regarding rock instability, rocks that have fallen from the roof are in direct contact with the concrete lining. The object of the evaluation was to determine whether the rock/concrete interface could be detected in an effective manner. Rock and concrete have similar dielectric values, and previous experience from void mapping indicated that the two materials were not easy to distinguish from each other.

Due to the uncertainty of the outcome and to conduct a more comprehensive study, a concrete wall was built at MnROAD. Rocks of different sizes were placed behind the wall and GPR measurements were performed. The results of the project (**Paper VII**) showed that in most cases the interface concrete/rock could not be detected.

However the interface rock/air resulted in a hyperbola signature, which can be used in the interpretation of GPR images. Ground-coupled antennas used at high frequencies produced the clearest response.

Further research could explore the accuracy and cost benefits of using ground-coupled GPR systems. It is thought that the use of GPR could bring significant benefits to tunnel maintenance, especially in Norway where a large number of tunnels have been constructed and that are now in need of preventive maintenance.

4.2.4. Airfields

Paper IV presents the Norwegian experience in airfield inspection using GPR and FWD. The backcalculation of layer materials' moduli has already been described in the literature (section 3.1.8), but research mostly relates to asphalt pavements.

The project took place at the military airport of Bardufoss, Norway. The initial objective was to calculate the PCN value of the runway. However, due to the apparent heterogeneity of the structure and lack of documentation, it was decided to carry out GPR measurements.

The GPR data first helped determine the overall structural condition. It was discovered that some sections were made of concrete (reinforced or not), some of asphalt, and some others consisted of asphalt over concrete. Knowing the type of material below the surface then helped the analyst interpret the value of E-moduli obtained from backcalculation of FWD data.

A critical eye is necessary to ensure quality data. However, GPR scanning conducted prior to FWD measurements can help understand suspicious variations in E-moduli and detect anomalies in the ground. GPR is not currently very much employed on airfields, although on a larger scale it could greatly improve the efficiency and effectivity of maintenance activities.

4.2.5. Frost depth and ice lenses

Norwegian infrastructures suffer from cold climate and strong seasonal changes, especially roads. The bearing capacity of pavement structures can vary significantly from freeze and thaw cycles and is at its lowest in spring, when moisture increases in the soil. The knowledge of frost penetration is therefore important for pavement design and rehabilitation activities.

The 3d-GeoScope has been tested with success in the detection of frost under the pavement surface (**Figure 25**). Measurements conducted at different times of the year (autumn, winter, spring) show the evolution of the frost line over time. The three-dimensional subsurface images are undeniably an advantage, since cross-profiles views can be produced. As can be seen on **Figure 26**, the frost front curves up when approaching roadsides. This is caused by the presence of a thick layer of

snow (about 1 m) on the sides, which has an insulation effect and slows down the propagation of frost in the ground.

Another process associated with frost is the formation of ice lenses in frost-susceptible soils, and frost heave. Heaving of the roadbeds complicates maintenance work and regularly raises poor performance and safety concerns (Øvstedal et al. 2012).

A series of GPR measurements was carried out with the aim to detect ice lenses. The surveys were often compounded by the presence of deicers in winter. Features could be detected, but it was not always possible to tell their nature. Due to their size, they could possibly be ice lenses, rocks or any other objects. Sometimes a phase inversion of the radar signal was observed (white/black/white instead of black/white/black), indicating that the reflection was caused by a material of lower dielectric permittivity. Still, the best way to confirm or invalidate the presence of ice lenses was to conduct the same GPR measurements in summer. By comparing two sets of data it often turned out that most objects detected in winter disappeared in summer, suggesting that they were indeed ice lenses.

Figure 27 gives an example of GPR measurements conducted both in summer and winter. The investigation took place in Malvik, Norway, on a county road with a pronounced depression of ≈ 3 m long and ≈ 40 cm deep. It was not known if the difference of level was due to a settlement of the 3 m long section or a heaving of the entire pavement. After investigation, it was found that the depressed area corresponded to a stone-filled trench with pipes in place. Objects were also detected in the base layer on either side of the trench. However they were no longer visible in summer, suggesting that they were ice lenses in a frost-susceptible soil, contributing to frost heave.

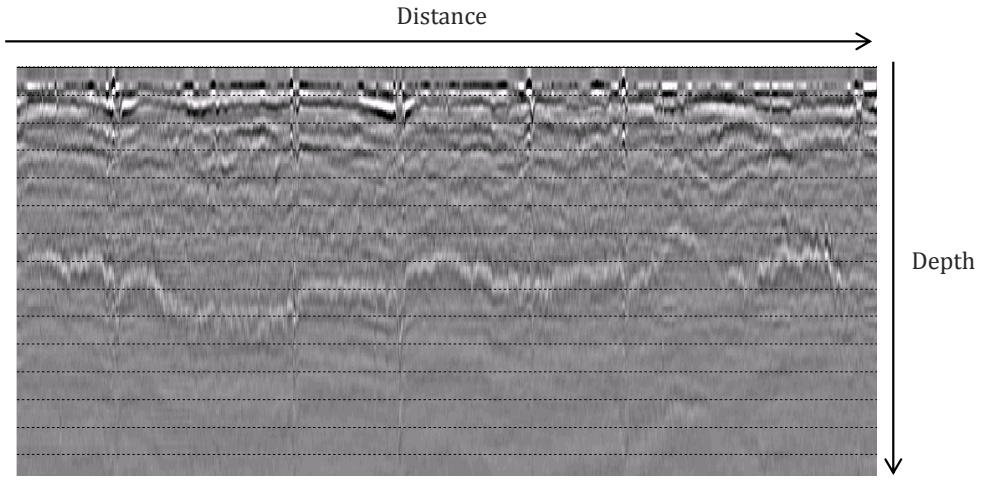

Figure 25 Frost line, longitudinal view

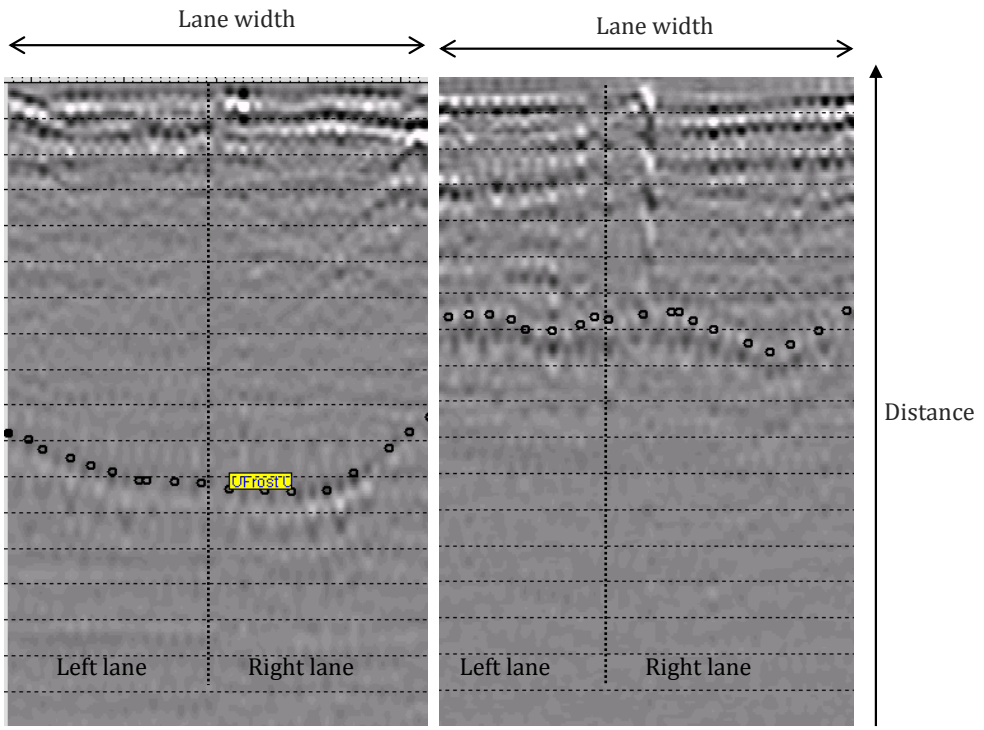

Figure 26 Frost line, cross profiles – winter (left), spring (right)

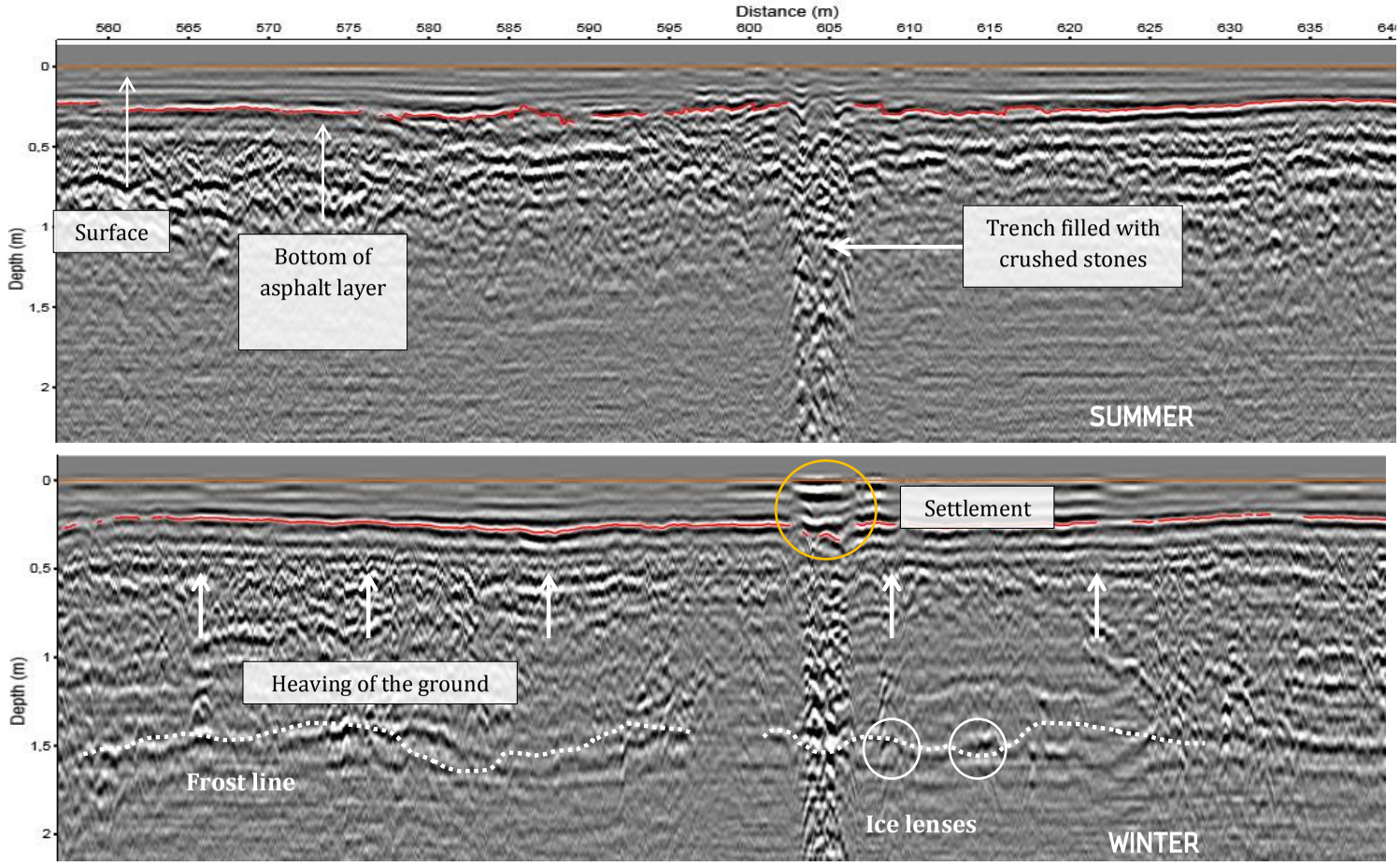

Figure 27 Frost line and ice lenses

4.2.6. Costs

This PhD work started, but also ended with a study on GPR accuracy for pavement layer thickness determination. After the intrinsic reliability of the system had been demonstrated (**Paper II**) and areas of applications investigated (**Papers I – VI**), questions around the financial advantages of GPR were raised. This is the subject of **Appendix A**, which is for now a draft report, but in which issues about the tradeoff between GPR accuracy and costs are addressed.

On the basis that QA/QC of new construction will further be performed in Norway and that the accuracy of measurements must be very high, the question regarding "how many calibration cores are enough?" can be posed. To the knowledge of the author, studies on cost/benefits analyses exist (section 3.1.8) but the issue of calibration has only been briefly addressed in a report from 2002 (Willett & Rister). Besides, few details about field testing and analyses are given in the report.

Knowing the number of manual measurements necessary to achieve a high accuracy is essential, especially in Norway where only one antenna array is at the disposal of the NPRA. As far as it is known, only air-coupled horn antennas are currently able to continuously calculate the dielectric permittivity along a section. The two main benefits of other types of GPR (non-destructive testing and cost savings) may then be reduced as the number of calibration cores increases.

During this research, the optimum number of calibration points was investigated at the pavement test track MnROAD. Results of this project are presented in **Appendix A**. The tested section was 70 m long and newly constructed. In spite of the homogenous structure, relatively large differences were observed in GPR error depending on whether calibration cores are taken. As illustrated in the paper, the overall GPR error varies for example from 5,32 % (ε = 5,83 applied to the entire section) to 11,83 % (ε = 4,63) for one calibration core. This is a considerable gap that must be minded.

Using multiple cores decreases the deviation in GPR errors, which reach the asymptotic limit of 5 %. The accuracy does not significantly improve above 3 calibration cores. However these results raise a question of the benefit of GPR on a cost level that should be further investigated.

Conclusion

The objective of this doctoral thesis was to reveal the advantages, limitations and possible areas of applications of Ground Penetrating Radar. The research was conducted as part of efforts to improve the efficiency of infrastructure inspection and rehabilitation strategies in Norway. Special attention was given to Norwegian problematics.

The conclusions that can be drawn from this study are as follows:

- GPR has an extensive range of applications and the potential to become an integral part of rehabilitation strategies of infrastructures.
- It can be used as a stand-alone tool, but should be used in combination with other NDT for a complete diagnostic. The technology, in its current state, is limited by the electrical properties of the investigated material.
- In the situation where distances and depths must be determined, calibration with ground-truth is indispensable. Expenses involved in field measurements can be overcome by using the technology at a network level.
- To get the most out of GPR surveys, it is important to carefully select the type of GPR system and antenna. Criteria such as speed of data collection, manageability, and size of the equipment have to be taken into account.
- GPR is ready for routine use in pavement thickness determination and forensic investigations. Data can be incorporated into Pavement Management Systems and improve the efficiency of rehabilitation strategies.
- GPR is ready for routine use in QA/QC and tunnel inspections, provided that the cost of implementation and equipment is assessed. It has the potential to substantially reduce the frequency of invasive interventions.
- The development of GPR in Norway is conditioned by the increase in skills and practical knowledge in GPR. The implementation of Ground Penetrating Radar on a project or network level will require training in both the theoretical understanding of the technology, the evaluation of the feasibility of the project, the field operation and the interpretation of the data.

The table below summarizes the status of research conducted to assess the feasibility of using GPR in infrastructure inspection.

Two innovative GPR applications are underway to produce meaningful results, and deserve further research and testing: the determination of salt quantity on roads, and the detection of ice lenses responsible of frost heave.
The measurement of the frost depth does not require further development and is ready for implementation, while GPR has already been deployed in the mapping of cavities behind tunnel linings. Equipment investment is required for quality assurance/quality control of new constructions and the detection of rock falls in tunnels. GPR may also be suited for bridge deck condition assessment, with immediate implementation.

It is hoped that the outcomes of this research project will have an impact on the development of the GPR technology in Norway and will be further embedded into maintenance and rehabilitation programs.

Table 10 Status of research

	Research phase	Development phase	Implementation phase
Salt quantity on winter roads	X		
Frost depth			X
Ice lenses	X		
QA/QC of pavements		X	
Airfields			X
Void mapping in tunnels			X
Rock falls in tunnels		X	

References

Abraham, O. & Dérobert, X., 2003. Non-destructive testing of fired tunnel walls: the Mont-Blanc Tunnel case study. *NDT & E International*, 36(6), pp.411–418.

Aho, S. & Saarenketo, T., 2006. *Design and repair of roads suffering from spring thaw weakening*, ROADEX III.

AL-Qadi, I.L. et al., 2010. Development of a time–frequency approach to quantify railroad ballast fouling condition using ultra-wide band ground-penetrating radar data. *International Journal of Pavement Engineering*, 11(4), pp.269–279.

Al-Qadi, I.L. et al., 2004. Effective Approach to Improve Pavement Drainage Layers. *Journal of Transportation Engineering*, 130(5), pp.658–664.

Al-Qadi, I.L. et al., 2010. In-Place Hot-Mix Asphalt Density Estimation Using Ground-Penetrating Radar. *Transportation Research Record: Journal of the Transportation Research Board*, 2152, pp.19–27.

Al-Qadi, I.L. & Lahouar, S., 2005. Measuring Rebar Cover Depth in Rigid Pavements with Ground-Penetrating Radar. *Transportation Research Record: Journal of the Transportation Research Board*, 1907, pp.80–85.

Al-Qadi, I.L., Lahouar, S. & Loulizi, A., 2002. Ground Penetrating Radar Evaluation for Flexible Pavement Thickness Estimation. In *Proceedings of the Pavement Evaluation Conference*. Roanoke, Virginia, USA: CD-ROM.

Al-Qadi, I.L., Lahouar, S. & Loulizi, A., 2005. *Ground-Penetrating Radar Calibration at the Virginia Smart Road and Signal Analysis to Improve Prediction of Flexible Pavement Layer Thicknesses*, Report No. FHWA/VTRC 05-CR7.

Al-Qadi, I.L., Lahouar, S. & Loulizi, A., 2003. Successful Application of Ground-Penetrating Radar for Quality Assurance – Quality Control of New Pavements. *Transportation Research Record: Journal of the Transportation Research Board*, 1861, pp.86–97.

Al-Qadi, I.L., Xie, W. & Roberts, R., 2008. Scattering analysis of ground-penetrating radar data to quantify railroad ballast contamination. *NDT & E International*, 41, pp.441–447.

Ariaratnam, S.T. & Guercio, N., 2006. In-pipe Ground Penetrating Radar for non-destructive evaluation of PVC lined concrete pipe. *Advances in Engineering Structures, Mechanics & Construction*, 140, pp.763–772.

Barnes, C.L. & Trottier, J., 2004. Effectiveness of Ground Penetrating Radar in Predicting Deck Repair Quantities. *Journal of Infrastructure Systems*, 10(2), pp.69–76.

Barnes, C.L. & Trottier, J., 2002. Phenomena and Conditions in Bridge Decks That Confound Ground-Penetrating Radar Data Analysis. *Transportation Research Record: Journal of the Transportation Research Board*, (1795), pp.57–61.

Benedetto, A., 2010. Water content evaluation in unsaturated soil using GPR signal analysis in the frequency domain. *Journal of Applied Geophysics*, 71(1), pp.26–35.

Berthelot, C. et al., 2009. Non-Destructive Structural Asset Valuation of a Saskatchewan Rural Airfield Before and After Structural Upgrade. In *Annual Conference of the Transportation Association of Canada*. Vancouver, British Columbia.

De Bold, R. et al., 2009. Aspects of GPR testing of a mixed railway trackbed. In *Proceedings of the 10th International Conference of Railway Engineering*. London, UK: Engineering Technics Press.

Bosela, P.A. et al., 2006. Field comparison of NDE methods for tunnel condition assessment. In *Proceedings of the Fourth Forensic Engineering Congress*. Cleveland, Ohio, pp. 620–640.

Cao, Y., 2011. *Full Waveform Analysis of Ground Penetrating Radar Measurements*. PhD dissertation: University of Minnesota.

Chen, D.-H. et al., 2003. Forensic Evaluation of Premature Failures of Texas Specific Pavement Study–1 Sections. *Journal of Performance of Constructed Facilities*, 17(2), pp.67–74.

Chen, D.H. & Wimsatt, A., 2010. Inspection and Condition Assessment Using Ground Penetrating Radar. *Journal of Geotechnical and geoenvironmental engineering*, 136, pp.207–214.

CIA, 2014. The World Factbook. Available at: https://www.cia.gov/library/publications/the-world-factbook/geos/no.html.

Clark, M., Gordon, M. & Forde, M.C., 2004. Issues over high-speed non-invasive monitoring of railway trackbed. *NDT & E International*, 37(2), pp.131–139.

Clark, M.. et al., 2001. Electromagnetic properties of railway ballast. *NDT & E International*, 34(5), pp.305–311.

Daniels, D.J., 2004. *Ground Penetrating Radar - 2nd Edition*, London, UK: The Institute of Electrical Engineers.

Dawson, A. et al., 2007. Design of Low-Volume Pavements Against Rutting: Simplified Approach. *Transportation Research Record: Journal of the Transportation Research Board*, 1989(1), pp.165–172.

Delatte, N. et al., 2003. Application of Nondestructive Evaluation to Subway Tunnel Systems. *Transportation Research Record: Journal of the Transportation Research Board*, 1845, pp.127–135.

Diamanti, N. & Redman, D., 2010. A Study of GPR Vertical Crack Responses in Pavement Using Field Data and Numerical Modelling. In *Proceedings of the 13th International Conference on Ground Penetrating Radar*. Lecce, Italy: IEEE.

Edwards, L. & Mason, Q., 2011. *Evaluation of Nondestructive Methods for Determining Pavement Thickness*, US Army Corps of Engineers: ERDC/GSL TR-11-41.

Eide, E. et al., 2005. Airfield Runway Inspection using 3- Dimensional GPR. In *Proceedings of the 3rd International Workshop on Advanced Ground Penetrating Radar: Iwagpr 2005*. Delft, the Netherlands: Delft University of Technology.

Eide, E., Hoff, I. & Værnes, E., 2001. *Undersøkelse av ballast under jernbane ved hjelp av georadar*, SINTEF Bygg og Miljø, STF22 A01319. In Norwegian.

Flintsch, G.W. et al., 2005. *Field Investigation of High Performance Pavements in Virginia*, Virginia Tech Transportation institute.

George, M. & Erdogmus, E., 2009. *Use of Ground Penetrating Radar for Construction Quality Assurance of Concrete Pavement*, Report No. P307: University of Nebraska – Lincoln.

Goel, A. & Das, A., 2008. Nondestructive testing of asphalt pavements for structural condition evaluation: a state of the art. *Nondestructive Testing and Evaluation*, 23(2), pp.121–140.

Gordon, M.O., Broughton, K. & Hardy, M.S. a., 1998. The assessment of the value of GPR imaging of flexible pavements. *NDT & E International*, 31(6), pp.429–438.

Grote, K. et al., 2005. Evaluation of infiltration in layered pavements using surface GPR reflection techniques. *Journal of Applied Geophysics*, 57(2), pp.129–153.

Gucunski, N. et al., 2010. Multiple Complementary Nondestructive Evaluation Technologies for Condition Assessment of Concrete Bridge Decks. *Transportation Research Record: Journal of the Transportation Research Board*, 2201, pp.34–44.

Gucunski, N. et al., 2012. *Nondestructive Testing to Identify Concrete Bridge Deck Deterioration*, Report No. SHRP 2 R06-A. Prepublication draft.

Gucunski, N., Hadidi, R. & Shokouhi, P., 2004. *Demonstration of Ground Penetrating Radar (GPR)*, Report No. GPR-RU4474: CAIT/Rutgers State University.

Hammons, M. et al., 2006. Detection of Stripping in Hot-Mix Asphalt. *Transportation Research Record: Journal of the Transportation Research Board*, 1949, pp.20–31.

Heitzman, M. et al., 2012. *Nondestructive Testing to Identify Delaminations between HMA Layers, Volume 1*, Report No. SHRP 2 R06-D. Prepublication draft.: Strategic Highway Research Program (SHRP) 2, National Research Council.

Hoff, I., Hoven, B. & Eide, E., 2008. Introduction of Ground Penetrating Radar in Pavement Rehabilitation in Norway. In *Transport Research Arena Europe*. Ljubljana, Slovenia.

Holzschuher, C., Lee, H.S. & Greene, J., 2007. *Accuracy and repeatability of Ground Penetrating Radar for surface layer thickness estimation of Florida roadways*, Report No. FL/DOT/SMO/07-505: Florida Department of Transportation.

Hugenschmidt, J., 2004. Accuracy and Reliability of Radar Results on Bridge Decks. In *Proceedings of the 10th International Conference on Ground Penetrating Radar*. Delft, the Netherlands, pp. 1–4.

Hugenschmidt, J., 2000. Railway track inspection using GPR. *Journal of Applied Geophysics*, 43(2-4), pp.147–155.

Hugenschmidt, J. & Loser, R., 2007. Detection of chlorides and moisture in concrete structures with ground penetrating radar. *Materials and Structures*, 41(4), pp.785–792.

Huisman, J.A. et al., 2003. Measuring Soil Water Content with Ground Penetrating Radar : A Review. *Vadose Zone Journal*, 2(4), pp.476–491.

Hyslig, J.P. et al., 2005. *Ground Penetrating Radar for Railroad Track Substructure Evaluation*, Report No. FHWA/DOT/FRA/ORD-05-04: Federal Railway Administration.

Ikiz, N.N., 2008. *Field and Laboratory Investigation of Anti-Icing/Pretreatment (PhD Thesis)*. PhD dissertation: Russ College of Engineering and Technology of Ohio University.

Infrasence, 2006. *Feasibility of Using Ground Penetrating Radar (GPR) for Pavements, Utilities, and Bridges*, Report No. SD2005-05-F: South Dakota Department of Transportation.

Infrasense, 2003. *Non-Destructive Measurement of Pavement Layer Thickness Final Report*, Report No. FHWA/CA/OR-2003/03: California Department of Transportation.

Jack, R. & Jackson, P., 1999. Imaging attributes of railway track formation and ballast using ground probing radar. *NDT & E International*, 32(8), pp.457–462.

Jol, H.M., 2008. *Ground Penetrating Radar: Theory and Applications*, Elsevier. ISBN: 978-0-444-53348-7.

Jørgensen, A.S. & Andreasen, F., 2007. Mapping of permafrost surface using ground-penetrating radar at Kangerlussuaq Airport, western Greenland. *Cold Regions Science and Technology*, 48, pp.64–72.

Kalogeropoulos, A., 2012. *Non-Destructive Determination of Chloride and Water Content in Concrete Using Ground Penetrating Radar*. Ecole Polytechnique Federale de Lausanne.

Karlovšek, J., Schuermann, A. & Willimas, D.J., 2012. Investigation of voids and cavities in Bored Tunnels using GPR. In *Proceedings of the 14th International Conference on Ground Penetrating Radar (GPR)*. Shanghai, China, pp. 496–501.

Kassem, E. et al., 2012. Measurements of asphalt pavement density using Ground Penetrating Radar and its relationship to performance. In *Transportation Research Board 91th Annual Meeting*. Washington D.C.

Keogh, T., Mesher, D.E. & Keegan, T.R., 2006. An Integrated System for Accurate Tie and Ballast. In *AREMA Conference*. Louisville, KY.

Klein-Paste, A., 2007. *Runway Operability under Cold Weather Conditions*. PhD dissertation: University of Science and Technology, Norway.

Kohler, E., Santero, N. & Harvey, J., 2006. *Final Report Pilot Project for Fixed Segmentation of the Pavement Network*, Report No. UCPRC-RR-2005/11: California Department of Transportation.

Lahouar, S. et al., 2002. Approach to Determining In Situ Dielectric Constant of Pavements Development and Implementation at Interstate 81 in Virginia. *Transportation Research Record: Journal of the Transportation Research Board*, 1806, pp.81–87.

Lahouar, S., 2003. *Development of Data Analysis Algorithms for Interpretation of Ground Penetrating Radar*. PhD Dissertation: Virginia Polytechnic Institute and State University.

Lahouar, S. & Al-Qadi, I.L., 2008. Automatic detection of multiple pavement layers from GPR data. *NDT & E International*, 41(2), pp.69–81.

Laurens, S. et al., 2005. Non-destructive evaluation of concrete moisture by GPR: experimental study and direct modeling. *Materials and Structures*, 38, pp.827–832.

Leng, Z. et al., 2009. Selection of Antenna Type and Frequency for Pavement Surveys Using Ground Penetrating Radar (GPR). In *Transportation Research Board 88th Annual Meeting*. Washington, D.C.

Leng, Z. & Al-qadi, I.L., 2009. Dielectric Constant Measurement of Railroad Application of STFT for GPR Data Analysis. In *Proceedings of the 7th International Non-Destructive Testing in Civil Engineering Symposium (NDTCE'09)*. Nantes, France, pp. 2–7.

Leng, Z., Al-Qadi, I.L. & Lahouar, S., 2011. Development and validation for in situ asphalt mixture density prediction models. *NDT & E International*, 44(4), pp.369–375.

Leng, Z. & Shangguan, P., 2012. Field Application of Ground Penetrating Radar for Asphalt Mixture Density Measurement : A Case Study of Illinois Route 72 Overlay. *Transportation Research Record: Journal of the Transportation Research Board*, 2304, pp.133–141.

Li, C., Miao, L. & Yue, J., 2010. Research on detection to Moisture Content of Flexible Pavement by GPR. In *Proceedings of GeoShanghai 2010*. American Society of Civil Engineers (ASCE), pp. 420–426.

Liu, J., Zollinger, D.G. & Lytton, R.L., 2008. Detection of Delamination in Concrete Pavements Using Ground-Coupled Ground-Penetrating Radar Technique. *Transportation Research Record: Journal of the Transportation Research Board*, 2087, pp.68–77.

Loizos, A. et al., 2011. A Practice towards Pavement Monitoring and Evaluation. In *Transportation Research Board 90th Annual Meeting*. Washington D.C.

Loizos, A. & Plati, C., 2007a. Accuracy of Ground Penetrating Radar Horn-Antenna Technique for Sensing Pavement Subsurface. *Sensors Journal*, 7(5), pp.842–850.

Loizos, A. & Plati, C., 2007b. Accuracy of pavement thicknesses estimation using different ground penetrating radar analysis approaches. *NDT & E International*, 40(2), pp.147–157.

Loizos, A. & Plati, C., 2011. Assessment of HMA Air-Voids and Stiffness Based on Material Dielectric Values. *Road Materials and Pavement Design*, 12(1), p.217 to 226.

Loulizi, A., 2001. *Development of Ground Penetrating Radar Signal Modeling and Implementation for Transportation Infrastructure Assessment*. PhD dissertation: Virginia Polytechnic Insitute and State University.

Lysbakken, K.R., 2013. *Salting of Winter Roads*. Trondheim, Norway: PhD dissertation: University of Science and Technology, Norway.

Maijala, P. & Herronen, T., 2011. *Benchmarking of GPR equipment for road surveys*,

Malvar, L.J., 2010. Detecting Voids Under Pavements. *Transportation Research Record: Journal of the Transportation Research Board*, 2170, pp.28–35.

Mardeni, R., Raja Abdullah, R.S.A. & Shafri, H.Z.M., 2010. Road pavement density analysis using a new non-destructive ground penetrating radar system. *Progress In Electromagnetics Research B*, 21, pp.399–417.

Maser, K., Martino, N., et al., 2012. Understanding and Detecting Bridge Deck Deterioration with Ground-Penetrating Radar. *Transportation Research Record: Journal of the Transportation Research Board*, 2313, pp.116–123.

Maser, K., Puccinelli, J. & Amestoy, J.K., 2012. Accuracy of Ground Penetrating Radar asphalt thickness data and its impact on pavement rehabilitation. In *Transportation Research Board 91th Annual Meetingth Annual Meeting*. Washington D.C.

Maser, K.R., 1996. Condition assessment of transportation Infrastructure using Ground Penetrating Radar. *Journal of Infrastructure Systems*, 2(2), pp.94–101.

Maser, K.R., 2009. Integration of Ground Penetrating Radar and Infrared Thermography for Bridge Deck Condition Evaluation. In *Proceedings of the 7th International Non-Destructive Testing in Civil Engineering Symposium (NDTCE'09)*. Nantes, France, pp. 1130–1136.

Maser, K.R. et al., 2003. Technology for quality assurance of new pavement thickness. In *Transportation Research Board 82nd Annual Meeting*. Washington D.C.

Maser, K.R. & Pucinelli, J., 2009. *Ground Penetrating Radar (GPR) Analysis, Phase I Report*, Report No. FHWA/MT-09-005/8201: Montana Department of Transportation.

Morcous, G. & Erdogmus, E., 2010. Accuracy of Ground-Penetrating Radar for Concrete Pavement Thickness Measurement. *Journal of Performance of Constructed Facilities*, 24(6), pp.610–621.

Morcous, G. & Sekpe, V., 2010. Inspection of Insulated Concrete Form Walls Using Ground Penetrating Radar. *International Journal of Construction Education and Research*, 6(4), pp.303–317.

Moropoulou, a. et al., 2002. Infrared thermography and ground penetrating radar for airport pavements assessment. *Nondestructive Testing and Evaluation*, 18(1), pp.37–42.

Nakano, T. & Sakai, H., 2008. Application of ground-penetrating radar and high-density electrical sounding for the study of seasonally frozen ground. *Bulletin of Glaciological Research*, 25, pp.27–35.

Narayanan, R.M. et al., 2004. Railroad track modulus estimation using ground penetrating radar measurements. *NDT & E International*, 37(2), pp.141–151.

Noureldin, A.S. et al., 2003. Network Pavement Evaluation with Falling-Weight Deflectometer and Ground-Penetrating Radar. *Transportation Research Record: Journal of the Transportation Research Board*, 1860, pp.90–99.

NPRA, 1997. *Håndbok R211 - Feltundersøkelser*, In Norwegian.

Øvstedal, E. et al., 2012. *Telehiv på nye norske veger*, Statens Vegvesen. In Norwegian.

Pailes, B.M., Gucunski, N. & Brown, M.C., 2013. Correlation of non-destructive testing results to improve assessment of corrosion and corrosion damage of a reinforced concrete deck. In *Transportation Research Board 92nd Annual Meeting*. Washington D.C.

Parkinson, G. & Ekes, C., 2008. Ground Penetrating Radar Evaluation of Concrete Tunnel Linings. In *Proceedings of the 12th Internarional Conference on Ground Penetrating Radar*. Birmingham, UK.

Plati, C. & Loizos, A., 2012. Using ground-penetrating radar for assessing the structural needs of asphalt pavements. *Nondestructive Testing and Evaluation*, 27(3), pp.273–284.

Poikajärvi, J. et al., 2012. Nondestructive Testing and Evaluation GPR in road investigations – equipment tests and quality assurance of new asphalt pavement. *Nondestructive Testing and Evaluation*, 27(3), pp.293–303.

Popik, M. et al., 2009. *Using Ground Penetrating Radar as an Assessment Methodology in Roadway Rehabilitation*, Report: Applied Research Associates/Florida Department of Transportation.

Quiroga, C., Kraus, E. & Overman, J., 2011. Strategies to Address Utility Challenges in Project Development. *Transportation Research Record: Journal of the Transportation Research Board*, 2262, pp.227–235.

Rajagopal, A., 2011. *Investigate Feasibility Of Using Ground Penetrating Radar In QC/QA of Rubblization Projects*, Report No. FHWA/OH-2011/15: Ohio Department of Transportation.

Rao, C., Von Quintus, H. & Schmitt, R.L., 2007. Calibration of Nonnuclear Density Gauge Data for Accurate In-Place Density Prediction. *Transportation Research Record: Journal of the Transportation Research Board*, 2040, pp.123–136.

Rmeili, E. & Scullion, T., 1997. Detecting Stripping in Asphalt Concrete Layers Using Ground Penetrating Radar. *Transportation Research Record: Journal of the Transportation Research Board*, 1568, pp.165–174.

Roackaway, T. & Rivard, J.A., 2010. Application of Ground Penetrating Radar in the Urban Environment. In *Proceedings of the 13th International Conference on Ground Penetrating Radar*. Lecce, Italy: IEEE.

Roberts, R. et al., 2006. Railroad Ballast Fouling Detection Using Ground Penetrating Radar – A New Approach Based on Scattering from Voids. In *Proceedings of 9th European Congress on Non-Destructive Testing (ECNDT 2006)*. Berlin, Germany.

Roberts, R. et al., 2009. *Subsurface Evaluation of Railway Track Using Ground Penetrating Radar*, Report No. FHWA/DOT/FRA/ORD-09/08: Federal Railroad Administration.

Ruthenberg, I.A., 1998. *Curve fitting and migration of GPR data for the detection of pipes and cables*. Bachelor thesis, University of Queensland (Australia).

Saarenketo, T., 2008. NDT Transportation. In H. M. Jol, ed. *Ground Penetrating Radar: Theory and Applications*. Elsevier. ISBN: 978-0-444-53348-7., p. 524.

Saarenketo, T., 2012. *Recommendations for guidelines for the use of GPR in asphalt air voids content measurement*, INTERREG: Mara Nord.

Saarenketo, T., Maijala, P. & Herronen, T., 2011. *Recommendations for guidelines for the use of GPR in road construction quality control Recommendations for guidelines for the Control*, INTERREG: Mara Nord.

Saarenketo, T. & Scullion, T., 2000. Road evaluation with ground penetrating radar. *Journal of Applied Geophysics*, 43(2-4), pp.119–138.

Schaus, L. & Popik, M., 2011. Frost Heaves: A Problem That Continues To Swell. In *Proceedings of the 2011 Annual Conference of the Transportation Association of Canada*. Edmonton , Canada.

Schmitt, R.L., Faheem, A. & Al-Qadi, I.L., 2012. Ranking System to Select Non-Destructive Technologies for Asphalt Pavement Compaction. In *Transportation Research Board 91th Annual Meeting*. Washington D.C.

Sebesta, S., Saarenketo, T. & Scullion, T., 2012. *Using Infrared and High- Speed Ground Penetrating Radar for Uniformity Measurements on New HMA Layers*, Report No. SHRP 2 S2-R06C-RR-1: Strategic Highway Research Program (SHRP) 2, National Research Council.

Sebesta, S. & Scullion, T., 2003. Application of Infrared Imaging and Ground-Penetrating Radar to Detect Segregation in Hot-Mix Asphalt Overlays. *Transportation Research Record: Journal of the Transportation Research Board*, 1861, pp.37–43.

Seung-veup, H. et al., 2003. An experimental study on a Ground Penetrating Radar for detecting water-leaks in buried water transfer pipes. In *International Symposium on Antennas, Propagation and EM Theory (ISAPE)*. Beijing, China: IEEE, pp. 596 – 599.

Shangguan, P. et al., 2013. An Innovative Approach for Asphalt Pavement Compaction Monitoring Using Ground Penetrating Radar. In *Transportation Research Board 92nd Annual Meeting*. Washington D.C.

Shangguan, P., Al-Qadi, I.L. & Leng, Z., 2012. Development of Wavelet Technique to Interpret Ground-Penetrating Radar Data for Quantifying Railroad Ballast Conditions. *Transportation Research Record: Journal of the Transportation Research Board*, 2289, pp.95–102.

Sivertsen, Å., 2012. *Sluttrapport for etatsprogrammet Salt SMART*, In Norwegian.

Sivertsen, Å. & Ofstad, S.I., 2014. *Mengderapportering vinteren 2013 / 2014*, In Norwegian.

Sterling, R., I. et al., 2009. *Encouraging Innovation in Locating and Characterizing Underground Utilities*, Report No. SHRP 2 S2-R01-RW: Strategic Highway Research Program (SHRP) 2, National Research Council.

Stoffregen, H. et al., 2002. Accuracy of soil water content measurements using ground penetrating radar : comparison of ground penetrating radar and lysimeter data. *Journal of Hydrology*, 267, pp.201–206.

Stokoe, K.H. et al., 2013. Development and Initial Testing of the Total Pavement Acceptance Device (TPAD). In *Transportation Research Board 92nd Annual Meeting*. Washington D.C.

Sund, E.K., 2012. *Hva vil det koste å fjerne forfallet på riksvegnettet ?*, Report No. 75/NPRA. In Norwegian.

Sussmann, T.R., 1999. *Application of Ground Penetrating Radar to Railway Track Substructure Maintenance Management*. University of Massachusetts Amherst.

Sussmann, T.R., Selig, E.T. & Hyslip, J.P., 2003. Railway track condition indicators from ground penetrating radar. *NDT & E International*, 36(3), pp.157–167.

Thodesen, C.C., Lerfald, B.O. & Hoff, I., 2012. Review of asphalt pavement evaluation methods and current applications in Norway. *The Baltic Journal of Road and Bridge Engineering*, 7(4), pp.246–252..

Thordarson, S., 2002. *Wind Flow Studies for Drifting Snow on Roads*. PhD dissertation: Norwegian University of Science and Technology, Norway.

Topp, G.C., Davis, J.L. & Annan, A.P., 1980. Electromagnetic determination of soil water content: Measurements in coaxial transmission lines. *Water Resources Research*, (16), pp.574–582.

Uddin, W., 2006. *Ground Penetrating Radar Study — Phase I Technology Review and Evaluation*, Report No. FHWA/MS-DOT-RD-06-182: Mississippi Department of Transportation.

White, J. et al., 2013a. Concrete tunnel lining evaluation using non-destructive techniques: A multi-method case study at Eisenhower tunnel. In *Transportation Research Board 92nd Annual Meeting*. Washington D.C.

White, J. et al., 2013b. Non-destructive evaluation of concrete linings at Hanging Lake tunnel. In *Transportation Research Board 92nd Annual Meeting*. Washington D.C.

Wightman, W.E. et al., 2003. *Application of Geophysical Methods to Highway Related Problems*, Report: Blackhawk GeoSciences/Federal Highway Administration.

Willett, D. a., Mahboub, K.C. & Rister, B., 2006. Accuracy of Ground-Penetrating Radar for Pavement-Layer Thickness Analysis. *Journal of Transportation Engineering*, 132(1), pp.96–103.

Willett, D.A. & Rister, B., 2002. *Ground Penetrating Radar "pavement layer thickness evaluation,"* Report No.KTC-02-29/FR101-00-1F: Kentucky Transportation Center.

Williams, R.R. et al., 2006. Evaluation of network level Ground Penetrating Radar effectiveness. In *Transportation Research Board 85th Annual Meeting*. Washington D.C.

Wimsatt, A. et al., 2012. *Mapping Voids , Debonding , Delaminations , Moisture, and Other Defects Behind or Within Tunnel Linings* Prepublica., Report No. SHRP 2 R06-G. Prepublication draft.: Strategic Highway Research Program (SHRP) 2, National Research Council.

Wu, R. et al., 2013. The Benefit of Ground Penetration Radar Thicknesses for Back-Calculation Using FWD Data. In *Transportation Research Board 92nd Annual Meeting*.

Xie, X. et al., 2007. Evaluation of grout behind the lining of shield tunnels using ground-penetrating radar in the Shanghai Metro Line, China. *Journal of Geophysics and Engineering*, 4(3), pp.253–261.

Yehia, S. et al., 2008. Ground-Penetrating Radar, Chain Drag, and Ground Truth: Correlation of Bridge Deck Assessment Data. *Transportation Research Record: Journal of the Transportation Research Board*, 2044, pp.39–50.

Zhang, F., Xie, X. & Huang, H., 2010. Application of ground penetrating radar in grouting evaluation for shield tunnel construction. *Tunnelling and Underground Space Technology*, 25(2), pp.99–107.

Zhang, Q. et al., 2010. Rail radar - a fast maturing tool for monitoring trackbed. In *Proceedings of the 13th Internarional Conference on Ground Penetrating Radar*. Lecce, Italy: IEEE, pp. 1–5.

Zhao, H. et al., 2011. Pavement Structure Segmentation Method Based on Ground-Penetrating Radar Data. In *Transportation Research Board 90th Annual Meeting*. Washington D.C.

PAPER I

Use of Ground Penetrating Radar for detection of salt concentration on Norwegian winter roads

A. Lalagüe & I. Hoff
SINTEF, Road and railway Engineering, Trondheim, Norway

E. Eide
3d-radar AS, Trondheim, Norway

A. Svanekil
Norwegian Public Roads Administration, Trondheim, Norway

ABSTRACT: The use of salt for ice and snow prevention and removal is practised in many countries in order to maintain a high level of mobility and safety during the wintertime. Today winter serviceability comes within a new scope where environmental considerations are very important. Due to lack of calibration of spreading methods, quantity of salt applied is usually not accurately determined. The Ground Penetrating Radar can be a useful tool in salting operations. It records the electric echoes induced by the dielectric properties differences between two materials. GPR can detect salted/non salted surfaces, especially when spread with brine. The amplitude of a single reflected signal is dependent on the brine concentration. This pilot study verifies this effect. However, the equipment and software used for the pilot need modifications to become a practical tool.

1 INTRODUCTION

1.1 *The context*

Because of snow and ice deposit, the adherence between tires and pavement is considerably reduced, which leads to an increase of traffic accidents. Snow can also disrupt the local economic activity when it impedes the road-users mobility. Optimization of salt use and better control of spreading are possible improvements. Targeted concentrations are often more effective, more economic and more eco-friendly than spreading on the entire section. This project work is related to the "bare pavement strategy" during winter, conducted by the Norwegian Public Roads Administration (NPRA), which consists to develop new tools and methods to keep the road snow- and ice-free.

1.2 *Background on road salt use*

De-icing is the process of removing ice from the pavement, while anti-icing consists in preventing ice deposit. De-icing can be done with chemicals. Snow removal is done by winter service vehicles and will not be discussed in this paper. Abrasives like sand increase friction. Sand does not have any chemical potential, and therefore does not affect the environment in the same way. On the other hand it is less efficient in many cases than salt. Chemicals are sodium chloride (NaCl), magnesium chloride ($MgCl_2$) or calcium chloride ($CaCl_2$). NaCl is by far the

most used. $MgCl_2$ and $CaCl_2$ are sometimes combined with NaCl, they reduce the reaction time and can be spread at very low temperatures (Vaa T. , 2004), but they are expensive, less easy and less safe to handle. $MgCl_2$ and $CaCl_2$ are not discussed in this paper.

1.3 *Research objectives*

Due to lack of calibration of spreading methods, quantity of salt applied is not normally accurately determined. Thus 140 000 tons of road salt are used each year in Norway; this amount is probably unnecessary high. The purpose of this project was to determine if the Ground Penetrating Radar (GPR) technique could be a relevant way to control the salt amount on roads. Laboratory tests were conducted at NTNU/SINTEF Road technology laboratory, in Trondheim. Tests have been carried with dry salt, brine and pre-wetted salt, all used by winter maintenance services.

2 THE MELTING ACTION OF SALT (VAA & SAKSHAUG, 2007)

2.1 *The eutectic point*

Salt is a "freezing point depressant": it lowers the freezing point of water (Environnement Canada, 2004). The freezing point varies in relation to the NaCl concentration. The lowest freezing point is called the "eutectic point". For a brine solution, it is reached at -21° C, for a salt percentage of 23.3%. In theory NaCl can be used for very low temperatures – down to -21°C. In practice, it is not recommended below -11°C. Even if NaCl is still able to melt ice at lower temperatures, it becomes less efficient.

2.2 *The role of salt in ice removal*

The melting action of salt is due to its hygroscopic property. It can absorb water from the pavement (rain, ice, snow) or humidity from the air if this is higher than 76%. Salt in contact with water will form brine that seeps in the ice/snow layer until it reaches the surface of the road. The bonds between pavement and ice are broken as brine flows along the crossfall. Remaining ice/snow is reduced to slush with traffic (Transportation Association of Canada, 1999).

2.3 *Dry salt applications*

Dry salt can be used on a bare pavement only in special occasions, in contemplation of a snowstorm for instance. It needs to be carefully spread, avoiding wheel path, because traffic sweeps it away from the road. Spread on ice/frost, dry salt is almost always efficient, but with a reaction time which can be high (>30 min). This delay corresponds to the necessary time for solid particles to absorb water and turn into brine. Below -7°/-8°, the water content in air is too low to initiate the melting process.

2.4 *Salt brine applications*

Liquid binds better than dry salt to the pavement, spreading can therefore be done at higher speeds. In addition to that, there is no delayed reaction time because there is no dry salt dissolution required. The treatment can be considered instantaneous, which is a real advantage. However, when ice starts melting, the brine is diluted. The salt concentration is getting lower as melting goes along and the solution becomes less efficient. It can even refreeze at low temperatures. The brine effectiveness is time limited.

2.5 *Pre-wetted salt applications*

The pre-wetting technique uses salt brine to wet dry salt. Thus it reduces the time needed for particles to dissolve and become active, and there is less dilution problem. Dry salt turns into

brine as ice melting goes along, and salt concentration remains the same until all of the dry salt is dissolved.

2.6 *Amount of salt to be applied according to pavement conditions*

The following guideline recommendations (Table 1) are issued by the Norwegian Public Roads Administration and used by the Norwegian winter maintenance services. The de-icing actions depend on the climatic conditions and state of the pavement. As indicated, dry salt can be applied only in case of high moisture content on the pavement surface so that it can turn into brine. Conversely, brine should not be applied when rainfalls occur to prevent a salt concentration lowering.

Table 1 Guiding salt quantity in grams/m2 (NPRA, 2003)

Pavement	Brine solution		Pre-wetted salt (dry + brine)		Dry salt	
	[0°; -5°]	[-5°;-10°]	[0°; -5°]	[-5°;-10°]	[0°;-5°]	[-5°;-0°]
Dry	10	15	4+2	4+3	inefficient	
Humid	15	20	8+3	9+4	inefficient	
Wet	inefficient		14+6	18+4	10	15
White frost	15	20	8+3	11+5	inefficient	
Thin ice	30	40	14+6	18+8	inefficient	
Thick ice	inefficient		18+8	21+9	inefficient	
Before rainfall	inefficient		14+6	18+8	inefficient	
Supercooled rain	inefficient		21+9	28+14	inefficient	
Snow	inefficient		20+0	25+0	20	25

3 ENVIRONMENTAL IMPACTS OF ROAD SALT USE

3.1 *Corrosion and infrastructure damage*

3.1.1 *Roads and bridges*

Salt can affect most structures by damaging concrete. Chlorides penetrate through concrete voids and corrode steel reinforcements. They dilate, which create cracks in the concrete. Today, new technologies and changes in construction practices have improved the corrosion-resistance of concrete, but old structures remains predisposed (Salt Institute, 2004).

3.1.2 *Vehicles*

Few years ago, vehicles corrosion was the costly consequence of road salt use. Today, even if some parts are still exposed to corrosion, automobile manufacturers have improved vehicle life span by using non-corrosive materials such as plastic and zinc-coated steel. As a consequence of ongoing improvements, vehicles corrosion has never been so low. But obviously, older vehicles still remain susceptible to salt damage (Salt Institute, 2004).

3.2 *Roadside vegetation*

Roadsides are often dry, man-made, harsh environments, and use of salt makes this situation worse. High chloride concentrations stop the absorption of soil humidity by the plants and make the leaves becoming brown. High sodium concentrations may affect plants growth, by modifying structure, permeability and aeration of the soil. The extent of the damages depends on several factors: amount of salt, type of soil, precipitation, distance from the road, wind direction and plant species. In a word, impacts are local and change from one site to another. Sensible salting can reduce the quantity of salt transported to side terrain (Transportation Association of Canada, 2003).

3.3 *Groundwater impacts*

The damages caused to vegetation are connected to impacts on groundwater. It depends on several factors such as the frequency of salt applications, size of the waterbody and distance from the road. During the snow melt, road runoffs are collected through waterpipes and mixed with sewage. At that time, the salt content can rise to more than 100 mg/l. If the runoffs are not previously diluted and directly discharged into the lake or river, the salt concentration can reach 5000 mg/l at the opening. However salted water is quickly diluted. Even if it can have a very high concentration of pollutants coming from the roadside in winter, the volume is generally very low. For these reasons roads are normally not considered an ecological hazard (Transportation Association of Canada, 2003).

3.4 *Fish tolerance towards salt*

High salt concentration in spring time may affect the aquatic life. To a certain extent, most fish types have a good tolerance to salt content, even if they are sensitive to long lasting impacts. Tolerated limit values range from 1000 mg Cl^-/l (plankton, larva) to 6000 mg Cl^-/l (trout). Obviously, the impact of salt on fishes depends on site characteristics and the turnover rate of water. If the flow rate is high, salt will be faster diluted (Salt Institute, 2004).

4 THE GROUND PENETRATING RADAR (GPR)

4.1 *Principle*

The GPR is a nondestructive method used to image the subsurface. It can detect all kinds of objects, cables, pipes, drains, waterways, groundwork, iron framework, anchorage etc. In geology and geotechnics, it determines the layout and the thickness of the different layers. If appropriately used, it is time-saving and improves the safety during construction works. The georadar transmits electromagnetic waves in the studied structure and records the electric echoes induced by the dielectric properties differences between two materials. It takes into account the round-trip time and the amplitude of the signal. An image is created when moving on the surface. Depth range and resolution depend on the several factors (Neal, 2004). If the electrical conductivity of the ground increases, the energy is likely to dissipate, then the penetration depth decreases. Likewise, high frequencies penetrate less into the soil than lower frequencies but give a better resolution. Sands, gravels, ballasts and rocks are easily penetrated. Concretes, due to their homogeneity, give goods images of their intern structure as well. On the contrary, clays and saline soils can constitute obstacles (Saarenketo, 2006).

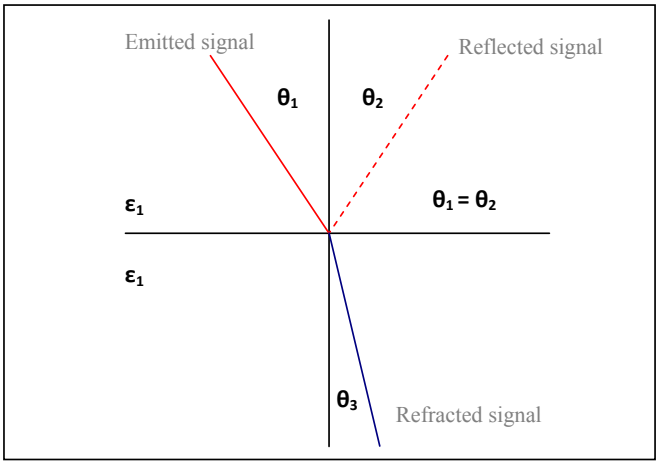

Figure 1 GPR principle

4.2 *Functions*

The Ground Penetrating Radar has many applications in numerous areas. Contrary to others systems which are limited to metal detection, it can locate all kinds of materials including synthetics such as PVC or polyethylene. It is therefore perfectly suitable for detection of piping and wiring systems in urban environment. It is also possible to determine the thickness of a material with the propagation speed. Surveys showed an error less than 10% when estimating ballasts thickness. As for roads, the GPR can be used in phase of excavation to estimate the quality of the subgrade and thus limit core drilling. In tunneling it enables the detection on voids and weakness zones. Stratigraphy, visualization of groundwater table or river bottoms, examination of polluted sites, seeking of voids, faults or cavities are others possible uses.

5 LABORATORY EXPERIMENT

5.1 *Equipment and materials*

- *Ground Penetrating Radar*
  - GeoScope™ GPR from 3d-radar AS
  - Frequency from 100 MHz to 2 GHz
  - Dwell time 2µs
  - Frequency step size 2 MHz
  - 31 elements (6 active for the tests)

- *Materials*
  - Sea salt, min. 99.9% NaCl, water content max. 3%, grain size max. 8mm.
  - Brine, nearly saturated with 23.3% salt by weight
  - Asphalt Concrete maximum grain size 11mm, samples 30cm x 30cm x 5cm
  - Foam microwave absorber, AN-79 by ECCOSORB®

5.2 *Test procedure*

The test consisted in:

– Placing the asphalt sample on top of the absorbent foam. The foam reflects less than -20 dB of normal incident energy above 600 MHz. It is thus easier to locate the asphalt layer on vertical pattern when analyzing data.

– Adding salt on top of asphalt, in the form of dry particles, brine or pre-wetted grains. Salt was spread as uniformly as possible, in ascending quantity order. It was not possible to follow the salt quantity guiding provided by NPRA. For practical reasons, it was difficult to use the low amount of salt. It sometimes even does not correspond to one salt grain. The salt quantity has therefore been exaggerated to fit the experience. Accurate salt concentrations can only be spread by using winter service vehicles (gritters, spreaders), for in-situ measurements.

– Pulling slowly the set board/foam/asphalt with the rope. It should be in motion to simulate the speed of the radar and to create the 3D-image. Movement is also necessary to avoid the static signal filter. Data are recorded with the GeoScope ™ GPR and analysed with Road Doctor ®.

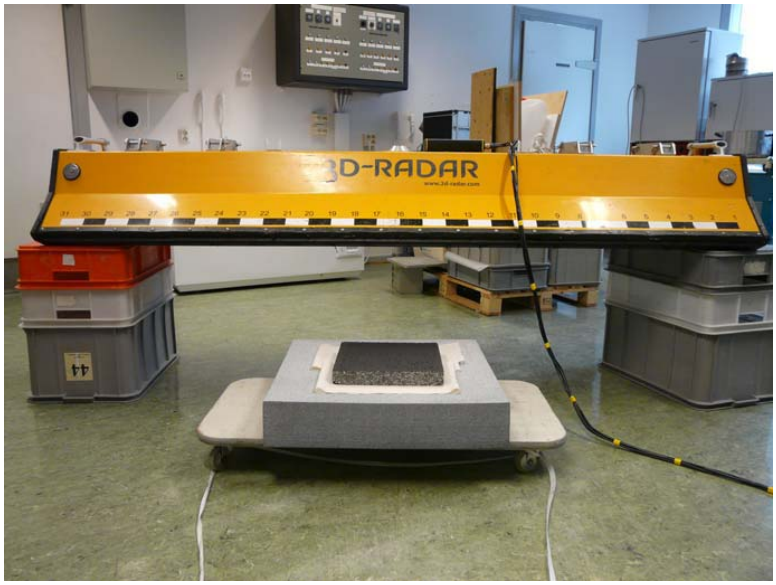

Figure 2 General setting

5.3 *Results*

The single scan views reveal pulses coming from the different interfaces (air/asphalt, asphalt/board and board/ground).

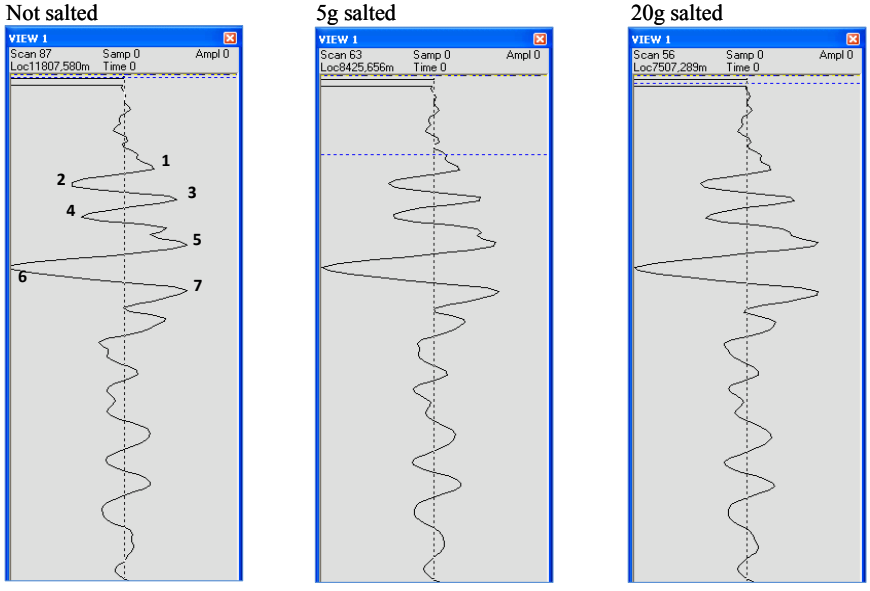

Figure 3 Single scans at different salt concentrations

Table 2 Correspondence between pulse peaks and interfaces

Peak number	Interface
1, 2	Asphalt surface
3, 4	Asphalt bottom/Top of the board
5, 6	Board bottom

For each quantity of salt (dry, diluted or pre-wetted), the pulse amplitudes were measured and listed in a table. Figures 4, 5 and 6 give the evolution of the amplitude in function of the salt amount spread on the asphalt surface. Legend refers to peaks as shown in figure 3.

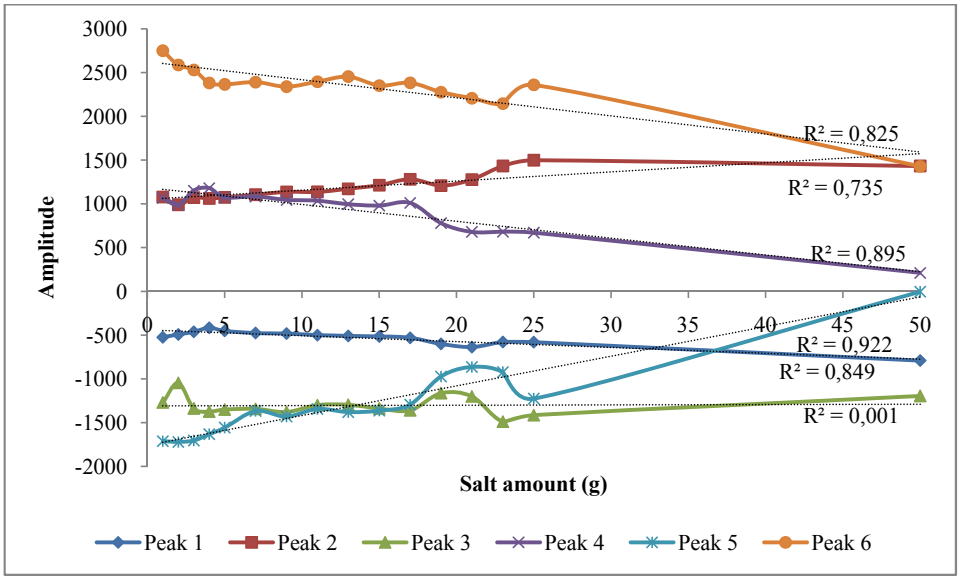

Figure 4 Evolution of the reflection amplitudes according to brine quantity

Table 3 Data analysis: brine

	Peak 1	Peak 2	Peak 3	Peak 4	Peak 5	Peak 6
	Descriptive statistics					
Mean	-534	1199	-1304	915	-1280	2335
Standard deviation	90	141	108	172	280	147
Relative standard deviation	17%	12%	8%	19%	22%	6%
	Regression statistics					
R	-0.92	0.86	0.04	-0.95	0.96	-0.91
R^2	0.85	0.74	0.00	0.90	0.92	0.83
Standard error	79.96	112.07	83.85	125.12	121.19	79.96

(Source: Excel 2007)

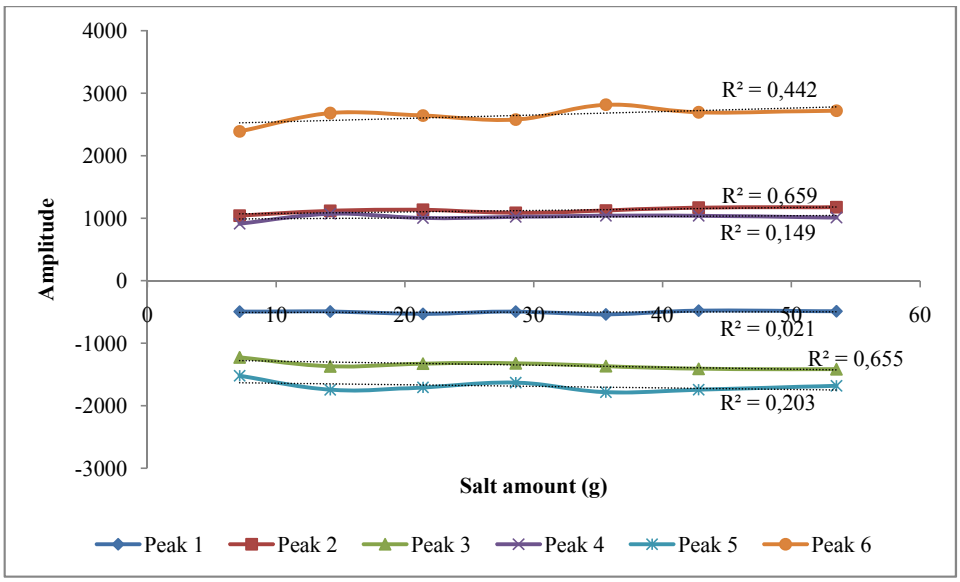

Figure 5 Evolution of the reflection amplitudes according to pre-wetted salt quantity

Table 4 Data analysis: pre-wetted salt

	Peak 1	Peak 2	Peak 3	Peak 4	Peak 5	Peak 6
	Descriptive statistics					
Mean	-502	1122	-1347	1015	-1687	2647
Standard deviation	23	47	65	50	90	135
Relative standard deviation	5%	4%	5%	5%	-5%	5%
	Regression statistics					
R	0.15	0.81	-0.81	0.39	-0.45	0.67
R^2	0.02	0.66	0.66	0.15	0.20	0.44
Standard error	24.62	30.33	41.63	50.84	87.57	110.19

(Source: Excel 2007)

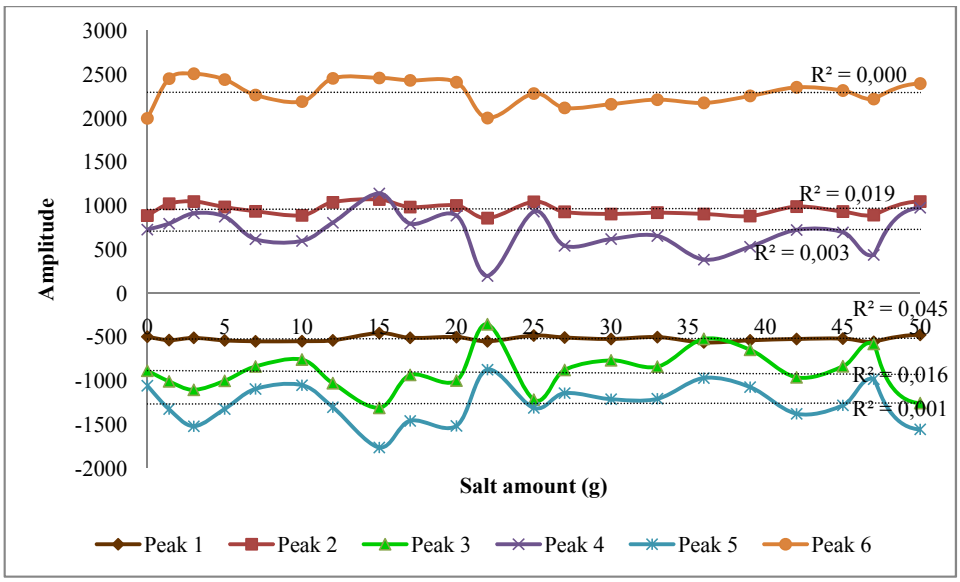

Figure 6 Evolution of the reflection amplitudes according to the dry salt quantity

Statistical analysis of the data showed no correlation between the peak amplitude and the amount of dry salt.

As expected, the signal amplitude seems to not be dependent on the dry salt quantity: correlation coefficients on figure 6 are close to 0. Dry salt is indeed not conductive and reflects the electromagnetic wave very slightly. It cannot be detected by the GPR in such small proportions. In pre-wetted salt case (Figure 5), the correlation is moderate ($|R|$ between 0.15 and 0.81). It comes from the fact that the salt is partly diluted. Figure 4 indicates a strong linear relationship between brine concentration and amplitude ($|R|$ between 0.86 and 0.96). The series 3 is an exception because it has an R-value close to 0: the correlation coefficient can be strongly attenuated by measurements errors. Even if the salt brine is only a thin film on the surface, it obviously also influences on the reflections from deeper interfaces. An increase in reflected signal strength (peaks 1 and 2) leads to energy loss of following waves (peaks 3, 4, 5 and 6). Reflection/transmission losses occur by absorption and each time the radiowaves pass through a boundary (Reynolds, 1997).

6 FIELD TESTING

In situ measurements have been carried out in order to corroborate results obtained in laboratory. Testing consisted in scanning a short road section - 500m - at regular time interval - 45min -, after passage of the salt spreader. At the same time quantity of salt was directly measured by use of a so-called saltstick SOBO-20 (Nygaard, 2003). This first trial was not conclusive by reason of unfavorable weather conditions. A number of factors should be considered in field testing such as width and pattern of salt spread, residual salt on the road surface, wind, humidity and temperature effect.

Figure 7 Dampening of a road section before use of the SOBO-20

7 CONCLUSION

The single pulse analysis comes to the following conclusion: salt is detectable by the Ground Penetrating Radar in presence of water (brine). Salted solution is highly conductive (100 mS/cm for brine); the conductivity is proportional to the salt concentration and since we get high R-values, the assumption of linear dependency between the salt concentration and the amplitude seems to be correct. These positive results concerning brine – the main point of interest – encourage us to continue research: they have yet to be substantiated with data from road trials. Field testing is currently in progress. To utilize the GPR as a practical tool, it would be necessary to develop a specialized equipment and software as well as calibrating GPR-measurement with other type of measurements.

REFERENCES

Environnement Canada. 2004. Principe d'utilisation des sels. Retrieved from http://www.ec.gc.ca/

Neal, A. 2004. Ground Penetrating Radar and its use in sedimentology: principles, problems and progress.

NPRA. 2003. Håndbok 111 - Standard for drift og vedlikehold. In norwegian.

NPRA. 2006. Salt befuktet med varmt vann. Forsøk sesongen 2005/2006 og videre anbefalinger. In norwegian.

Nygaard, H. 2003. Rapport om restsaltsmåleren SOBO 20. In norwegian.

Reynolds, J. M. 1997. *An introduction to applied and environmental geophysics*. Wiley.

Saarenketo, T. 2006. Electrical properties of road materials and subgrade soils and the use of Ground Penetrating Radar in traffic infrastructures surveys.

Salt Institute. 2004. Le sel de voirie et notre environnement. In french.

Transportation Association of Canada. 2003. Gestion de la végétation. In french.

Transportation Association of Canada. 2003. Gestion du drainage et des eaux de ruissellement. In French.

Transportation Association of Canada. 1999. Road salt and snow and ice control.

Vaa, T. 2004. Norwegian experience with use of Magnesium Chloride.

Vaa, T., & Sakshaug, K. 2007. Salting av veger – En kunnskapoversikt. In norwegian.

ADDITIONAL RESOURCES

Eide, E. 2000. Radar Imaging of Small Objects Closely Below the Earth Surface.

Svanekil, A. 2007. Forsøk med varmbefuktet salt for å bedre friksjonen på vinteren. In norwegian.

Mangold, T. 2000. Road salt use for winter maintenance.

Stidger, R. W. 2003. The basics of salting and sanding. Better Roads magazine .

Sensors & Software Inc. Notes on Ground Penetrating Radar principles, procedures & applications.

PAPER 2

Accuracy of Ground Penetrating Radar in Bituminous Pavement Thickness Evaluation

Anne Lalagüe
MSc, PhD candidate
SINTEF Road and Railway Engineering
Trondheim, Norway
anne.lalague@sintef.no

Inge Hoff
Professor
NTNU Department of Civil and Transport Engineering
Trondheim, Norway
inge.hoff@ntnu.no

Abstract

The Ground Penetrating Radar technology is a non-destructive method used to investigate the subsurface, by transmitting electromagnetic waves and recording the electric echoes induced by dissimilar dielectric properties. One primary GPR application in pavements is evaluation of the layer thicknesses. Accuracy in predictions is essential for rehabilitation design, pavement management and quality control. Many studies have confirmed the accuracy of the GPR method, which generally range from 2% to 10%. However, the accuracy is greatly dependent on the dielectric properties of the materials, which are often unknown or roughly estimated. The objective of the presented study is to perform a comparative analysis of asphalt layer thickness estimation between GPR data and drilled cores values, while considering the dielectric permittivity.

1. Introduction

The GPR technology has become a valuable method over the past ten years in pavement investigations, and its use is nowadays well-spread in several countries. However, the technique has been a recent development in Norway, since the first Ground Penetrating Radar destined to road investigation purposes was purchased in 2006 by the Norwegian University of Science and Technology (NTNU), in cooperation with the research organization SINTEF.

The purpose of this investment has hitherto been to investigate the structures prior to rehabilitation. When the weakest sections have been identified, the optimal method for rehabilitation and design can be selected (Hoff, Hoven, & Eide, 2008).

Rehabilitation design required a range of information that can be obtained by GPR. One of the most useful data is the pavement layer thickness. Traditionally, this has been determined by drilling cores. This method is time-consuming, expensive and do not provide a continuous thickness profile. The GPR technique, as a fast, non-destructive and continuous method, represents an interesting alternative.

Much work has been carried out to determine the accuracy of GPR data, using in most cases horn antennas. GPR results have generally been compared to drilled cores and differences vary between 2 and 10% (Al-Qadi et al, 2005; Evants et al, 2008). New pavement layers seem to give

the best accuracy, ranging from 3 to 5% (Saarenketo T. , 2009). The highest accuracy (2,5mm) has been reported by Maser et al. (2003) by testing the horn antenna technique.

Ground Penetrating Radar purchased by NTNU and SINTEF is a three-dimensional step-frequency (SF) system using a bowtie antenna array. It can generate waveforms from 100 MHz up to 3 GHz. Tests previously conducted using a similar SF GPR demonstrated its capabilities in different civil engineering applications (Scott, Gagarin, Mills, & Oskard, 2006). An accuracy of 1,9% in average is obtained, comparing mean asphalt thickness along a ten mile section, and the design asphalt thickness.

This paper presents the results obtained from research on SF GPR accuracy, by comparing GPR with in situ core data. Each single asphalt layer thickness is assessed, as well as the total asphalt thickness, which constitutes the pavement.

2. Data collection

2.1 GPR measurements

Tests were carried out on a site awaiting rehabilitation works. The pavement structure consists of several thin asphalt layers over an aggregate base.

GPR data were collected using two SF GPRs operating respectively in the frequency ranges 100 MHz – 2 GHz and 100 MHz – 3 GHz. The measurements were performed with 31 antenna pairs, a distance travelled between each data collection location of 10 cm and the full bandwidth.

Two measurements were performed. The first testing took place before the rehabilitation works with the 2 GHz GPR. After the asphalt resurfacing was completed, the second measurement was performed using the 3 GHz GPR. A higher frequency gives a better resolution and enables to differentiate several asphalt layers. The accuracy of GPR data was evaluated for both asphalt/asphalt and asphalt/base interfaces.

Ten cores were collected at 2m intervals in the right wheel path, for each GPR measurement.

2.2 Dielectric measurement

The electrical properties of materials describe the propagation and reflection of electromagnetic waves. One of the most important properties is the dielectric permittivity ε. From this, the depth of the target can be determined. Therefore, it is essential to assign a correct value when analysing GPR data (Saarenketo T. , 2006).

The dielectric value of the cores was measured in the laboratory with the help of Percometer. This instrument calculates the real part of the complex relative dielectric permittivity from the change in the electrical capacity of the probe, cause by the sample under test. As recommended by the device manufacturer and as previously presented by Loizos & Plati (2007), the cores were first sawed to enable a perfect fit of the probe on the surface.

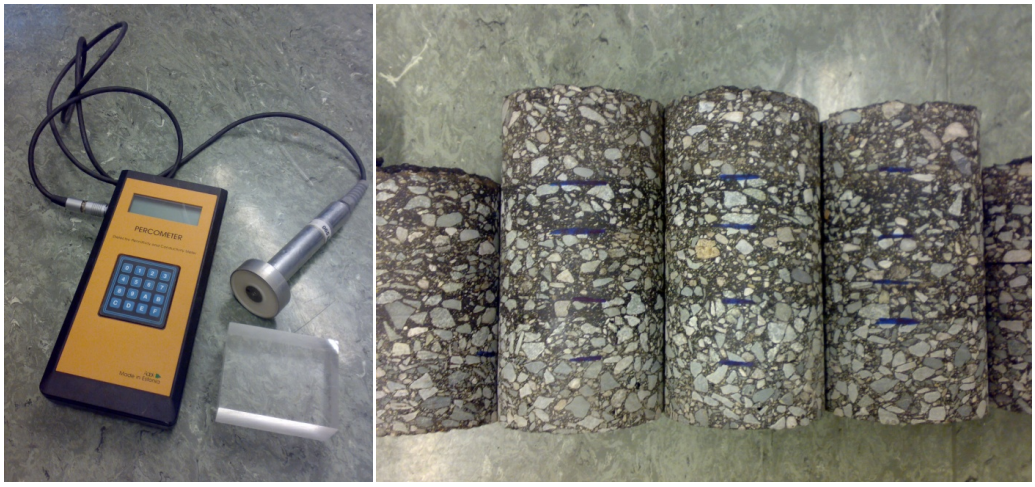

Figure 1 Percometer is used to measure the dielectric constant of cores

3. Results

The present section shows the results from GPR testing. Core thicknesses are considered as the reference values. The discrepancy between the true values (core thicknesses) and the GPR data is described by the relative error, which is the absolute error divided by the true value, expressed in percentage.

3.1 Total asphalt thickness using a 2 GHz-antenna

Figures 2 and 3 compare the GPR data with the core thicknesses. Figure 3 presents a quite good fit, with R^2 of 0,825. The slope value is slightly above 1, which indicates a general tendency for the GPR data to overestimate the asphalt thickness. Percent error ranges from 0,7 to 10% (Table 1), and has an average of 3,6%.

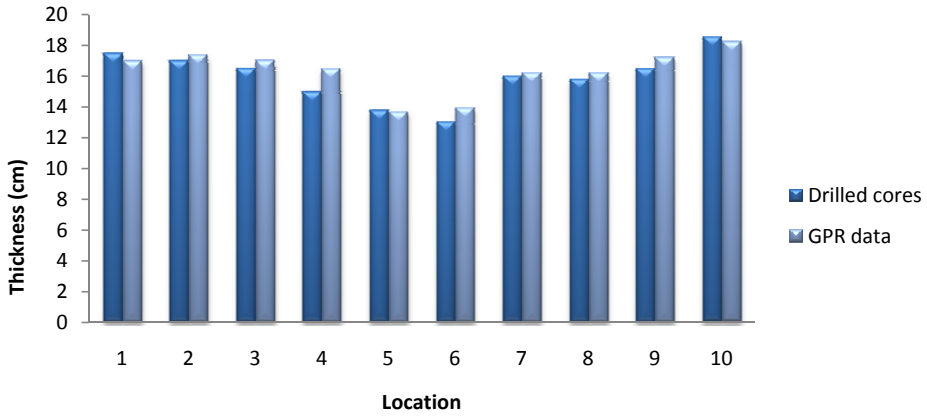

Figure 2 Comparison of cores and GPR thicknesses

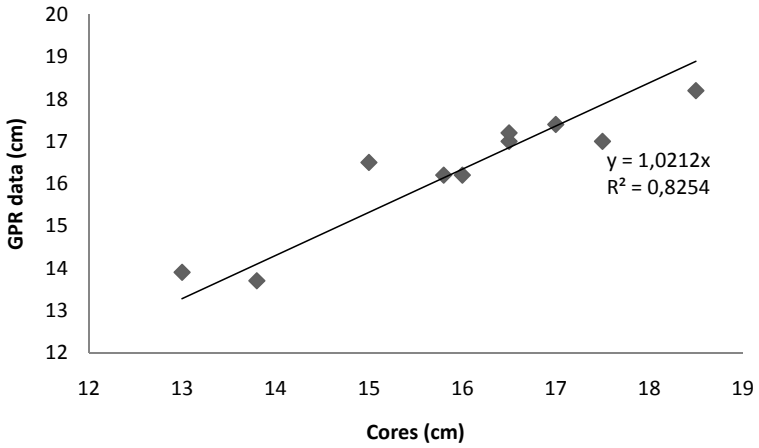

Figure 3 Correlation between cores and GPR thicknesses

Table 1 GPR relative errors compared to reference thicknesses measured on cores

Position	1	2	3	4	5	6	7	8	9	10	Average
%	2,9	2,4	3,0	10	0,7	6,9	1,3	2,5	4,2	1,6	3,6

3.2 Total asphalt thickness using a 3 GHz-antenna

Figures 4 and 5 compare the GPR data with the core thicknesses. Figure 5 presents a better fit than in the previous case, since R^2 is equal to 0,968. The slope is very close to 1, and indicates a general tendency for the GPR data to underestimate the asphalt thickness. Percent error ranges from 0 to 6,6% (Table 2), and has an average of 3,3%.

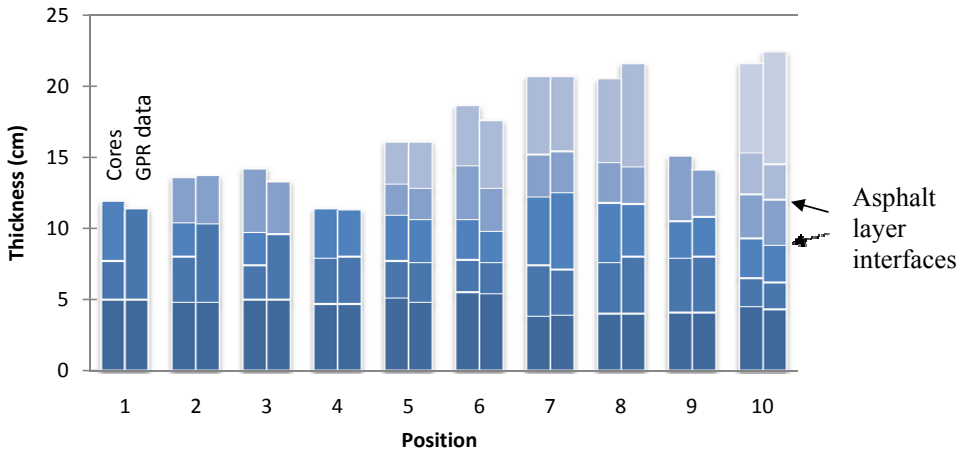

Figure 4 Comparison of cores and GPR thicknesses

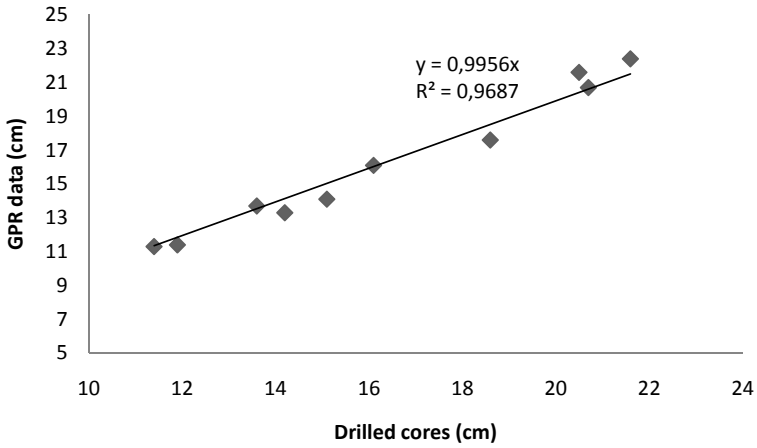

Figure 5 Correlation between cores and GPR

Table 2 GPR relative errors compared to reference thicknesses measured on cores

Position	1	2	3	4	5	6	7	8	9	10	Average
%	4,2	0,7	6,3	0,9	0,0	5,4	0,0	5,4	6,6	3,7	3,3

3.3 Asphalt layers thicknesses using a 3 GHz-antenna

Figure 4 compares as well the different asphalt layers thicknesses with GPR data.

Even if data are more scattered, Figure 6 presents a quite good fit with a R^2 of 0,863. The slope is slightly below 1, and indicates a tendency for the GPR data to underestimate the asphalt layers thicknesses. This leads to a general tendency to undercalculate the total asphalt thickness (cf. section 3.2). Percent error ranges from 0 to 25,4% (Table 3), and has an average of 8,2%.

Even if few values are available for the layers 4, 5 and 6, Table 3 shows an increase of the relative error with the depth.

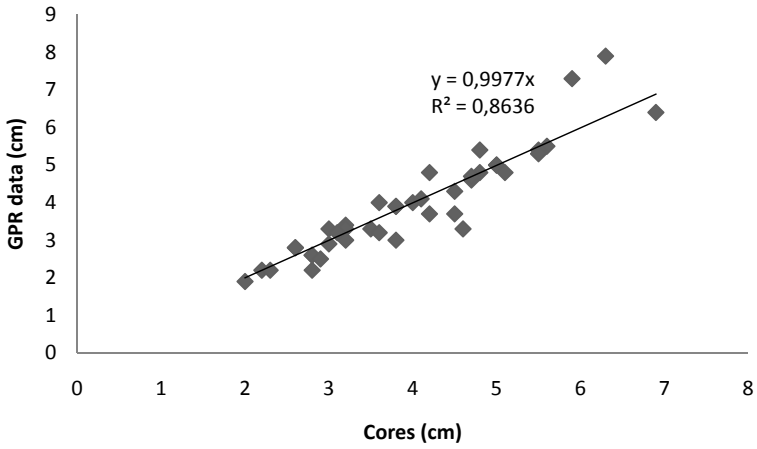

Figure 6 Correlation between cores and GPR

Table 3 GPR relative error compared to reference thicknesses measured on cores

	1	2	3	4	5	6	7	8	9	10	Average
layer 1	0	0	0	0	5,9	1,8	2,6	0	0	4,4	1,5
layer 2	7,2*	1,8*	2,1*	3,1	7,7	4,3	11,1	11,1	2,6	5	6,4
layer 3				5,7	6,2	21,4	12,5	11,9	7,7	7,1	10,4
layer 4		6,25	17,8		0	21	3,4	7,1	28,3	3,2	10,9
layer 5					10	14,3	3,6	23,7		13,8	13,1
layer 6										25,4	25,4

* Some asphalt interfaces where not directly visible on GPR data, in test locations 1, 2 and 3.

4. Conclusion

The present study aimed to determine the accuracy of the Step Frequency GPR used in Norway for maintenance and rehabilitation purposes. Tests performed on the field produced satisfactory results. It seems that the 3 GHz antenna gives a better accuracy (3,3%) than the 2GHz (3,6%), which is coherent with the GPR theory. Detection of several asphalt layers and estimation of the thicknesses have been made with an accuracy of 8,2%, which is an acceptable value for practical use. The accuracy is dependent on the value of ε. To secure confidence in the measured GPR data, supplementary cores and Percometer test could be performed.

The accuracy obtained shows that GPR is a useful tool for quality control of new asphalt layers and as a surveying tool before rehabilitation.

5. References

1. Hoff, I., Hoven, B., & Eide, E. (2008). 'Introduction of Ground Penetrating Radar in Pavement Rehabilitation in Norway', *Transport Research Arena Europe 2008*, Ljubljana, Slovenia.
2. Al-Qadi, I. L., Lahouar, S., Jiang, K., McGhee, K. K. & Mokarem, D. (2005). 'Accuracy of Ground Penetrating Radar for Estimating Rigid and Flexible Pavement Layer Thicknesses', *Journal of the Transportation Research Board, Issue number* 1940*,* pp. 69-78.
3. Evants, R., Frost, M., Stonecliffe-Jones, M. & Dixon, N. (2008). 'Review of Pavement Assessment Using Ground Penetrating Radar (GPR)', *12th International Conference on Ground Penetrating Radar*, Birmingham, England.
4. Saarenketo, T. (2009). 'NDT Transportation'. In H. M. Jol, *Ground Penetrating Radar: Theory and Applications,* pp. 395-444, Elsevier.
5. Maser, K. R., Holland, T. J., Roberts, R., & Popovics, J. (2003). 'Technology for quality assurance for new pavement thickness', *International Symposium on Non-Destructive Testing in Civil Engineering (NDT-CE)*, Berlin, Germany.
6. Scott, M., Gagarin, N., Mills, M. K., & Oskard, M. (2006). 'Step Frequency GPR Evaluation of the Natchez Trace Parkway: Pavement and Infrastructure Measurement and Assessment for FHWA Digital Highway Measurement Vehicle Applications'. *Highway Geophysics - NDE Conference.* St-Louis, Missouri.
7. Saarenketo, T. (2006). *Electrical properties of road materials and subgrade soils and the use of Ground Penetrating Radar in traffic infrastructure surveys (Doctoral dissertation).* Oulu University, Finland.
8. Loizos, A., & Plati, C. (2007). 'Accuracy of pavement thicknesses estimation using different ground penetrating radar analysis approaches', *NDT&E International, Volume* 40*, Issue* 2*,* pp. 147-157.

PAPER 3

Determination of space behind pre-cast concrete elements in tunnels using GPR

Anne Lalagüe
SINTEF Road and Railway Engineering
Trondheim, Norway
anne.lalague@sintef.no

Inge Hoff
NTNU Road and Transport Engineering
Trondheim, Norway
inge.hoff@ntnu.no

Abstract - **Many tunnels in Nordic countries are lined with prefabricated concrete elements to protect against frost and leakages. This protective lining is fixed to the rock face in a few points, but when installed renders the rock surface inaccessible, owing to the lack of predesigned inspection hatches. Safety inspections have hitherto consisted of random drilling into the concrete lining. However, such random inspection is both unreliable and expensive. Therefore Ground Penetrating Radar has been introduced in the vault walls to map the contours of the gap more systematically. Such scanning technology provides satisfactory data, given optimal location of apertures. The scanning technique is therefore extended to the vault roof to pinpoint potential rockfalls.**

Keywords – Ground Penetrating Radar; tunnel engineering; safety inspection

I. INTRODUCTION

Due to its mountainous areas and fjords that make the coastline extremely rugged, Norway has acquired an international reputation in tunnel and bridge construction. However, the Norwegian expertise has suffered a serious setback three years ago: on December 25th 2006 night, the concrete roof of the Hanekleiv tunnel (Vestfold County, south of Norway) caved in and 200m^3 of rock, reinforcement and concrete fell down on the lanes (Fig. 1). Thanks to the late hour on Christmas Day, no car was present and nobody was injured. Rubble extended over 30m long, and piled up until they reached the former tunnel's roof. A few weeks later, an investigation showed that the tunnel was insufficiently secured.

Despite the prompt renovation and the resignation of the director of the Norwegian Public Road Administration, concerns about tunnels safety resurfaced. The decision was made to inspect the rock surface of a majority of tunnels in Norway.

II. TUNNEL ENGINEERING

A. Construction method

Geologically, Norway is a typical hard rock province: about 2/3 of the bedrock is Precambrian (gneiss, granite, gabbros and quartzite) and 1/3 is Palaeozoic (mica schist, marble and greenstone). From a rock engineering point of view, most of the rocks found in Norway seem to be of high quality [1]. For this reason, the Drill & Blast technique is widely employed, rather than excavation with the Tunnel Boring Machine (TBM). The first operation consists in drilling holes in tunnel's face by the percussive method. They are partially filled with high strength explosives which are then detonated with detonators. In contrast to the smooth finish with the TBM technique, the contour of the tunnel is rough because of the blast, even if smaller charges are often used close to the contour.

The type of rock supports selected depends on the rock conditions [2]. In poor rock, a concrete lining for stabilization is preferable. In good quality rock, a minimum of support is required. Most of Norwegian tunnels fall into this category. Nevertheless, due to the cold climate, they often need a light concrete protection against water leakages and frost damages.

Figure 1. Rockfall in Hanekleiv tunnel

B. The inner lining

The inner lining should provide an efficient protection against water, frost, fire, pollution, high pressure cleaning and load. Visual criteria such as reflection of light and optical alignment must be considered as well. Several technical solutions exist. However, experience from the Nordic countries reveals that pre-fabricated concrete elements are not only the most common linings, but also the best durable in high-traffic

tunnels [3]. They offer a good protection against frost and water leakages. However they are expensive and not versatile with regards to geometry.

The inner lining is fastened to the rock by rock bolts but is not intended to be a rock support. The rock surface is hard to access because the linings were often not designed with inspection hatches. The access to the rock mass surface is therefore solely possible by cutting openings through the concrete walls.

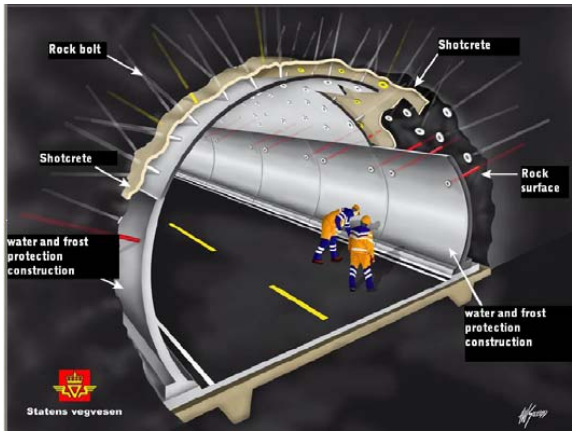

Figure 2. Tunnel cross section showing the inner lining (Statens Vegvesen)

C. *Tunnel safety*

Inspections of tunnels have to be carried out according to the geological situation and the installed safety measure, as stipulated by the Norwegian regulation [4]. If these are not assessed and registered, a condition evaluation including material examination and rating takes place each year. Otherwise, the control frequency is five years.

D. *Rock inspection*

Several methods of inspection exist, but they generally require a direct access to the rock face. Since most of the concrete vaults were not designed with hatches, it is necessary to create apertures in positions that give the inspector best possible visual access to the rock surface. The space between the wall and the rock surface is not usually known, so Ground Penetrating Radar has been used to scan the concrete lining continuously along the tunnel.

Figure 3. Space between the concrete vault and the rock surface

III. GPR PRINCIPLES

Ground Penetrating Radar (GPR) is a nondestructive method used to image the subsurface. It is able to detect objects, such as cables, pipes, drains, waterways, groundwork, iron framework and anchorages. In geology and geotechnics, it is employed to determine the layout and the thickness of the different layers. If appropriately used, it is time-saving and improves the safety during construction works.

GPR transmits electromagnetic waves into the structure to be studied and records the electric echoes induced by the dielectric properties differences between two materials. It takes into account the round-trip time and the amplitude of the signal. An image is created when the operator moves the device across the surface. Depth range and resolution depend on the several factors. If the electrical conductivity of the ground increases, the energy is likely to dissipate into heat, then the penetration depth decreases. While high frequencies penetrate less deeply into the soil than lower frequencies, they provide a better resolution. Sands, gravels, ballasts and rocks are easily penetrated. Concretes, due to their homogeneity, create goods images of their intern structure as well. In contrast, clays and saline soils can constitute obstacles.

IV. FIELD EQUIPMENT AND DATA ACQUISITION

A. *Equipment*

The equipment used is a GeoScope, designed and manufactured by 3D-RADAR. It consists of a GeoScope Radar Unit which constitutes the core of the assemblage. It generates the digital signals (electromagnetic waves) and stores the collected data. The frequency ranges from 100MHz to 2GHz. The air-coupled antenna array is 60cm wide using 7 active elements. The space between two elements is 7.5 cm that gives a maximum scan width equals to 52,5cm, suitable for tunnel inspections. The Distance Measurement Interval (DMI) is an optical encoder which measures the distance. It is placed on the wheel and connected to the GeoScope unit. An Operator PC is used for configuring the parameters (frequency range, selection

of active elements, measurement interval) and displaying data acquisition.

B. Wall scanning

To fit vertical surfaces, an arm has specially been designed. This is assembled to a lightweight frame which is directly mounted to the vehicle's bumper. The following figure shows the system at work:

Figure 4. Vehicle bracket with arm mounted to allow surveying tunnel walls.

In case of obstacles (road signs, emergency exit, parking space, extinguishers…), the antenna was lifted with ropes and an electric winch.

Each tunnel side was measured at two different heights: approximately 1,5m and 2m (Fig. 5). With careful driving, it was possible to maintain a constant height along the walls.

The longitudinal distance was measured in one go. The traffic was either closed or restricted, and did not impede with the measurements which were performed relatively quickly.

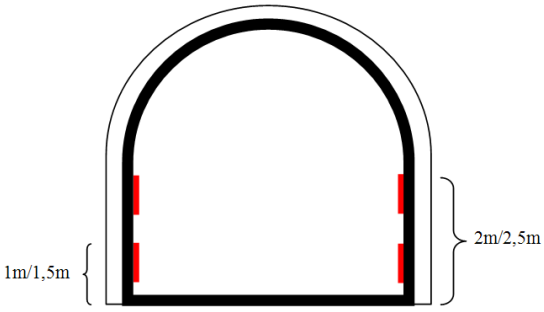

Figure 5. Tunnel cross section

C. Roof scanning – pilot study

Although it is useful to map the cavity, it is still necessary to conduct a manual inspection of the bedrock surface to detect loose rocks and materials located on the roof.

To investigate whether the radar can be used for such purposes, a little test was carried out by hooking up some sand bags on the inside of the vault in one of the investigated tunnels. Fig. 6 shows plastic bags filled with moist crushed stones placed inside the cavity. They are hung on crossbars at 1m high. Each bag weighs from 15 to 20 kg.

Figure 6. Bags with wet sand placed on the inside of the protective wall

V. RESULTS AND DISCUSSION

A. Wall scanning

The radar data were processed and displayed using the program Road Doctor, developed and distributed by Roadscanners Oy. The interpretation phase follows the processing operation and is done manually or semi-automatically. Thirteen tunnels were investigated, with lengths ranging from lengths from 200 to 5000 m:

TABLE I. TUNNELS INVESTIGATED

Tunnel	Road number	Length (m)
Hitra	RV714	5645
Hell	E6	2573
Grillstadhaug	E6	750
Svølgja	RV30	700
Være	E6	1625
Håggå	E6	290
Brattli	E6	210
Brattås	RV18	523
Hove	RV18	541
Steinbrekka	RV18	184
Blindheim	EV39	≈ 1000
Furnes	RV61	≈ 175
Skuggen	EV136	≈ 200

For all these tunnels (except one, see below), it was relatively easy to find bedrock surface and the back of the vault. Since the dielectric constant (ε) is constant for air, the cavity's width can be calculated with good accuracy. The distance varies greatly from a few centimeters (contact) up to more than one meter. From the profiles the best placement for inspection hatches can be found (Fig. 7).

B. Special case in Væretunnel

The second examined tunnel (Væretunnel, east of Trondheim), gave no clear results. Reflections were dampened, as if the waves could not penetrate the concrete lining. Upon closer investigation it turned out that the vaults were built of lightweight concrete with LECA balls (Lightweight Expanded Clay Aggregate) as aggregates.

This mixture of LECA balls with a very low density and mortar with a high density could diffuse the waves so that it is not possible to interpret the reflections. Fortunately, this type of vault is unusual in Norway and this problem no longer happened thereafter.

C. Roof scanning – pilot study

After interpretation of the results the following observations could be made (Fig. 8):

- Joints can easily be spotted.
- The sandbags result in a parabola (small black trace on the print screen). The red parabola is manually added with an interpretation tool, the average object size can be determined from this.
- The others object dimensions can be found from the cross section and time slice.

One should admit that the interpretation was easier because the sandbags location was known. If it was not the case, the parabola could have been missed in the interpretation. The pilot study gave promising results and a full scale testing was performed.

VI. FURTHER RESEARCH

The equipment worked very well to determine space between the inner lining and the rock face. Several tunnels have been studied. From the profiles the best placement for inspection hatches could be found.

In some tunnels, it is difficult to implement a manual inspection because there is simply too little space to climb on the lining in a secure way. For these tunnels, it may be relevant to use Ground Penetrating Radar to look for stone that lies on top of the vault. Such loose stones that have fallen will be a danger signal that the rock mass is unstable and that it must be investigated manually.

Through a pilot project, it was shown that the equipment is well suited to find material that is in contact with the vault. Before such investigations can be carried out, a system must be developed to examine the roof of the tunnel and not just the walls that today's equipment does. This can be done relatively easily by using for example a self-propelled lift. Cost of renting is modest and it is possible to rent such equipment over almost the entire country.

VII. CONCLUSION

The following conclusions can be drawn from the completed surveys:

- The equipment has proven to be reliable and useful for determining the distance between the inside of the vaults and the rock surface.
- For vaults with lightweight concrete with LECA as aggregates, it appears that the method can not be used.
- It is possible to find objects that are in contact with the vault
- Investigations of the tunnel's roof require some customization work but it is probably worthwhile.

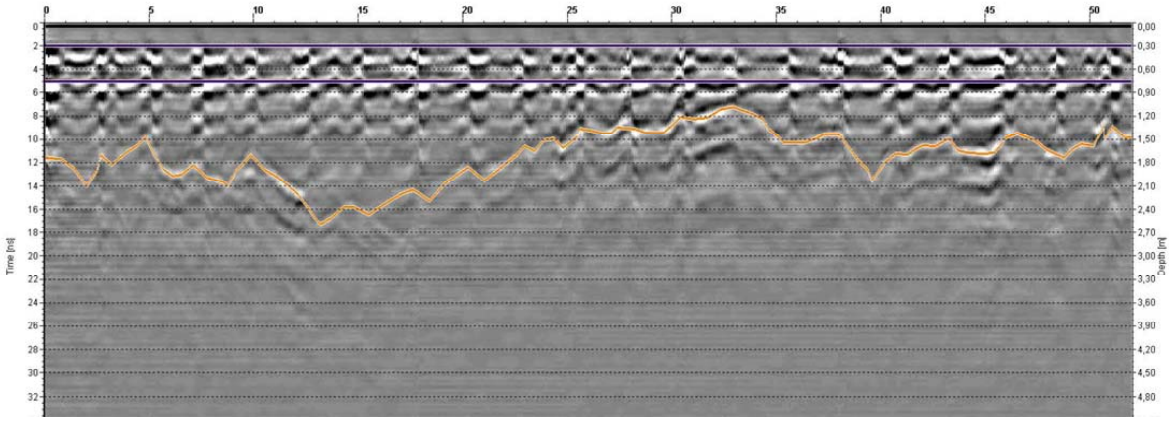

Figure 7. Extract of radargram

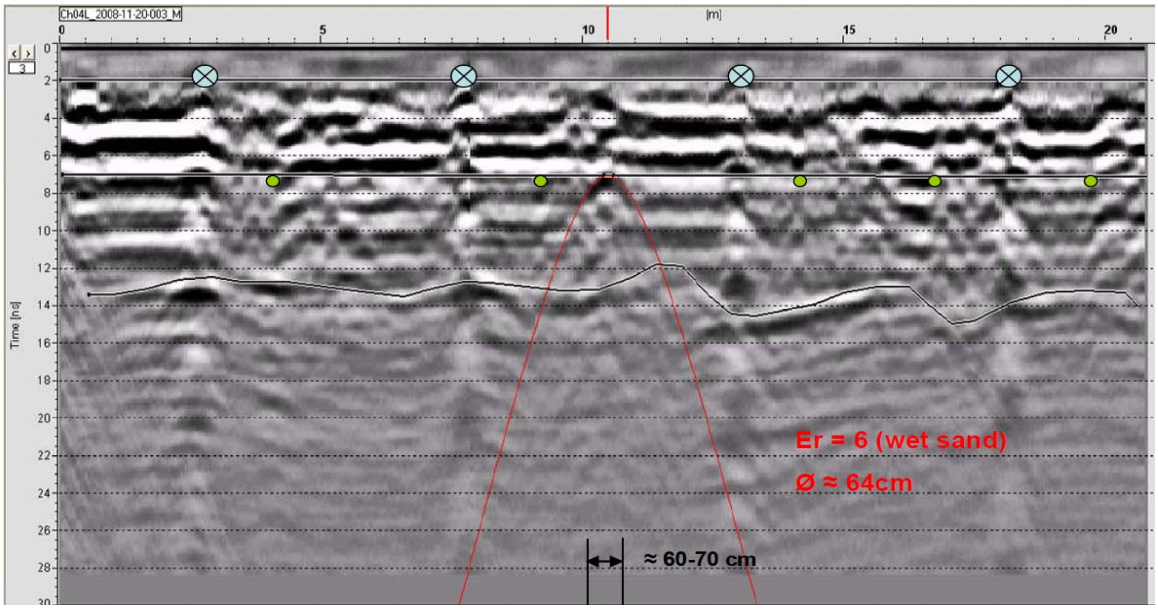

Figure 8. Interpretation of the pilot study

REFERENCES

[1] B. Nilsen and A. Thidemann, "Rock Engineering", Volume no.9 in the Hydropower development series, published by Norwegian Institute of Technology, 1993, pp. 156, ISBN 82-7598-017-8.

[2] B. Nilsen and A. Palmstrøm, "Engineering Geology and Rock Engineering. Handbook no.2", published by the Norwegian Soil and Rock Engineering Association, 2000, pp. 249. ISBN 82-91341-33-8.

[3] E.Broch, E.Grøv and K.I.Davik ,"The inner lining system in Norwegian traffic tunnels", Tunneling and Underground Space Technology, volume 17, issue 3, 2002, pp 305-314.

[4] Norwegian Public Road Administration, "Håndbok 111- Standard for drift og vedlikehold", 2003, in norwegian.

PAPER 4

Bearing capacity of airfield pavements – In situ survey, measurements and calculations using GPR and FWD

A. Lalagüe
Department of Civil and Transport Engineering, Norwegian University of Science and Technology (NTNU), Trondheim, Norway

D. Gryteselv
SINTEF Road and Railway Engineering, Trondheim, Norway

I. Hoff
Department of Civil and Transport Engineering, Norwegian University of Science and Technology (NTNU), Trondheim, Norway

ABSTRACT: Runways, taxiways and aprons must have documented their bearing capacity with PCN value (Pavement Classification Number), preferably by a technical evaluation. On new structures this is normally relatively simple to accomplish. On older parts with unknown layer structure and material properties this can be a challenging task. SINTEF/NTNU has been using data from FWD (Falling Weight Deflectometer) in combination with GPR (Ground Penetration Radar) to estimate the PCN value both of asphalt and concrete pavements. GPR is used to estimate layer structures, layer thickness and to a certain extent the type and characteristics of material in each layer. Backcalculation of FWD data is used to estimate the modulus of elasticity of each material layer. By using GPR data, FWD data and aircraft traffic data as input in a suitable calculation program system the PCN value can be estimated. Despite several challenges and many uncertain factors this could be a cost-effective way to estimate PCN values compared to other extensive destructive investigations and material testing.

KEY WORDS: Bearing Capacity, in-situ survey, GPR, FWD.

1 INTRODUCTION

Airfields owners must document the bearing capacity giving a PCN value (Pavement Classification Number). The PCN value must be assessed for each main section of the airfield, preferably by a technical calculation or evaluation. This means that each runway, taxiway and apron should be evaluated separately if the structure and/or the traffic/load vary. With new structures and known materials and layer thicknesses, this is relatively simple to accomplish. A structural design based on equivalent traffic and load is normally also done prior to construction.

Old structures are usually far more difficult to evaluate. Construction data are commonly unknown. To obtain layer thicknesses and material properties, an extensive destructive examination together with time consuming laboratory and/or field tests is necessary.

By combining two nondestructive technologies such as Ground Penetrating Radar (GPR) and Falling Weight Deflectometer (FWD), it is possible to reduce the time to collect data about existing structure. GPR is used to measure layer thickness and identify the main type of material (i.e. bituminous, non-bituminous, and concrete). To a certain extent also some material properties can be detected. Nevertheless a few destructive investigations like core drilling or excavating to calibrate GPR data is still indispensable.

This paper presents experiences from investigating some Norwegian airfields with emphasis on the use of GPR to examine the existing structure and the use of FWD to estimate the structure stiffness with the purpose of assessing the PCN value.

2 USING 3D-GPR

2.1 Principle

Ground Penetrating Radar (GPR) is a nondestructive method used to map the subsurface. It sends electromagnetic waves to the ground and registers the reflected signals induced by the dielectric properties differences between two materials. An image is then created when moving along the surface. Depth range and resolution depend mainly on the operating frequency and the electrical conductivity of the ground. High frequencies penetrate less into the soil than lower frequencies but give a better resolution. Exploration depth is very limited in highly-conductive soils such as clay and saline soils, but sand, gravel, ballast and bedrock are easily penetrated.

GPR can detect all kinds of objects, as long as they are of substantial size (5 – 10 cm) and have dissimilar dielectric properties from the host environment. Cables, pipes, drains, waterways, groundwork, iron framework, anchorage are thus usually easily detected. In road engineering, GPR is used in quality control to determine the layout and the thickness of the different layers. Non reinforced concretes, found in most Norwegian airfields, usually give good response as well.

If appropriately used, the GPR technology is time-saving, cost effective and provides more valuable information than any other ground exploration methods.

2.2 Case study from Norwegian airports

The GPR technique has successfully been used in Norway to identify the airfield structure. Airfield structures usually fall into two categories: flexible (asphalt) and rigid (concrete) pavements. Concrete can be reinforced or not, and may sometimes be covered by an asphalt layer. The thickness of the design is directly correlated to the bearing capacity of the structure and is a key parameter in quality control investigations.

The Figures below show typical airfield structures that can be found in Norway, along with the corresponding radar profile:

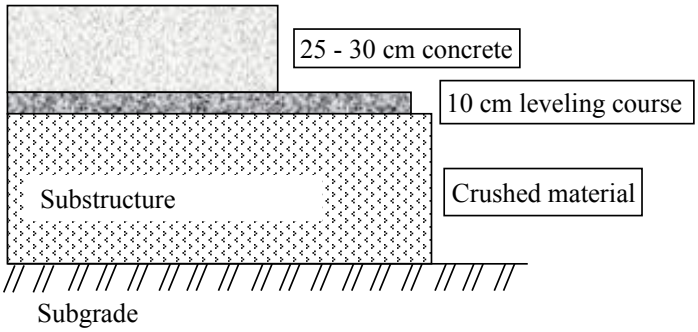

Figure 1: Typical Norwegian rigid pavement structure

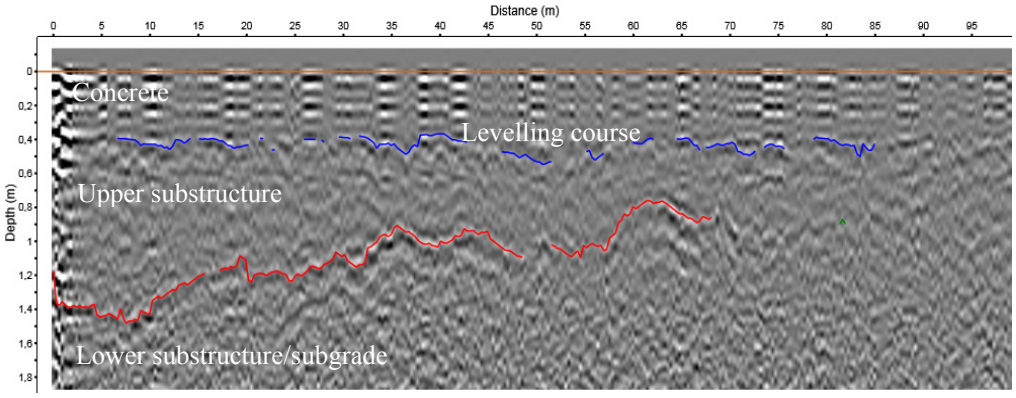

Figure 2: Non-reinforced concrete pavement - GPR profile (inline view)

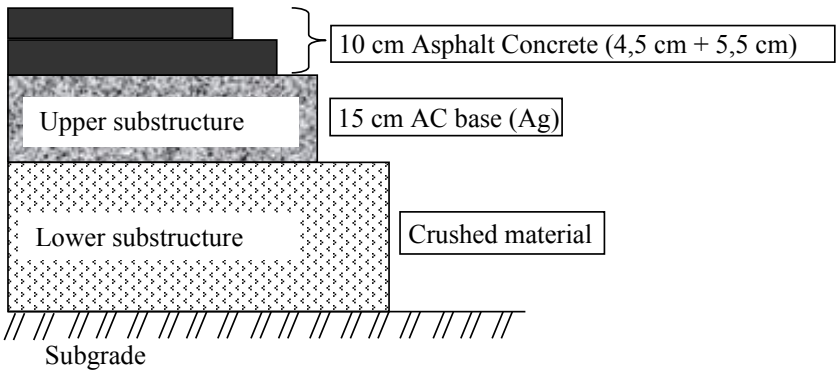

Figure 3: Typical Norwegian flexible pavement structure

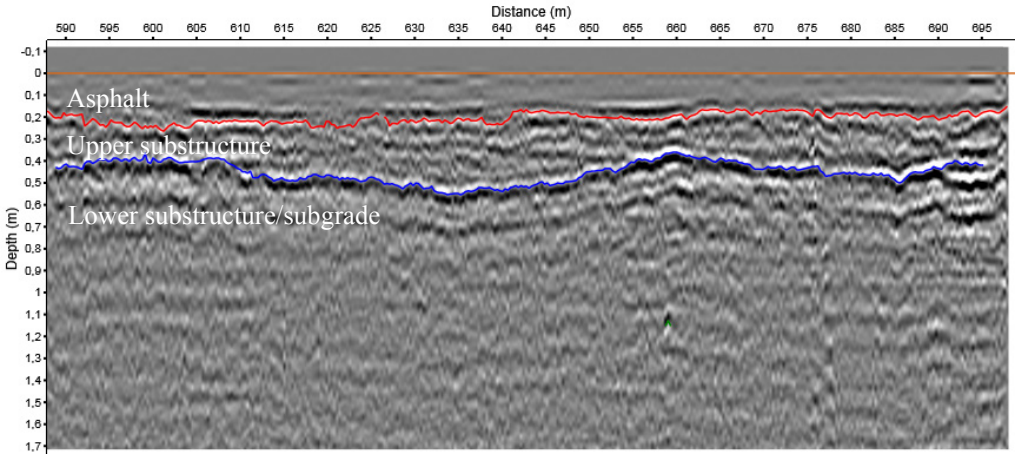

Figure 4: Asphalt pavement – GPR profile (inline view)

As can be seen in Figures 2 and 4, layers are not always homogenously defined and thicknesses may vary greatly. In the absence of documentation, an application of GPR would be to locate abrupt changes in layers thicknesses (Figure 5) or subsurface defects (settlements par example).

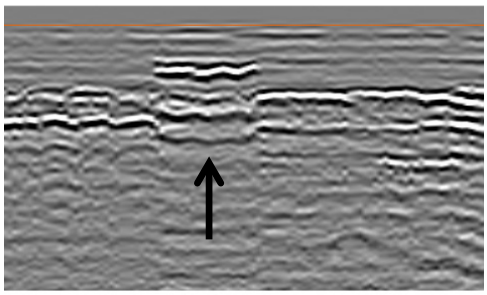

Figure 5: Change in the pavement structure resulting from rehabilitation works (GPR profile - inline view)

Sometimes, asphalt overlays are laid over concrete slabs to rehabilitate runways. Again, when works are not sufficiently documented or if information is missing, GPR can successfully be used to map asphalt and concrete areas. The total pavement thickness is usually different and can be plotted on a color depth map (top view, Figure 7). However, the depth of penetration depends greatly on the surveyed material and may be limited in concrete pavements. Uncertainties (poor signal strength) are therefore not interpreted or sometimes indicated by a dashed line.

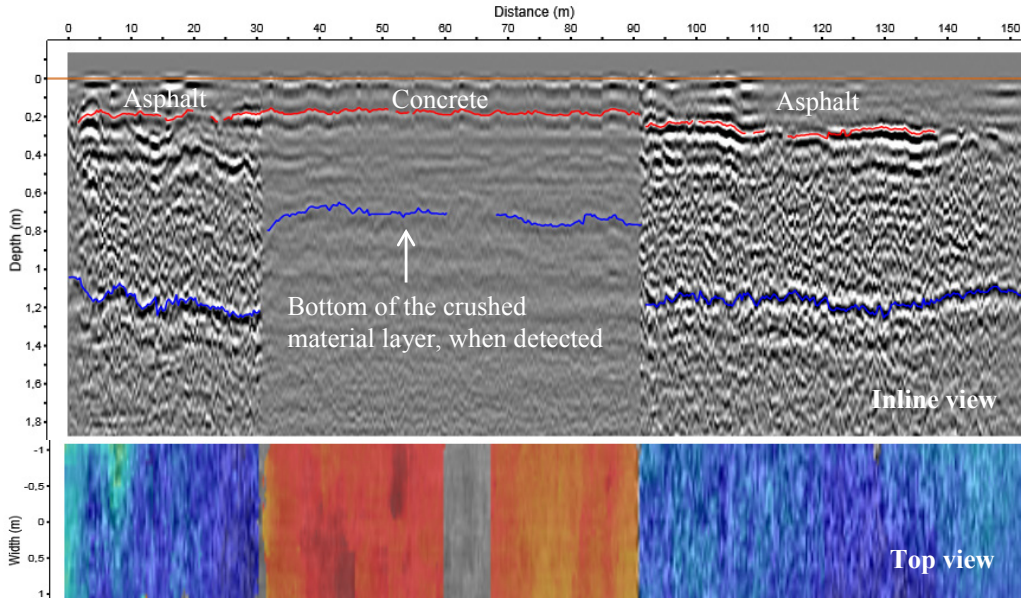

Figure 6: Asphalt and concrete structures

GPR is also commonly used to locate any anomaly or buried object in the ground. The Figure below shows an asphalt pavement GPR profile taken from a Norwegian airfield. In asphalt/base course materials the depth of penetration is usually very good and objects are easily detected. The anomaly number 1 has a size of about 1 m x 0,5 m and is 1,25 m deep. GPR detects changes in dielectric properties but does not provide much information about the nature or type of the surveyed material. Object number 1 can for example be a cavity, a plate or another buried structure. Object number 2 is about 0,70 m wide and minimum 2 m long. Thanks to the cross profile and top views that display the shape of the object, it can be assumed that it is a pipe.

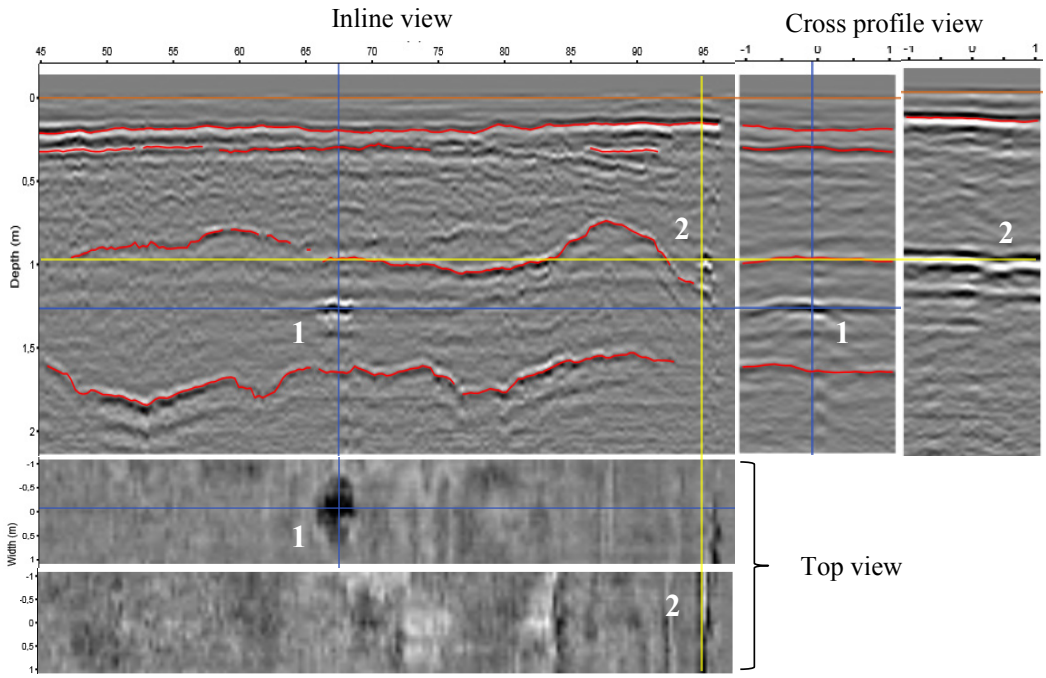

Figure 7: Located objects in the ground

GPR is a reliable geophysical method used to map the subsurface, detect anomalies in the pavement structure and locate buried objects. It has some performance limitations caused mostly by the environment. Highly-conductive soils (clay, peat) and brine from winter maintenance should be avoided to ensure effective results. The method becomes more powerful when used in combination with conventional site investigations such as drilling; soil surveys are consequently more comprehensive and thorough, cost-effective and time-saving.

3 USING FWD

FWD - Falling Weight Deflectometer is used to estimate the structural capacity of the overall pavement structure; surface deflections are then an input for the backcalculation of the individual layers stiffness (E-moduli). Layer thicknesses and main material types (i.e. concrete, bituminous, non-bituminous) can be found from GPR measurements and analysis. In this example a Dynatest 8000 FWD (Figure 8) is used. Normally the load will be approximately 130 kN with a contact stress of 1.8 MPa. This is somewhat less than the load of most design aircrafts. Since the materials involved normally show a non-linear stiffness, an insufficient load will underestimate the layer moduli.

Figure 8: FWD operated by the Norwegian Public Road Administration (NPRA), Region North

The measured stiffness can vary a lot along a section. Figure 9 shows this quite clearly where deflection basins for three locations on the same section are illustrated.

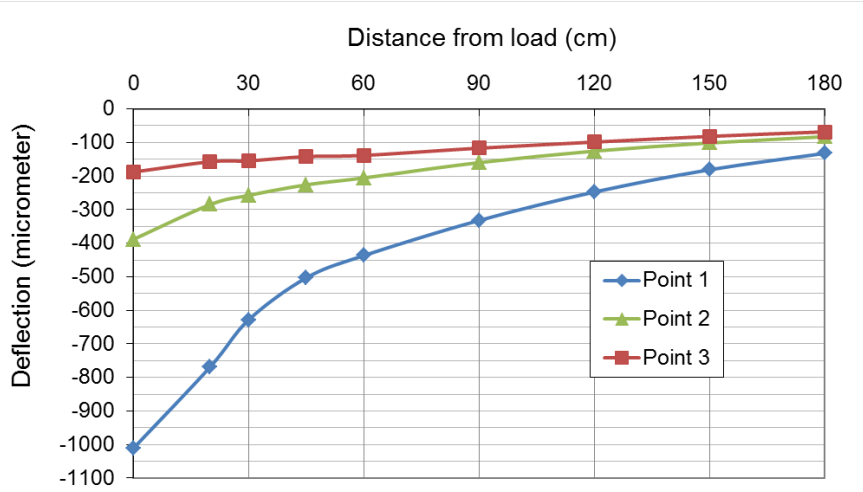

Figure 9: Example of deflection basin for three different locations on the same section

Obviously the structure could be expected to be different in the three locations shown in Figure 9. This is not always true. Thus local weaknesses or strengths can be discovered in this way. Even with only 30 – 50 meters between the drops it will not be possible to locate every weakness. By using the continuous GPR scanning profile it is possible to become aware of local suspicious variations along the sections that could need closer examinations.

Figure 10 shows variations along a taxiway. The tests have been done in two lines, 5 m from the centerline. The spacing between points is 50 m. Stiffness is here simply defined as maximum stress divided by maximum deflection. Even if local variations may be important, it

is easy to see the change in response at about 1400 m when the structural response is completely different.

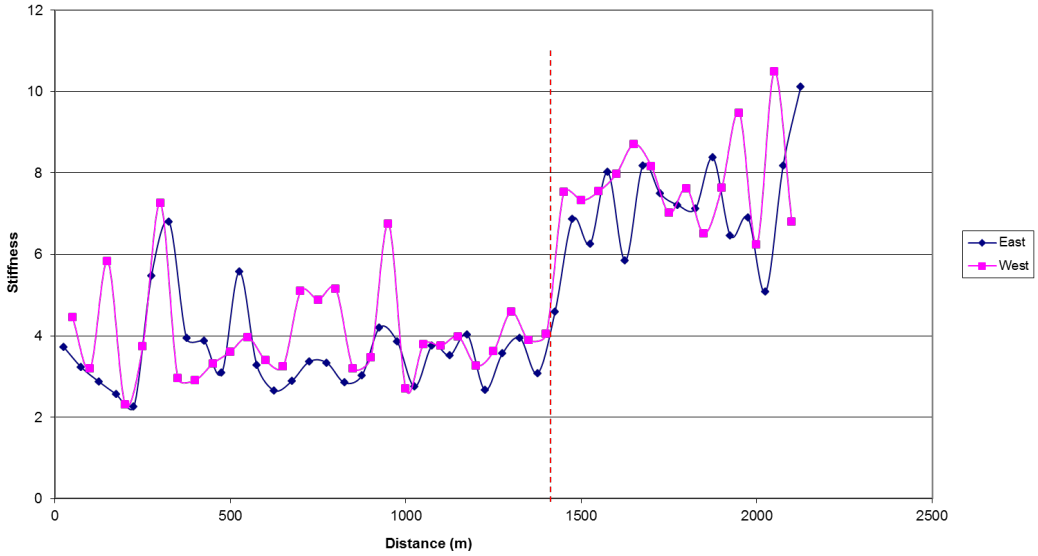

Figure 10: Variation of the structure stiffness along one of the taxiways.

In our work we used the 90-percentile value of measured stiffness from FWD as an input to backcalculation analysis to avoid using the extreme high values you always will find. Even with good knowledge of layer thickness and good FWD data available it will be necessary to apply engineering judgment to secure useful results. Backcalculation will often place too high stiffness in one layer and too low in the next.

Table 1: Backcalculated values and values used for resilient modulus (MPa)

Layer	Thickness	5 m east	5 m west	Average	Value used in analyses
Asphalt	100 mm	12618	20811	16715	4 000
Asphalt base course	150 mm	706	100	403	1 100
Glacial gravel	500 mm	153	2845	1499	310
Soil	N/A	416	312	364	250

As can be seen from Table 1 the difference between the calculated stiffness and the stiffness based on engineering judgment can vary quite a bit. The values used for analyses give the same total deflection for the FWD-blow, but the distribution of stiffness (and by this the deflection bowl) is quite different. The table above illustrates the problem with inaccurate determination of layer thickness. If the real layer thickness deviates from what is used in modeling the calculated stiffness will be affected quite extensively.

4 CALCULATION / ESTIMATION OF PCN

The ACN/PCN (Aircraft/Pavement Classification Number) method is used to calculate the bearing capacity of an airport i.e. the aircraft with the highest ACN number that can drive the airport without causing need for excess maintenance. The PCN does not give any information about the risk for immediate failure of a single especially heavy plane. The Norwegian regulations require the PCN value to be published for all airports, but the regulations do not specify how this should be done.

Two different tools have been used for calculating PCN: Pavers and PCASE. Both can use data from FWD as an input to accomplish backcalculation of layer parameters. Both can use fatigue models for estimating the number of design aircraft passages allowed before permanent damage occur (cracking or deformation). Pavers is as far as we have found out easier to use because of better handling of FWD data and easier use of metric units. PCASE can be faster in estimating PCN value if construction data and material properties are known.

Fatigue modeling of asphalt pavements is not straight forward and several models have been proposed and are in use. The choice of model will greatly influence the resulting estimation of pavement fatigue life. For the analyses of the Norwegian airports the fatigue model called DWW F78 in the Pavers system has been used:

$$\log N = 26{,}676 - 7{,}327 \times \log(E) + 0{,}769 \times \log2(E) - 5{,}851 \times \log(\varepsilon)$$

Where:
N = Number of load repetitions until fatigue
E = Young's modulus
ε = Horizontal strain at the bottom of the asphalt layer.

For soil another «fatigue»-model was used:

$$\text{Log } N = 25{,}305 - 7{,}14 \times \log(\varepsilon(z))$$

Where ε(z) is vertical strain in the soil layer.

The Pavers system does not consider other distress modes like permanent deformations in the layers above the soil. The method is also quite sensitive for small changes in input parameters. Nevertheless, used together with good input data and sound engineering judgment the method gives reasonable results for typical structures and common traffic situations. For more untypical structures or traffic, more advanced analyses should be considered.

5 CONCLUSIONS

SINTEF/NTNU has been using data from FWD in combination with GPR (Ground Penetration Radar) to estimate the PCN value both of asphalt and concrete pavements. GPR is used to estimate layer structures, layer thickness and to a certain extent the type and characteristics of material in each layer. Backcalculation of FWD data is used to estimate the modulus of elasticity of each material layer. By using GPR data, FWD data and aircraft traffic data as input in a suitable calculation program system, the PCN value can be estimated. Despite several challenges and uncertain factors this could be a cost-effective way to estimate PCN values compared to other extensive destructive investigations and material testing.

REFERENCES

Adolf, M. et al., 2010. *PCASE 2.09. User manual*. US Army Corps of Engineers. Transportation System Center & Engineering Research and Development.

CROW. *Guideline on PCN Assignment in the Netherlands.* CROW-report 05-06.

CROW. *PCN procedure for technical evaluation of flexible and rigid pavements.* www.crow.nl

CROW. *The PCN Runway Strength Rating and Load Control System*. CROW-report 04-09

Eide, E., Sandnes, P. A., Nilssenand, B. and Tjora, S. T. 2005. *Airfield runway inspection using 3 dimensional GPR*. Proceedings of the 3rd International Workshop on Advance Ground Penetrating Radar (IWAGPR), pp 87-91, Delft, The Netherlands.

Garba, R. and Horvli, I. 2002. *Prediction of Rutting Resistance of Asphalt Mixtures.* Proceedings of the Sixth International Conference on the Bearing Capacity of Roads, Railways, and Airfields, Lisbon, Portugal.

Mork, H. *Utrekning av bæreevne frå nedbøyingsmålingar*. Notat 432, Institutt for Veg og jernbanebygging, NTH. Trondheim 1987 (in Norwegian).

Saarenketo, T. 2006. *Electrical properties of road materials and subgrade soils and the use of Ground Penetrating Radar in traffic infrastructure survey.* PhD thesis. ISBN 951-42-82221.

Samferdselsdepartementet. *Forskrift om utforming av store flyplasser*. FOR-2006-07-06-968 (in Norwegian).

Thompson, M. Gomez-Ramirez, F., Gervais, E. and Roginski, M. 2006. *Concepts for Developing a Mechanistic-Empirical Based CAN Procedure for New Generation Aircraft*. Proceedings of the 10th International Conference on Asphalt Pavements (ICAP), Québec City, Canada.

PAPER 5

Is not included due to copyright

PAPER 6

Accuracy of Ground Penetrating Radar in Pavement Thickness Evaluation – Impact of Interpretation Errors

Anne Lalagüe[a*], Matthew A. Lebens[b], Inge Hoff[c]

[a]*SINTEF Building and Infrastructure, Trondheim, Norway*
[b]*Minnesota Department of Transportation, Maplewood, MN, USA*
[c]*Norwegian University of Science and Technology,Trondheim, Norway*

Abstract

Ground penetrating radar (GPR) is a nondestructive technique used by road engineers to evaluate the condition and the layer thickness of the pavement structure. The reliability of the method is related to the characterization of the dielectric constant Ɛ of the material, which can be determined from core samples or GPR data. Although numerous research studies report an accuracy of the layer thickness ranging from 3 % to 10 %, the level of confidence of the GPR data is still questioned. This lack of confidence is not only related to the GPR capabilities but is also affected by the interpretation process of the recorded data.
In this project, an asphalt pavement was scanned and then analyzed both manually and using a semi-automatic software layer tracking tool. Despite the large amounts of GPR data that are usually collected during road surveys, it is often necessary to interpret the data manually. It was shown in this study that an incorrect layer tracking results in an asphalt thickness error of 19,9 % instead of 3,6 % when using manual interpretation.

Keywords: GPR; Pavement layer thickness, Accuracy, Manual and semi-automatic interpretation

Résumé

Le radar à pénétration de sol (ou GPR pour Ground Penetrating Radar) est une méthode géophysique non destructrice couramment utilisée par les ingénieurs routiers pour évaluer la qualité de la structure des chaussées. La précision des données obtenues dépend en grande partie de la constante diélectrique Ɛ des matériaux sondés, qui peut être déterminée soit à partir d'échantillons de chaussées, soit à partir des profils radar. La plupart des études sur la précision du GPR rapportent des marges d'erreur de seulement 3 – 10 %. Pourtant, les capacités de l'appareil sont parfois encore remises en doute. Ce manque de confiance n'est pas seulement lié à la performance du radar géologique, il est aussi causé par le processus d'interprétation des données.
Dans ce projet, une chaussée en asphalte a été scannée puis analysée à la fois manuellement et de façon semi-automatique avec un logiciel. Malgré les grandes quantités de données qui sont habituellement collectées, il est souvent nécessaire de les interpréter manuellement. Cette étude montre qu'une interprétation incorrecte des profils radar engendre une erreur de 19,9 % pour l'asphalte, au lieu de 3,6 % lorsque l'interprétation est faite manuellement.

Mots-clé: Radar à pénétration de sol, GPR, Précision, Interprétation manuelle et semi-automatique

Abbreviations and nomenclature

GPR Ground Penetrating Radar
ε Dielectric constant

1. Introduction

1.1. Context

Non-destructive methods are increasingly used by highway agencies to evaluate the pavement condition. Among them, the ground penetrating radar (GPR) technology is particularly suited to subsurface exploration, as it is time efficient and cost-effective in mapping the road profile.
One of the most useful data sets in preventive maintenance and road rehabilitation is the layer thickness of the pavement structure. The accuracy and repeatability of the GPR data have been studied by government agencies, academic institutions and GPR providers (Maser & Pucinelli, 2009; Saarenketo, 2008). However, the reliability of the technique is still questioned, and GPR is still not fully implemented in many countries.
In the assessment of GPR accuracy, most research studies concentrate on the instrument parameters and the soil properties. However they often neglect difficulties encountered in the data interpretation, which is known to be subjective and requires specialized experience.

1.2. Research objective

The objective of this paper is to increase the understanding of inaccuracies due to data interpretation errors. A successful GPR project often provides clear data, but with somewhat wide interfaces that separate the pavement layers. Manually picking the center of the interface that corresponds to the maximum signal amplitude is not always straight-forward, and can be very time-consuming with large data files. Semi-automatic tools available in interpretation softwares are convenient, but can lead to significant errors if used without close operator supervision. This study, conducted in cooperation with the Minnesota Department of Transportation, will attempt to evaluate the impact of semi-automatic layer tracking vs. manual interface selection on the accuracy of GPR data in pavement thickness assessment.

2. Ground Penetrating Radar technology

2.1. Measuring principle

Ground penetrating radar (GPR) is a geophysical survey method used to remotely and non-destructively obtain a representative image of the subsurface materials. The technique is based on the propagation of electromagnetic waves in dielectric materials, as depicted in Figure 1.

- Short pulses are emitted at a certain frequency by a radar transmitter in an antenna.
- Reflected waves are received by the antenna and recorded.
- The radar signal is returned differently at distinct, abrupt dielectric non-homogeneities in the surveyed materials.
- A representation of the subsurface layers is created by graphing the differing signal travel times and amplitude.

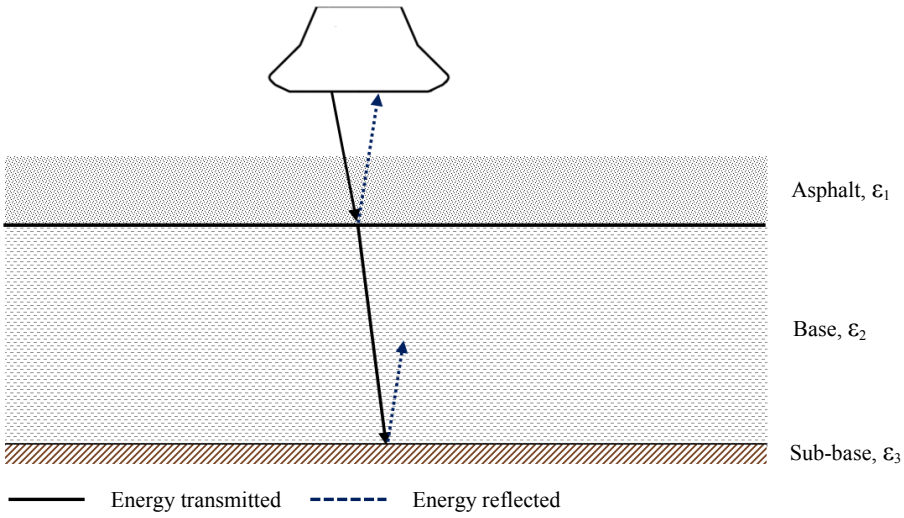

Fig. 1. Propagation of electromagnetic waves in a medium

GPR is used in a variety of applications, from geological and archaeological investigations to road and structure inspections. Typical road surveys include: layer thickness assessment, utility mapping, detection of underground cavities or structures, asphalt and concrete evaluation (pavement condition, void content, rebar spacing, frost depth), groundwater profiling.

The GPR technique is rapid, accurate and non-destructive, which makes it particularly timesaving and well-suited for many subsurface investigations. However, it has some limitations inherent in the wave propagation theory. The dielectric properties of the targeted structures or layer boundaries must have sufficient contrast with the host environment in order to be detected. Poor results are generally achieved in high-conductive media, such as clay, peat and saline soils, or in moist conditions. In addition, the selection of the operating frequency directly affects the depth of exploration. A high frequency GPR will have good resolution but a limited depth of penetration. Conversely, at low frequencies greater depths can be probed, but to the detriment of accuracy and clarity. Thus a trade-off between depth and resolution must be found during the feasibility study to achieve the best possible results.

2.2. GPR systems

Air-launched GPR systems are generally positioned 20 – 50 cm from the structure to be investigated. They allow the calculation of the dielectric constant of the material and subsequently are a more accurate estimate of the distance to the targeted object. Air-launched antennas are particularly suited for pavement surveys since they can be operated at normal driving speed.

With ground-coupled systems, the antenna is directly in contact with the structure to be investigated. The calculation of the dielectric constant from the data is not possible and it is necessary to use calibration cores or drilling to obtain accurate thickness data. Data is collected at a slower speed than with an air-launched GPR. However, at equivalent frequency ground-coupled antennas provide better energy penetration with reduced interference, and are usually preferred for concrete investigations.

Step-frequency GPR systems collect simultaneous data across the frequency domain: they generate waveforms at a series of discrete frequencies during certain times called "dwell times". The frequency at which the radar waves are transmitted increases in discrete steps. Data is then converted into the time-domain through an inverse Fourier Transform (Hoff, Hoven, & Eide, 2008; Scott, Arnold, & Gibson, 2010). Such GPRs provide variable exploration depths without deteriorating resolution. However the calculation of the dielectric constant is not possible at the current state of practice and drilling is still required.

3. Data Collection and Interpretation

3.1. GPR measurements

Field measurements were performed in Sør-Trøndelag, Norway, using a 100 MHz – 3 GHz step-frequency GPR system (Figure 2). The antenna array is capable of using 29 channels spaced by 7,5 cm, covering a scan width of 1,8 m, however only a limited number were selected in this test to allow a reasonable survey speed.
The 12 km long road section consists of a dense-graded asphalt pavement and a crushed stone base.
The positioning of the GPR data was done with GPS and kilometres markers. GPS coordinates were recorded at both the start and end points of the road section.

Fig. 2. GPR data collection equipment

3.2. Soil sample collection

Core samples were collected every 500 m in the right wheel path prior to GPR measurements. On several occasions, an indication of the sampling could be seen in the radar profiles (Figure 3). In these cases the thickness can be precisely determined in the GPR profiles at the exact location where cores were collected.

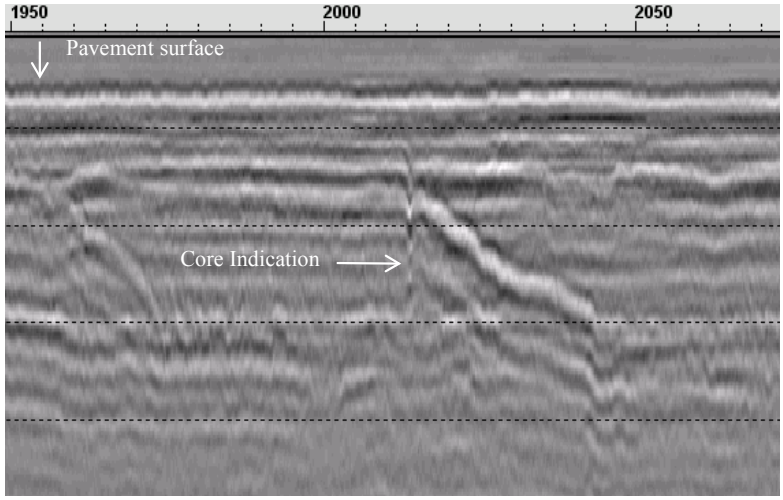

Fig. 3. Sampling trace

3.3. Calibration

The electrical properties of materials determine the propagation and reflection of electromagnetic waves. From the dielectric permittivity ε, the depth of the target can be determined using the following equation:

$$h = (c \times t)/(2\sqrt{\varepsilon}) \quad (1)$$

Where:
c = speed of light in free space (≈ 300 m/s)
h = layer thickness, in m
t = two-way travel time, in s
ε = dielectric constant of the material

Therefore it is essential to assign a correct value to ε when analyzing GPR data. The accuracy of the formula principally depends on to what extent the dielectric properties of the material are known. The following methods are available:

- The dielectric constant can be assumed from experience, or obtained from dielectric tables (Daniels, 2004; Saarenketo, 2006) without core calibration. Typically, the dielectric constant of asphalt ranges from 4 to 6.
- If the pavement layer thickness is precisely known at one location (i.e. from cores or drilling), ε can be calculated using Equation 1.
- If core samples are available, the dielectric constant can also be measured using a Percometer (Loizos & Plati, 2007).
- If GPR data collection was performed using an air-launched horn antenna, the dielectric constant can be calculated from surface reflections (Maser & Scullion, 1990). This method provides accurate and continuous results.

As the calculation of ε is not currently possible using the GPR system described in section 3.1, pavement cores and soil samples were obtained and average dielectric constants were computed, and are summarized in Table 1.

Table 1. Measured dielectric constants

Layer	ε
Asphalt	5,58
Gravel	10,71
Limestone gravel	10,68
Sandy gravel	6,78

3.4. Data interpretation

The GPR data was analyzed using the Road Doctor software. Each layer can be tracked manually or semi-automatically. When using semi-automatic tracking, the user teaches the program which interface to follow by clicking a few times on the screen at the interface. The program then attempts to follow the maximum amplitude of the selected interface as long as possible. This tool functions well but there can be inaccuracies in the tracking, especially when an interface is wide and not very well delineated (Figure 4).

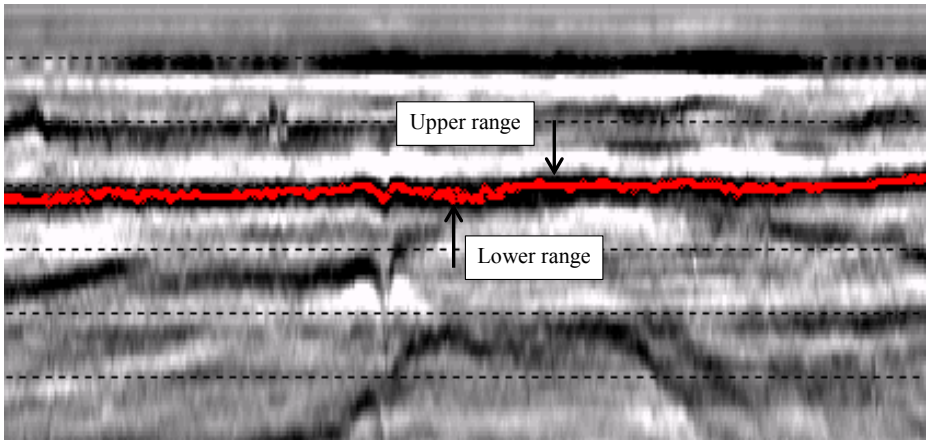

Fig. 4. Inaccuracies in layer tracking

4. Results

4.1. HMA layer

A test was conducted to compare the GPR measurement of an HMA layer to known thickness of 19 cores.
On 19 collected core samples of the HMA layer:

- 2 were used for calibration only
- 3 were outliers and not used
- 14 were usable for analysis and are shown in Table 2

Outliers have values that are unusually distant from the rest of the data. Outliers can be caused by measurement errors such as inaccuracies in location, such as when the sample trace is not visible on GPR profiles.
Based on the 14 usable measurements, the relative error of GPR data for the asphalt layer is **3,6 %** (Table 2). A similar study carried out with the same equipment also revealed an error of 3,6 % (Lalagüe & Hoff, 2010)
.

Table 2. GPR relative errors compared to reference thicknesses measured on cores (asphalt)

Thickness (cm)	Samples														Average
Core	25	23	27	20	20	20	20	20	25	20	38	25	25	23	23,6
GPR (lower)	23,2	21	21,4	14,9	14	14,4	14,5	17,7	19,4	16,9	32,4	24,1	19	20,6	19,5
GPR (center)	25,8	23,6	26,6	21	20,1	19,2	19,6	22	25	21,1	38,8	25	23,7	25	24
GPR (upper)	31,8	31,5	32,3	29,4	26,3	25	24,5	25	27,2	24,5	41,8	27,2	25,9	27,6	28,6
% Error	**3,2**	**2,6**	**1,5**	**5**	**0,5**	**4,0**	**2,0**	**10**	**0**	**5,5**	**2,1**	**0**	**5,2**	**8,7**	**3,6**

The chart below (Figure 5) shows the error range of the thickness measurements of each sample, based on an inaccurate interpretation by the software. Accurate coring and manual GPR data lie in the blue boxes. They differ in average by 3,6 %. Error bars are thicknesses obtained from an incorrect semi-automatic interpretation of GPR data. For example, sample 1 has:

- an exact core thickness of 25 cm
- a GPR thickness of 25,8 cm

} Blue boxes

- a maximum GPR thickness of 32 cm
- a minimum GPR thickness of 24 cm

} Error bars

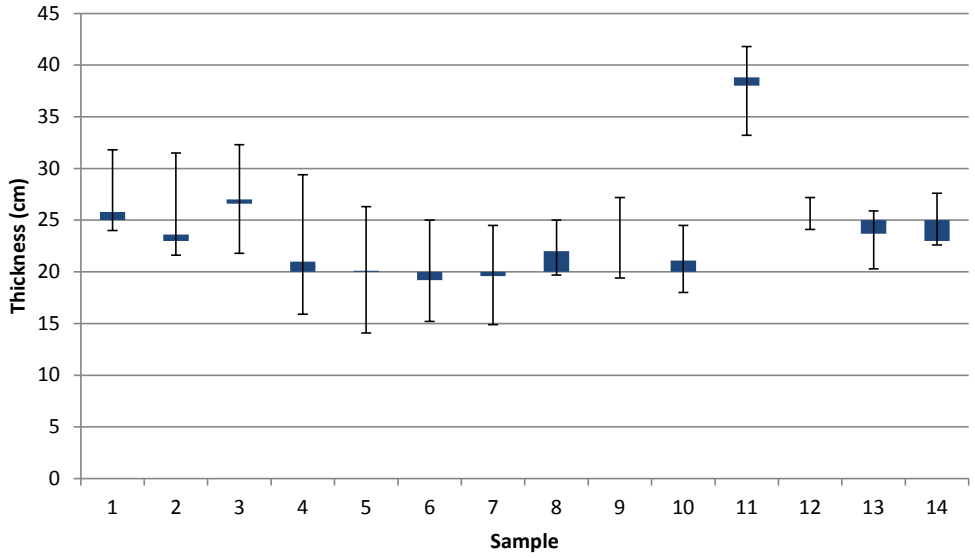

Fig. 5. Range of error of GPR data (asphalt)

It was found that an incorrect software layer picking can lead to an average relative error of **19,9 %.** This percentage should not necessarily be interpreted as an inaccuracy of the GPR data, but it rather highlights the limitations of the semi-automatic interpretation of the data.

4.2. Base layer

The GPR measurement was compared to known thickness of 40 soil samples.
On 40 measured thicknesses of the base layer:

- 4 were used for calibration only
- 4 were outliers and not used
- 10 were not detected by GPR (insufficient contrast with the adjacent layers)
- 22 were usable and are shown in Table 3

Based on the 22 measurements, the relative error of GPR data for the base material is **5,1 %** (Table 3).
A slight decrease in accuracy as a function of depth is expected, as radar energy is scattered and absorbed by passing through materials - which in turn leads to a loss of resolution and clarity.

Table 3. GPR relative errors compared to reference thicknesses measured on cores (base)

Thickness (cm)	Samples											Average
Core	50	34	35	8	25	30	36	50	25	50	35	
GPR (lower)	47,5	31	32,9	6	20,7	28,4	31,9	43,2	20	43,6	27,9	
GPR (center)	52,2	33,6	37,3	8	26,3	30,4	34,8	48,8	24	48,6	33,4	
GPR (upper)	62,7	39,5	43,1	9,3	30	36,7	38,6	56,4	26,8	51,8	36	
% Error	**4,4**	**1,2**	**6,6**	**0,0**	**5,2**	**1,3**	**3,4**	**2,5**	**4,2**	**2,9**	**4,8**	
Core	40	25	25	25	50	55	62	35	25	35	27	35,5
GPR (lower)	35,6	23,7	20,3	24,8	48	52,4	53,1	27	23,2	35,3	21,8	31,7
GPR (center)	37,8	26,7	24,7	26,2	54,4	57,8	58	31	27	37,5	25,1	35,6
GPR (upper)	44	35	33,4	29,3	57	63,7	65,7	32,3	29,2	35	27	40,3
% Error	**5,8**	**6,8**	**1,2**	**4,8**	**8,8**	**5,1**	**6,9**	**12,9**	**8,0**	**7,1**	**7,6**	**5,1**

In this example, an inaccurate software interpretation of the base layers (too high or too low) leads to an average relative error of **13,4 %** (Figure 6). This percentage is lower than the error seen with asphalt thicknesses. This may be partially due to a decreasing ratio of the widths of interfaces/total depth, as the depth of observation increases.

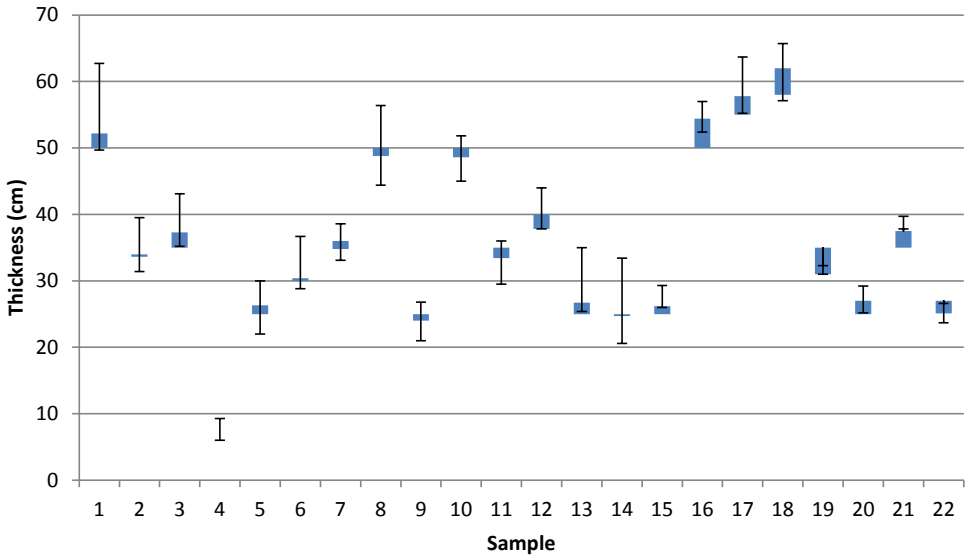

Fig. 6. Range of error of GPR data (base)

5. Discussion and Conclusion

The results of this study show that GPR can be very accurate when determining the pavement layer thickness. However the success of a GPR survey is strongly dependent on a known dielectric constant Ɛ, the location match between core samples and the GPR profile data, the flatness of the surface, the depths of observation, and the data interpretation method employed.
Although the GPR error in controlled studies with manual interpretation can be as low as 3 – 5 %, the process required is too painstaking to be able to maintain this level of accuracy with large data sets. GPR data is often collected in large amounts and manual layer tracking can become very time-consuming.
Semi-automatic layer tracking tools can be convenient and timesaving, but as shown in this study they must be used carefully. A small deviation of the tracking from the middle of the interface may result in significant interpretation errors and a subsequent decrease in overall accuracy.
This preliminary study will be extended in the future to additional factors affecting the data interpretation process, such as the type of antenna and software used, and the operator's experience.

References

Daniels, D. J. (2004). *Ground Penetrating Radar - 2nd Edition*. London, UK: The Institute of Electrical Engineers.

Hoff, I., Hoven, B., & Eide, E. (2008). Introduction of Ground Penetrating Radar in Pavement Rehabilitation in Norway. In *Transport Research Arena 4th Conference*. Ljubljana, Slovenia.

Lalagüe, A., & Hoff, I. (2010). Accuracy of Ground Penetrating Radar in Bituminous Pavement Thickness Evaluation. In *Transport Research Arena 5th Conference*. Brussels, Belgium.

Loizos, A., & Plati, C. (2007). Accuracy of pavement thicknesses estimation using different Ground Penetrating Radar analysis approaches. *NDT & E International*, *40*(2), 147–157. doi:10.1016/j.ndteint.2006.09.001.

Maser, K. R., & Pucinelli, J. (2009). *Ground Penetrating Radar (GPR) Analysis HWY-308813-RP, Phase I Report*.

Maser, K. R., & Scullion, T. (1990). Automated detection of pavement layer thickness and subsurface moisture using Ground Penetrating Radar. Final Report. Texas Transportation Institute, College Station.

Saarenketo, T. (2006). *Electrical properties of road materials and subgrade soils and the use of Ground Penetrating Radar in traffic infrastructure surveys*. University of Oulu.

Saarenketo, T. (2008). NDT Transportation. In H. M. Jol (Ed.), *Ground Penetrating Radar: Theory and Applications* (p. 524). Elsevier.

Scott, M., Arnold, J., & Gibson, D. (2010). *Step Frequency Ground Penetrating Radar Characterization and Federal Evaluation Tests*. Federal Highway Administration.

PAPER 7

Detection of Rock Fragments on Tunnel Concrete Lining with Ground Penetrating Radar (GPR)

Anne Lalagüe[a] (corresponding author), Matthew A. Lebens[b], Inge Hoff[c], Eivind Grøv[a]

[a] SINTEF Building & Infrastructure, Høyskoleringen 7A, 7465 Trondheim, Norway. Emails: anne.lalague@sintef.no; eivind.grov@sintef.no.

[b] Minnesota Department of Transportation - Office of Materials and Road Research, 1400 Gervais Avenue, Maplewood, MN 55109, USA. Email: matthew.lebens@state.mn.us.

[c] Norwegian University of Science and Technology, Department of Civil and Transport Engineering, Lerkendalsbygget 2-051 Høyskoleringen 7A, 7465 Trondheim, Norway. Email: inge.hoff@ntnu.no.

Abstract

This article describes research works aimed at developing a new tunnel inspection method using Ground Penetrating Radar (GPR). The feasibility of six GPR systems was assessed for:

- Remote mapping of cavities behind concrete linings
- Detect rock fragments that have fallen from the tunnel roof onto the inner lining of e.g. precast concrete segments

Research studies conducted both in Norway and the USA conclude that the GPR technique is a simple and reliable method to assist stability inspection in existing Norwegian tunnels. The ground-coupled GPR systems represent a step forward in remote detection of rock fragments on tunnel concrete linings, applying particularly well to self-standing inner linings. The analysis of the data is relatively straightforward with reasonable accuracy.

Keywords: Ground Penetrating Radar, GPR, tunneling, concrete lining, loose rocks, safety.

1. Introduction

1.1. Context

Norway is a long and narrow country with a broken coastline 103 000 km long, cut by numerous fjords and thousands of islands. To meet the demands of the population and improve road safety, mountain roads and ferry connections have gradually been replaced by tunnels. As of 2012 in Norway, there were around 1050 road tunnels totaling almost 1000 km and approximately 720 railway tunnels with a total length of almost 300 km. One of them, Lærdal, is the world's longest road tunnel at 24,5 km long. Norway has acquired an international reputation in tunnel and bridge construction, producing time- and cost-effective solutions to fit challenging environmental and traffic conditions. One important aspect of this concept is the installation of free standing inner tunnel linings. Several different lining methods have

been employed, some with pre-cast concrete segments and others comprised of PE-foam covered by sprayed concrete. The lining methods typically result in a small volume of void space (typically 10 - 60 cm) between the inside of the lining and the rock contour (Broch et al., 2002). These "unbounded" linings do not contribute to the tunnel stability.

The Norwegian tunneling industry experienced a serious incident during the night of December 25 in 2006, when a cave-in took place through the concrete lining of the Hanekleiv tunnel (Vestfold County, southern Norway), less than 10 years after the construction. A total volume of 250 m^3 of rock, reinforcement and concrete fell down onto the traffic lanes. Rubble extended over 30 m long, and was piled up to the former tunnel's roof; however due to the late hour on Christmas Day no vehicles were present and no injuries occurred. An investigation showed that the tunnel was insufficiently designed to support a weak zone containing swelling clay (Bollingmo et al., 2007). Despite the prompt renovation, concerns about tunnel safety have persisted. The Norwegian Public Road Administration (NPRA) responded with the decision to conduct manual inspections of tunnel stability by physically entering the void space between the inner lining and the rock surface of a majority of tunnels in Norway. In addition, all new road tunnels were to be built with an increased cross section both side to facilitate the access to this void space.

1.2. Ground Penetrating Radar applications in tunnels

There have been several tunnel investigations made with GPR, although many are of a different nature from that presented in this paper. Most studies focus on lining structures and backfill grouting:

The thickness of the concrete lining is generally known, as it is usually made of prefabricated elements. However it is sometimes so deteriorated that the thickness is not constant anymore, and the mechanical strength is compromised. This situation was encountered in the Mont-Blanc tunnel, after the deadly fire that occurred in 1999 (Abraham & Dérobert, 2003). Seismic refraction and Ground Penetrating Radar measurements were then conducted to evaluate the extent of the damage to the concrete lining. The GPR data revealed cracks and variations in the lining thickness.

Reinforcement mesh and other steel components in concrete linings are generally easily detected by GPR and several studies reported positive results (White et al., 2013a, 2013b). The detection of delamination is, however, not as clear (Bosela et al. 2006). The extent of the deterioration has to be sufficiently large (voids size and moisture area) to be easily observed on radargrams (Wimsatt et al. 2012). More broadly, Parkinson & Ekes (2008) reported use of GPR for the detection of concrete honeycomb, embedded wooden timbers, liner-rock contact and voids.

To reinforce the tunnel structure, grout mortar is commonly injected between the inner lining and the bedrock. Although the quantity and pressure of grout are regulated by standards, the quality of the injection is not always met and some gaps may remain unfilled. Xie et al. (2007) recently used GPR to verify the homogeneity of a newly placed backfill grouting. Measurements were conducted using a 200

MHz ground-coupled antenna to better penetrate the reinforcement mesh. Because the water content varies a lot during the curing time, the dielectric permittivity was measured in situ, from a known point at the time of the measurements. The survey appeared to be successful, as the grout mortar showed sufficient contrast with the tunnel lining and the surrounding soil.

Few years later the same authors expanded their research to 250 MHz, 500 MHz and 1 GHz frequencies. The tests also showed satisfactory results, with the 500 MHz GPR system giving the most promising results (Zhang, Xie, & Huang, 2010). Further on this topic, Karlovšek et al. (2012) studied the feasibility of GPR to detect voids at 400 MHz, 1 GHz and 1,5 GHz frequencies and also reported encouraging results.

Research similar to ours is that of Cardarelli et al. (2003), who used geophysical techniques to assess the stability of the rock after a landslide. The study focuses on seismic methods, but also employs GPR to provide information about fractures and possible concrete-rock contact.

1.3. Research objective

This paper describes research project aimed at developing a new tunnel inspection method using Ground Penetrating Radar (GPR). The main objective is to improve the safety and effectiveness of inspection maintenance operations in existing Norwegian tunnels, using a remote and non-destructive procedure to:

- Remotely scan the rock surface during geological inspections and assess the void cavity behind the inner lining.
- Detect rock fragments that have fallen from the rock surface / tunnel roof onto the inner linings (of e.g. precast concrete segments).

A modern road tunnel is a complicated structure with various installations using a wide range of material types and construction. GPR has the capability to penetrate concrete linings, but materials such as bolts, reinforcements, trapped moisture etc. can confuse and attenuate the signal.

2. Norwegian tunneling

Geologically, Norway is a typical hard rock region: about 2/3 of the bedrock is Precambrian (gneiss, granite, gabbro and quartzite) and 1/3 is Paleozoic (mica schist, marble and greenstone). From a rock engineering point of view, much of the rock mass found in Norway is of good quality (Nilsen and Thidemann, 2008), but may change rapidly to poorer quality in certain zones. For this reason, the Drill & Blast (D&B) tunnel construction method is more widely used than the Tunnel Boring Machine (TBM) and a variety of support and inner lining types are normally used. In contrast to the smooth finish with the TBM technique, the rock contour of a D&B-tunnel will be rough and irregular because of the blasting, even if careful blasting is specified.

The type of rock supports and lining selected depends on the rock conditions (Nilsen and Palmstrøm, 2000). In areas of extremely poor rock, a reinforced concrete lining for stabilization may be applied. In good quality rock, bolts and sprayed concrete may be sufficient. Between these extremes, different thicknesses of reinforced sprayed concrete are used. Also, due to the cold, moist climate, Norwegian tunnels often need protection against water leakages and frost damages, so-called Water and Frost Protection (the inner lining).

The inner lining should provide satisfactory protection against water, frost, fire, pollution, high pressure cleaning and load. Several technical solutions exist but the experience of the Nordic countries reveals that pre-fabricated concrete elements are the most common and durable linings in high-traffic tunnels (Broch et al., 2000).

The required type and thickness of insulation is determined according to the frost index F10 (h°C) of the site, defined as the sum of the negative air temperature multiplied by the number of hours per occurrence of negative temperatures (Statens Vegvesen, 2006). The choice of type of inner lining and its dimensions are governed by the AADT. In case precast concrete linings are required they are usually 150 mm thick (for two-lane highways). The concrete lining is fastened to the rock by fixation bolts and is not intended to form a part of the rock support. The void between the backside of the walls and the bedrock is typically left open (Figure 1).

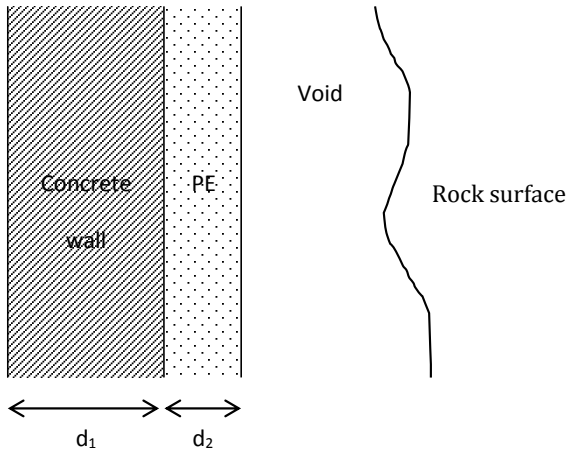

Figure 1 Cross-section of an inner lining of pre-cast segments of concrete with PE-foam for insulation

Tunnel inspections generally require a direct access to the rock face. Since most of the concrete linings were not designed with enough access hatches, it has been necessary to create apertures through the walls in positions that give the inspector best possible visual access to the rock surface. The space between the wall and the rock surface is not usually known, so Ground Penetrating Radar has been used to attempt to scan the concrete lining and interior voids along the tunnel.

3. Ground Penetrating Radar

Ground Penetrating Radar (GPR) is a geophysical survey method used to remotely and non-destructively obtain an image of the subsurface materials. The technique is based on the propagation of electromagnetic waves in dielectric materials:

- Short pulses are emitted at a certain frequency by a radar transmitter in an antenna.
- Reflected waves are received by the antenna and recorded.
- Pulses are returned differently at any distinct, abrupt dielectric inhomogeneities in the surveyed materials.
- A representation of the subsurface layers is created by graphing the differing signal travel times and amplitude.

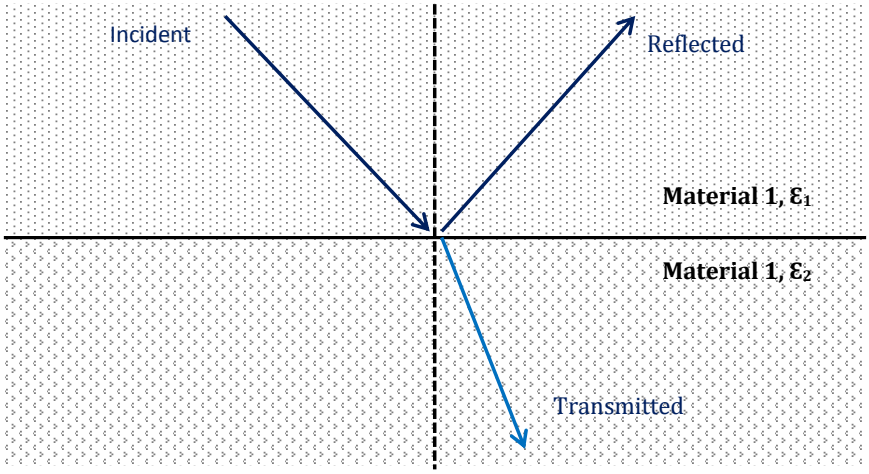

Figure 2 Principle of GPR measurement

GPR is used in a variety of applications, from geological and archaeological investigations to road and structure inspections (Saarenketo, 2008). Typical road surveys include: layer thickness assessment, utility mapping, detection of underground cavities or structures, asphalt and concrete evaluation (pavement condition, void content, rebar spacing, frost depth), groundwater profiling.

The GPR technique is rapid, accurate and non-destructive, which makes it particularly timesaving and well-suited for many subsurface investigations. However, it has some limitations inherent in the wave propagation theory. The dielectric properties of the targeted structures or layer boundaries must have sufficient contrast with the host environment in order to be detected. Poor results are generally achieved in high-conductive media, such as clay, peat and saline soils, or in moist conditions. In addition, the selection of the operating frequency directly affects the depth of exploration. A high frequency GPR will have a good resolution but a limited depth of penetration. Conversely, at low frequencies greater depths

can be probed, but to the detriment of accuracy and clarity. Thus a trade-off between depth and resolution must be found during the feasibility study to achieve the best possible results.

GPR systems, antennas and manufacturers used in this study are presented in Table 1.

Table 1 Overview of GPR systems used in the study

GPR systems	Frequency	Manufacturer
Ground-coupled	400 MHz	GSSI (USA)
Ground-coupled	1,5 GHz	GSSI (USA)
Ground-coupled	2,6 GHz	GSSI (USA)
Air-launched, horn antenna	1 GHz	GSSI (USA)
Air-launched, horn antenna	2 GHz	GSSI (USA)
Step-Frequency, antenna array	100MHz – 3GHz	3d-Radar (Norway)

Air-launched GPR systems (Figure 3) are generally positioned 20 – 50 cm from the structure to be investigated. They allow the calculation of the dielectric constant of the material and subsequently are a more accurate estimate of the distance to the targeted object. Air-launched antennas are particularly suited for pavement surveys since they can be operated at normal driving speed.

With ground-coupled systems, the antenna is directly in contact with the structure to be investigated. The calculation of the dielectric constant from the data is not possible and it is necessary to use calibration cores or drilling to obtain accurate thickness data. Data is collected at a slower speed than with an air-launched GPR. However, at equivalent frequency ground-coupled antennas provide better energy penetration with reduced interference, and are usually preferred for concrete investigations.

Step-frequency GPR systems (Figure 4) collect simultaneous data across the frequency domain: they generate waveforms at a series of discrete frequencies during certain times called "dwell times". The frequency at which the radar waves are transmitted increases step by step. Data is then converted into the time-domain through an inverse Fourier Transform (Hoff et al., 2008; Scott et al., 2010). In this present study, the frequency ranged from 100 MHz to 3 GHz. Such GPRs provide a good exploration depth without deteriorating resolution. However the calculation of the dielectric constant is not possible at the moment, and drilling is required.


Figures 3a - 3b Air-launched (left) and ground-coupled (right) antennas

4. Free-space mapping behind concrete walls

The first step in the tunnel investigations was to develop a system to apply the step-frequency GPR to the interior surface of a concrete lining. This was done to evaluate the free space and identify potential access panel locations.

A road tunnel near Trondheim, Norway was selected for this test. To conform to the interior vertical surfaces, an "arm" was specially designed. This is attached to a lightweight bracket which is mounted to the vehicle's bumper. The following figure shows the system in operation:

Figure 4 Vehicle bracket with arm mounted to allow surveying tunnel walls

In case of obstacles (road signs, emergency exit, extinguishers, etc), the antenna was lifted out of the way with an electric winch and ropes. Each side of the tunnel was measured at two different heights: approximately 1 m and 2 m. The traffic in the lane being tested was restricted, and did not impede with the measurements, which were performed relatively quickly (≈ 5 km/h).

The radar data was processed and displayed using the Road Doctor software, developed and distributed by Roadscanners Oy, Finland. An interpretation phase follows the processing operation and is done manually or semi-automatically. For all investigated tunnels, it was relatively easy to find bedrock surface and the back of the vault since the dielectric constant (ε) is constant for air. The cavity's width could then be calculated with good accuracy. The distance varies greatly from a few centimeters (almost contact) up to more than one meter. The profiles of the void and location of joints were then observed to identify sections with sufficient space (> 50 cm) for installing inspection apertures (Figure 5).

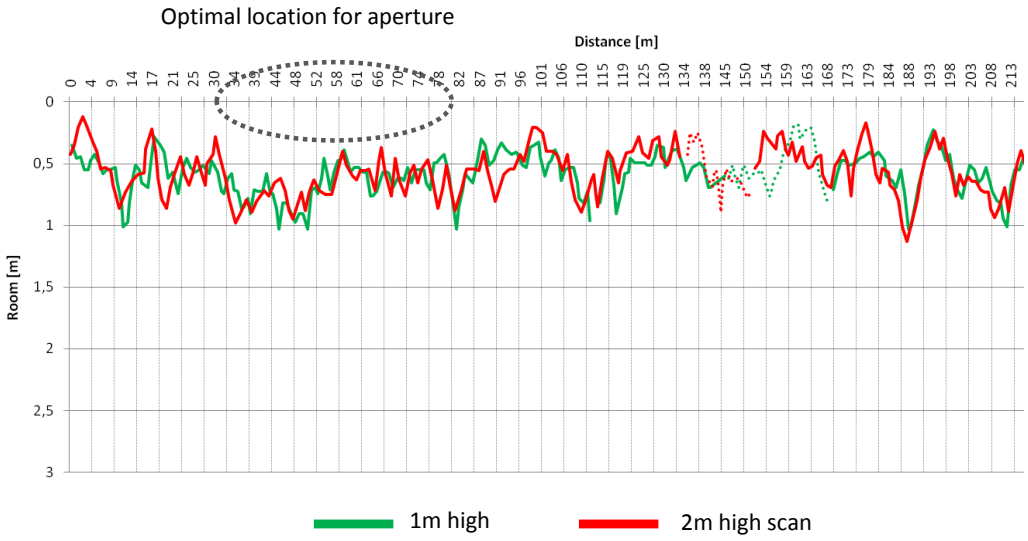

Figure 5 Rock surface profile

5. Detection of loose rocks on top of the concrete lining

5.1. Using step-frequency GPR

Mapping of space behind concrete linings makes inspection easier, but it is still necessary to climb on top of the concrete vault to inspect the tunnel's roof. Such an operation is hazardous since it is wet, slippery, dark and narrow. An evacuation after an accidental fall would be very difficult. In good rock mass conditions the blasting would normally leave little space between the wall and the rock surface. This is very cost-effective in the construction phase, but makes it impossible to carry out manual inspection operations after the wall is in place; therefore the NPRA instructed an increased cross section by adding 200 mm on both sides.

Unstable rock areas could potentially be identified because material may fall from the tunnel's roof, before a larger scale collapse occurs. By detecting loose rocks on top of the lining, an early and targeted inspection could be possible.

To investigate whether GPR can be used for such purposes, an experiment was carried out by applying bagged rocks of varying size on the inner lining side (Figure 6) of Grillstad tunnel, Norway. Data was processed using Examiner software, from 3d-Radar AS, Norway.

Figure 6a, 6b In-situ field testing in Norway using a step-frequency GPR

The GPR system used in this study (Figure 4) has the benefit of being multi-channelled. With a scan width of 50 cm, the number of passes can be considerably reduced. Furthermore, the wide bandwidth (100 MHz – 3 GHz) allows a variable depth of penetration without sacrificing resolution.

Results of this preliminary study were mixed. On some profiles, rocks (and more precisely their backside) could be easily observed, as in Figure 7. However some scans required further data processing in order to identify the rocks (Figure 8) and for some others, rocks did not appear at all (Figure 9). It appeared that a close coupling with the surface caused ringing and interference which slightly reduce the effectiveness of the step-frequency GPR.

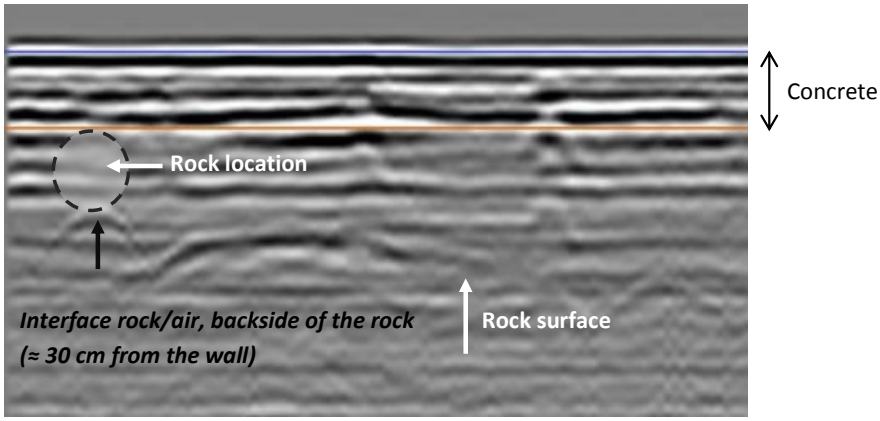

Figure 7 Successful step-frequency GPR measurement in finding rocks (1)

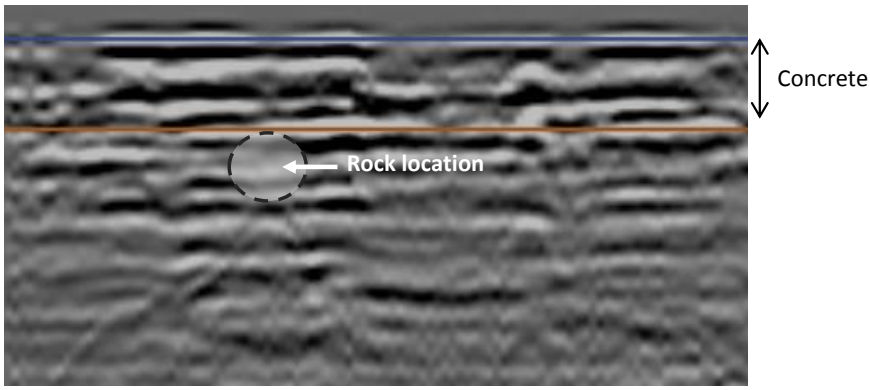

Figure 8 Successful step-frequency GPR measurement in finding rocks (2)

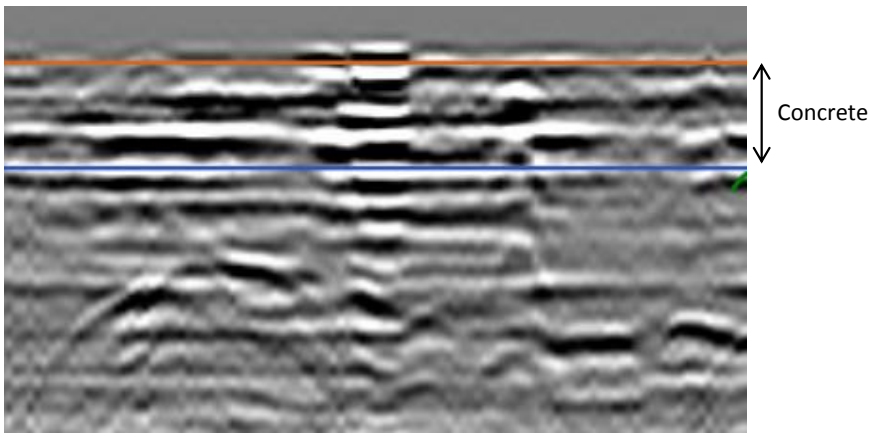

Figure 9 Unsuccessful (unclear) step-frequency GPR measurement

5.2. Using air-launched and ground-coupled GPR

In order to better characterize the feasibility of GPR to detect loose rocks behind concrete slabs, a research study was conducted in collaboration with the Minnesota Department of Transportation (MnDOT) using both air-launched and ground-coupled antennas.

5.2.1. Wall construction

Concrete test elements similar to the ones used in Norwegian tunnel were built at the Minnesota Road Research Project (MnROAD), a pavement and materials test facility owned and operated by the Minnesota Department of Transportation. The structural linings design and the concrete mix design comply scrupulously with the Norwegian requirements. Elements are 15 cm thick, of type B45 (strength class) and MF40 (durability class, exposure to salt/frost). The concrete mix contains silica fume, fly ash, 2 kg/m^3 of micro polypropylenfibers. The water-to-cement ratio is below 0,40 and the entrapped air content around 5 %.

Concrete elements were reinforced with two welded wire meshes. As steel interferes the most with GPR signal propagation, different configurations were examined. In Panel 1, the two meshes were aligned. Panel 2 have nonaligned meshes and represents the most difficult case. Conversely, Panel 3 does not have welded wire meshes. The spacing of the meshes is 14 cm x 14 cm.

Figure 10 shows the type of reinforcement in each panel. Panels are 2,4 m long and 1,2 m high.

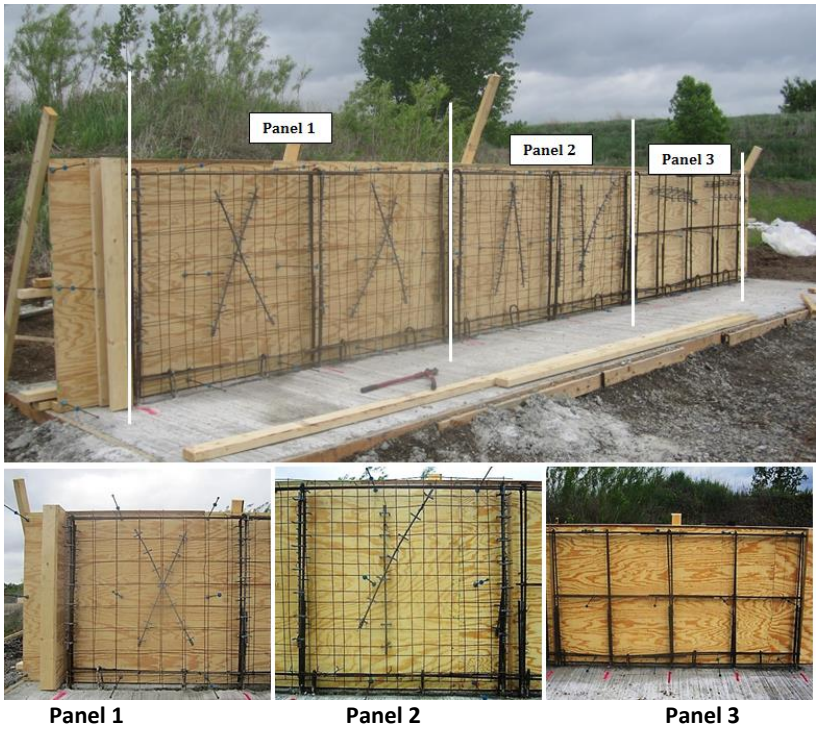

Figure 10 Construction of the simulated tunnel wall at MnROAD

5.2.2. GPR measurements and data interpretation

Rocks of varying size (from 5 cm to 50 cm) were placed on the backside of the concrete wall. All GSSI ground-coupled and air-launched GPR systems from Table 1 were tested and rated according to their ability to detect rocks. An aluminium plate was placed next to the rocks for reference. A second series of measurements was then carried out with rocks wrapped in aluminium foil, in order to assist with the data analysis process using Road Doctor and RADAN softwares.

To verify the GPR profiles, each scan was then compared to the corresponding picture showing the exact rocks location.

Figure 11a, 11b Wrapped small and medium rocks (left), large rock (right)

5.2.3. Results

When no rock is placed on the backside of the wall, the following GPR profiles are obtained (Figure 12). The backside of the wall is visible, the outer mesh, the inner mesh when not aligned with the latter, and the rebars.

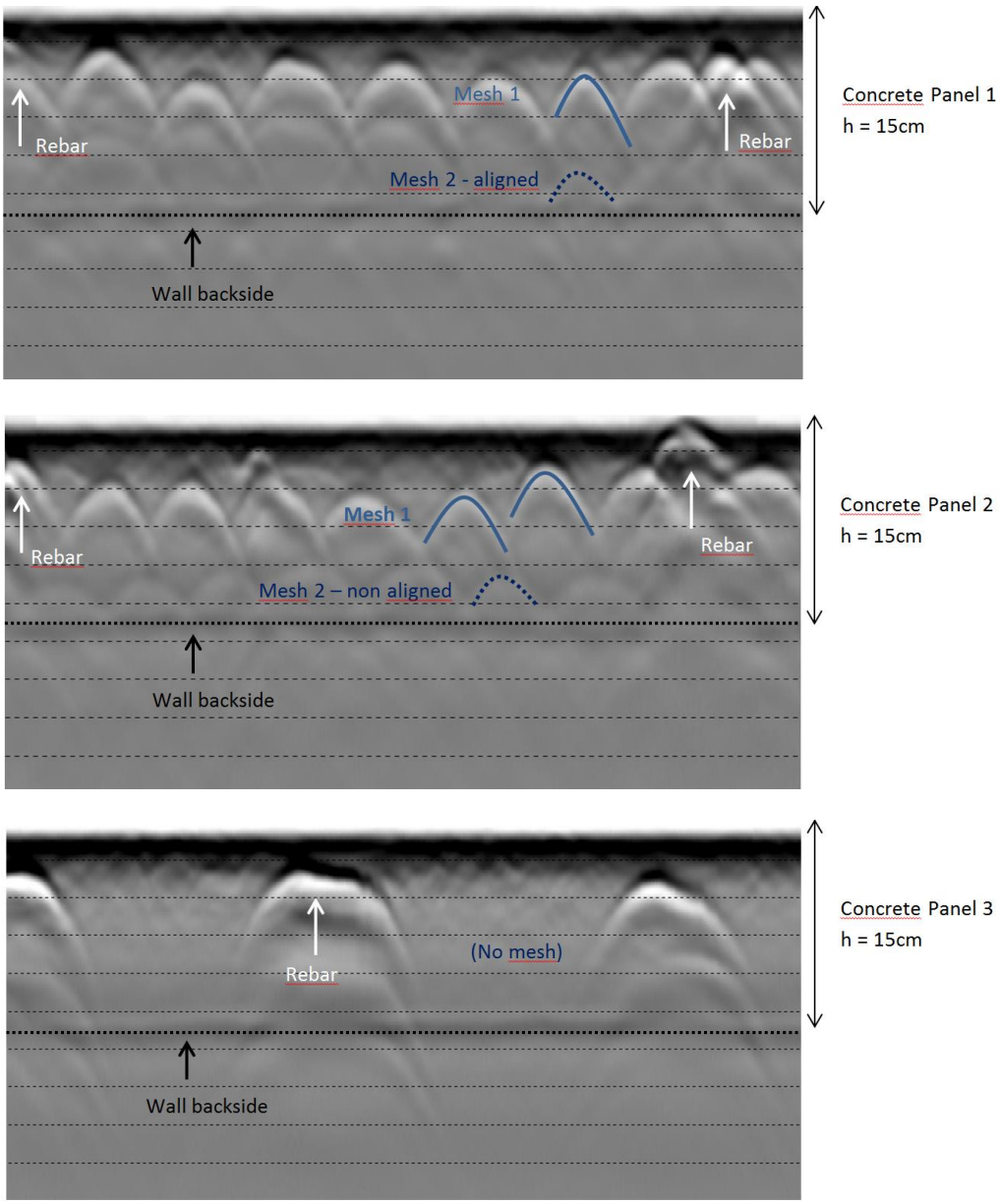

Figures 12a, 12b, 12c GPR profiles of the concrete walls, 2.6 GHz GPR

- Results of ground-coupled 400 MHz measurements

As expected, ground-coupled 400 MHz measurements were not successful. The depth of penetration depends on the operating frequency, the transmitter power and the material itself. At low frequencies, radar waves are less likely to be attenuated by the electrical conductivity. However, the loss of resolution can be significant. Low frequencies GPR systems are appropriate for deep geological surveys but not for shallow investigations.

- Results of ground-coupled 1,5 GHz measurements (Table 2)

Ground-coupled 1,5 GHz measurements gave the best overall results. Large and medium-sized rocks could easily be identified on the radar profiles. No advanced data processing or filtrering was necessary. However smaller rocks (< 10 cm) could not be detected with sufficient confidence.
It was possible to see about 1 m behind the concrete backside. Please note that this is actually the interface between rock and air that is detected, the contrast in dielectric constant between concrete (9) and rock (8 – 10) being too small.

- Results of Ground-coupled 2,6 GHz measurements (Table 3)

Ground-coupled 2,6 GHz measurements gave the best radar images for small and medium rocks (very small rocks are somewhat uncertain). However large rocks could not be detected, due to the limited depth of exploration (about 50 cm) inherent to such high-frequency GPR.

- Results of air-launched 1 GHz measurements (Table 4)

Air-launched 1 GHz measurements gave satisfactory results for large rocks only. It is possible to see up to 1 m behind the concrete backside but because of energy loss between the antenna and the concrete surface, the signal quickly drops off to an unusable level.
Efforts were made during the measurements to keep the antenna at a constant distance from the wall (about 50 cm). However small variations occurred and this explains why the concrete surface (blue line) is wavy.

- Results of air-launched 2 GHz measurements

Air-launched 2 GHz measurements were not successful. The high operating frequency combined with the energy loss between the antenna and the surface does not allow a proper depth of exploration. Such GPR systems are typically used for thin asphalt pavements surveys.

Table 2 Overview of 1,5 GHz ground-coupled GPR profiles

	Panel 1	Panel 2	Panel 3
Large rock	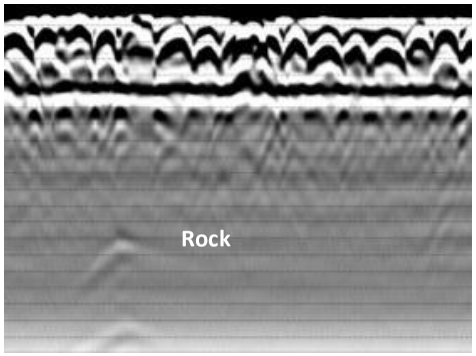	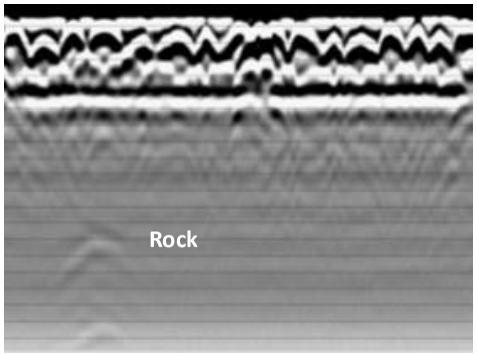	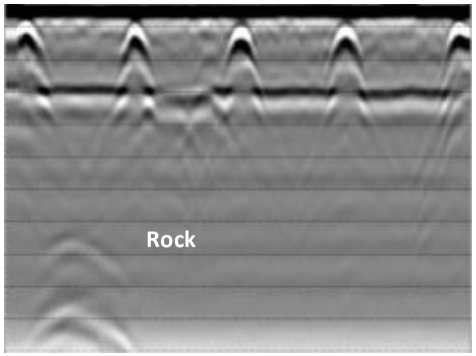
Small and medium rocks	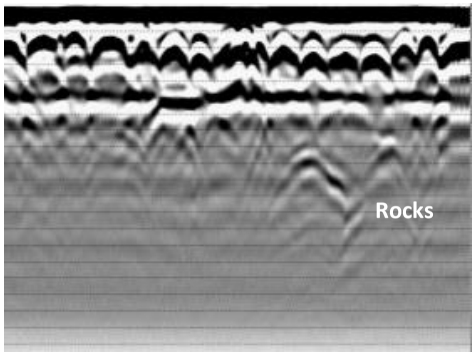	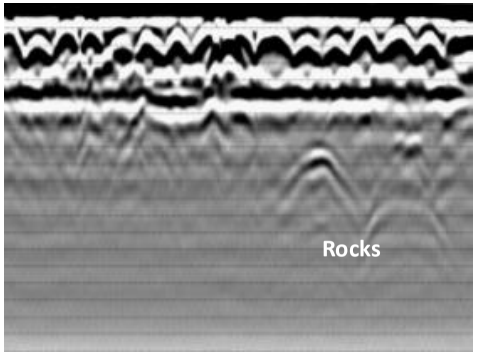	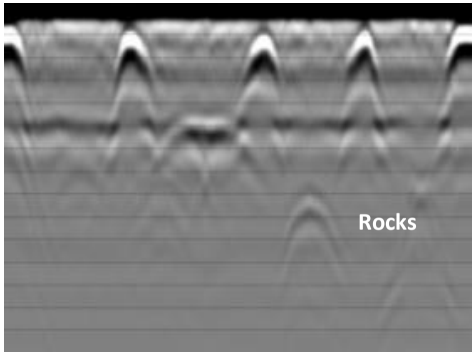

Table 3 Overview of 2,6 GHz ground-coupled GPR profiles

	Panel 1	Panel 2	Panel 3
Large rock	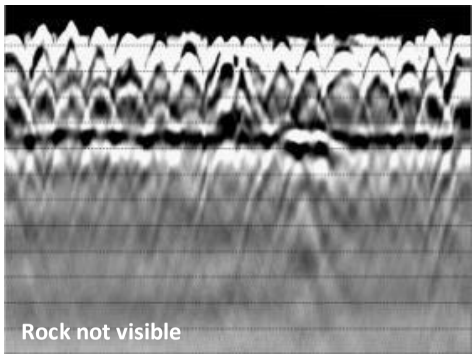	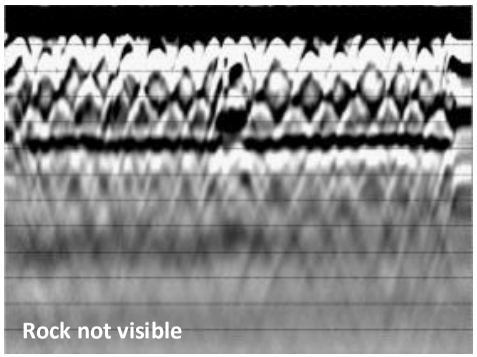	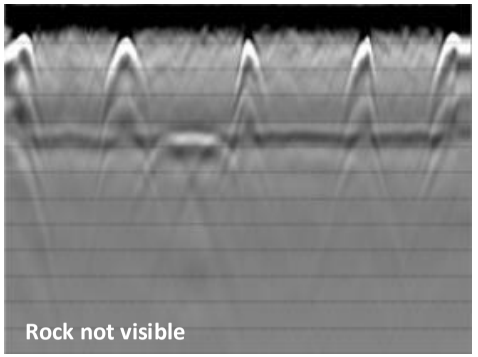
Small and medium rocks	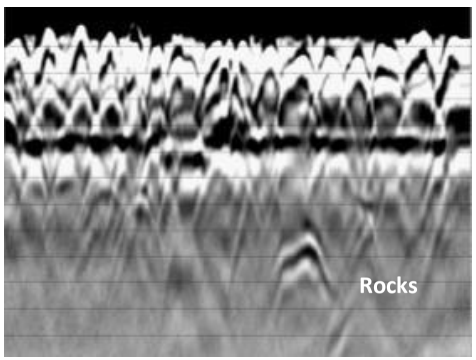	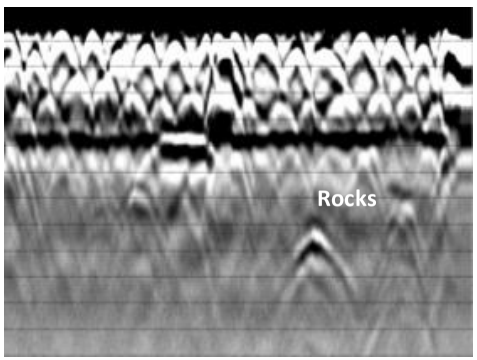	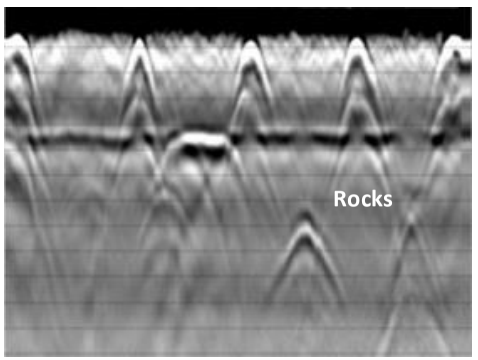

Table 4 Overview of 1 GHz air-launched GPR profiles

	Panel 1	Panel 2	Panel 3
Large rock	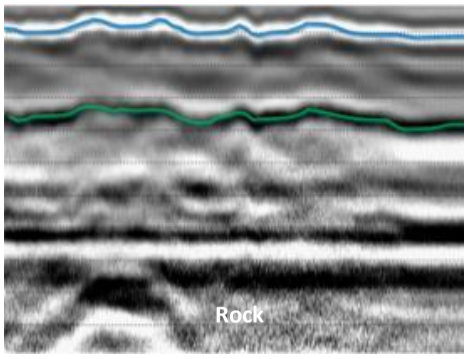	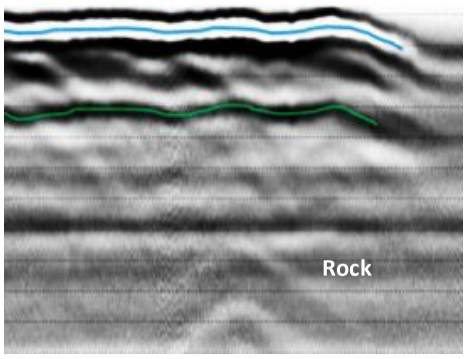	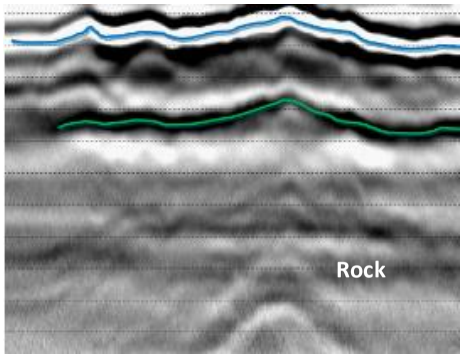
Small and medium rocks	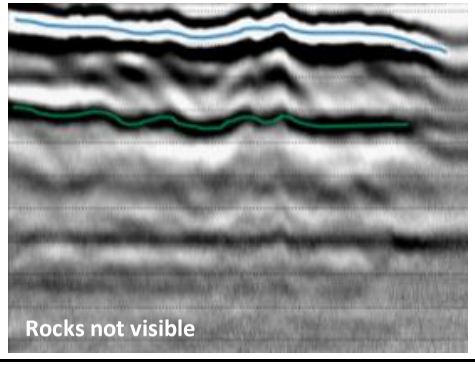	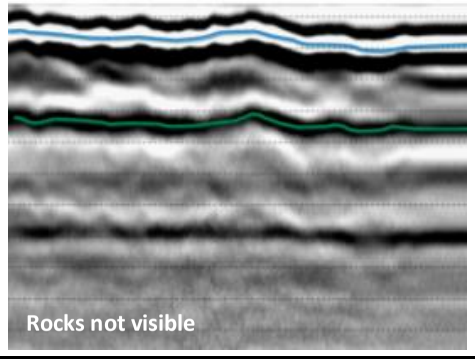	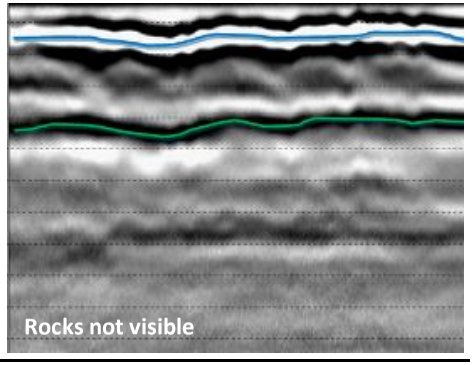

6. Conclusions and Recommendations

The following conclusions can be drawn from the completed surveys:

- GPR has proven to be reliable and useful for determining the distance between the inside of the concrete linings and the rock surface. The step-frequency GPR from 3d-Radar, with its wide bandwidth and antenna array, is particularly adapted to such investigations.

- Ground-coupled GPR systems give by far the best results in detecting loose rocks on top of concrete linings. They must be operated at walking speed but offer unequalled signal penetration and reliable, repeatable data. The 1,5 GHz antenna is the most effective of the systems tested.

- Medium high frequency air-launched antennas (1 GHz) give satisfactory results when detecting large rocks (> 40 cm). However surface coupling and interference with metallic items (such as lightning system, frame and bracket) may significantly reduce the quality of the GPR data and render the interpretation difficult.

Levels of GPR capabilities in detecting loose rocks on concrete linings are summarized in the table below.

Table 5 GPR measurements summary

GPR System	**Ground-coupled**			**Air-launched**		**Step-frequency**
Frequency	400 MHz	1,5 GHz	2,6 GHz	1 GHz	2 GHz	100 MHz – 3 GHz
Large rocks (D ≥ 30 cm)	-	+++	-	++	-	+
Small and medium rocks (5 cm < D < 20 cm)	-	++	+++	-	-	+

Based on the assessments results, the following remarks and recommendations can be drawn:

- To maximize the GPR survey effectiveness, two ground-coupled antennas could be used: 1,5 GHz for the detection of large rocks and 2,6 GHz for a more accurate detection of small/medium rocks.

- The tunnel lining should be scanned right after the tunnel construction and regularly rescanned for comparison highlighting any changes that occur.

- Further research could explore the accuracy and cost benefits of using ground-coupled arrays. Such GPR systems may provide improved profiles while reducing significantly the number of scans and the duration of data analysis.

- Concrete linings in Norwegian railways tunnels are typically thicker (200 mm instead of 150 mm) with heavier steel reinforcement. This may not significantly impact the overall conclusion of the field experiments, as the difficult case of non-aligned reinforcements (which is not always true in actual constructions) was also successfully tested with this simulated wall.

Acknowledgment

This project was funded by the Norwegian Public Road Administration (NPRA) and the Norwegian National Railway Administration (NNRA). The authors wish to thank Ine Gressetvold (NPRA) for conceptualizing this project. The authors gratefully acknowledge the field support and resources provided by Maureen Jensen from the Minnesota Department of Transportation (MnDOT). Special thanks to MnDOT Research Engineers Ally Akkari, Dr. Shongtao Dai, Dr. Bernard Izevbekhai and Ben Worel for their guidance and assistance in duplicating the Norwegian concrete mix design. The authors also gratefully acknowledge Jack Herndon, Steve Olson, Len Palek and other MnROAD Engineers and Technical Experts whose efforts and dedication to the wall design and construction were greatly appreciated.

References

Abraham, O., & Dérobert, X. (2003). Non-destructive testing of fired tunnel walls: the Mont-Blanc Tunnel case study. *NDT & E International*, *36*(6), 411–418. doi:10.1016/S0963-8695(03)00034-3

Bollingmo, P., Nilsen, B., & Nordgulen, Ø. (2007). *Raset i hanekleivtunnelen 25. desember 2006, Rapport fra undersøkelsesgruppen*. In Norwegian.

Bosela, P. A., Lek-udom, S., Mullangi, S., & Delatte, N. (2006). Field comparison of NDE methods for tunnel condition assessment. In *Proceedings of the Fourth Forensic Engineering Congress* (pp. 620–640). Cleveland, Ohio. doi:10.1061/40853(217)50

Broch, E., Grøv, E., Davik, K.I., 2002. The inner lining system in Norwegian traffic tunnels, Tunneling and Underground Space Technology, volume 17, issue 3, pp 305-314.

Hoff, I., Hoven, B., & Eide, E. (2008). Introduction of Ground Penetrating Radar in Pavement Rehabilitation in Norway. In Transport Research Arena Europe. Ljubljana, Slovenia.

Jol, H., 2009. Ground Penetrating Radar, Theory and Applications, Elsevier. ISBN 978-0-444-533487.

Karlovšek, J., Schuermann, A., & Willimas, D. J. (2012). Investigation of voids and cavities in Bored Tunnels using GPR. In *Proceedings of the 14th International Conference on Ground Penetrating Radar (GPR)* (pp. 496–501). Shanghai, China. doi:10.1109/ICGPR.2012.6254916

Lalagüe, A., Hoff, I., 2010. Determination of space behind precast concrete elements in tunnels using GPR. In: Proceedings of the 13th International Conference on Ground Penetrating Radar, Lecce, Italy. Doi: 10.1109/ICGPR.2010.5550195.

Nilsen, B., Palmstrøm, A., 1993. Rock Engineering, Volume no.9, Norwegian Institute of Technology. ISBN 82-7598-017-8.

Nilsen, B., Palmstrøm, A., 2000. Engineering Geology and Rock Engineering - Handbook no.2, Norwegian Soil and Rock Engineering Association. ISBN 82-91341-33-8.

Norwegian Public Road Administration (NPRA), 2003. Håndbok 111- Standard for drift og vedlikehold". In Norwegian.

Parkinson, G., & Ekes, C. (2008). Ground Penetrating Radar Evaluation of Concrete Tunnel Linings. In *Proceedings of the 12th Internarional Conference on Ground Penetrating Radar*. Birmingham, UK.

Saarenketo, T. (2008). NDT Transportation. In H. M. Jol (Ed.), *Ground Penetrating Radar: Theory and Applications* (p. 524). Elsevier.

Scott, M., Arnold, J., & Gibson, D. (2010). *Step Frequency Ground Penetrating Radar Characterization and Federal Evaluation Tests*. Federal Highway Administration.

Statens Vegvesen. (2006). *Vann- og frostsikring i tunneler - Håndbok 163*. In Norwegian.

White, J., Wolf, J., Shokouhi, P., Hurlebaus, S., & Wimsatt, A. (2013a). Concrete tunnel lining evaluation using non-destructive techniques: A multi-method case study at Eisenhower tunnel. In *Transportation Research Board 92nd Annual Meeting*. Washington DC.

White, J., Wolf, J., Shokouhi, P., Hurlebaus, S., & Wimsatt, A. (2013b). Non-destructive evaluation of concrete linings at Hanging Lake tunnel. In *Transportation Research Board 92nd Annual Meeting*. Washington DC.

Wimsatt, A., White, J., Leung, C., Scullion, T., Hurlebaus, S., Zollinger, D., … Saarenketo, T. (2012). *Mapping Voids , Debonding , Delaminations , Moisture, and Other Defects Behind or Within Tunnel Linings* (Prepublica.). Report No. SHRP 2 R06-G. Prepublication draft.: Strategic Highway Research Program (SHRP) 2, National Research Council.

Xie, X., Liu, Y., Huang, H., Du, J., Zhang, F., & Liu, L. (2007). Evaluation of grout behind the lining of shield tunnels using ground-penetrating radar in the Shanghai Metro Line, China. *Journal of Geophysics and Engineering*, *4*(3), 253–261. doi:10.1088/1742-2132/4/3/S03

Zhang, F., Xie, X., & Huang, H. (2010). Application of ground penetrating radar in grouting evaluation for shield tunnel construction. *Tunnelling and Underground Space Technology*, *25*(2), 99–107. doi:10.1016/j.tust.2009.09.006

Appendix A

Use of Ground Penetrating Radar in quality assurance of new asphalt pavements

Anne Lalagüe, PhD student, Norwegian University of Science and Technology
Matt Lebens, Research Project Engineer, Minnesota department of Transportation
Inge Hoff, Professor, Norwegian University of Science and Technology

1. INTRODUCTION

Pavement layer thickness and density are two important factors for the quality of newly constructed asphalt pavements. They are directly related to the pavement life, and non-compliance to standards and requirements may lead to reduced quality and economic consequences.

Ground Penetrating Radar (GPR) is the most advanced technology for measuring the pavement layer thickness and air voids variations. It is a quick, reliable method, and is not-destructive. Surveys can be performed at driving speeds; they give a continuous profile of the pavement, and do not damage it.

For quality assurance projects, it is very important to achieve a high level of accuracy. As many measuring instruments, GPR needs to be calibrated. The reliability and accuracy of GPR depends greatly on how well the dielectric properties of the surveyed medium are known. The most important dielectric property is the *dielectric permittivity ε*, and is used to convert the two-way travel time of the GPR waves into depth.

Some GPR systems are able to calculate the dielectric permittivity automatically (air-coupled horn-antennas). Other systems cannot (ground-coupled and step-frequency systems): it is therefore necessary to extract one or several cores to determine the permittivity from it/them. The value of permittivity is then used for the entire section.

The GPR technology is supposedly non-destructive, core extraction is costly and time-consuming. As the same time, quality assurance requires a very high accuracy in the measurements, which can mainly be achieved by calibration on asphalt samples. Therefore there is a trade-off to be found, between high level of accuracy and cost of core extraction.

The purpose of this study, carried out in cooperation with the Department of Transportation of Minnesota, is to help understand the benefit of core samples on the overall accuracy of pavement thickness and density measurements. Calibration cores are necessary, but for economic reasons it is important to extract them as little as possible. This project attempts to quantify: "how much is enough".

2. THE GROUND PENETRATING RADAR TECHNOLOGY

2.1 Measuring principle

Ground penetrating radar (GPR) is a geophysical survey method used to remotely and non-destructively obtain a representative image of the subsurface materials. The technique is based on the propagation of electromagnetic waves in dielectric materials, as depicted in the figure below.

- Short pulses are emitted at a certain frequency by a radar transmitter in an antenna.
- Reflected waves are received by the antenna and recorded.
- The radar signal is returned differently at distinct, abrupt dielectric non-homogeneities in the surveyed materials.
- A representation of the subsurface layers is created by graphing the differing signal travel times and amplitude.

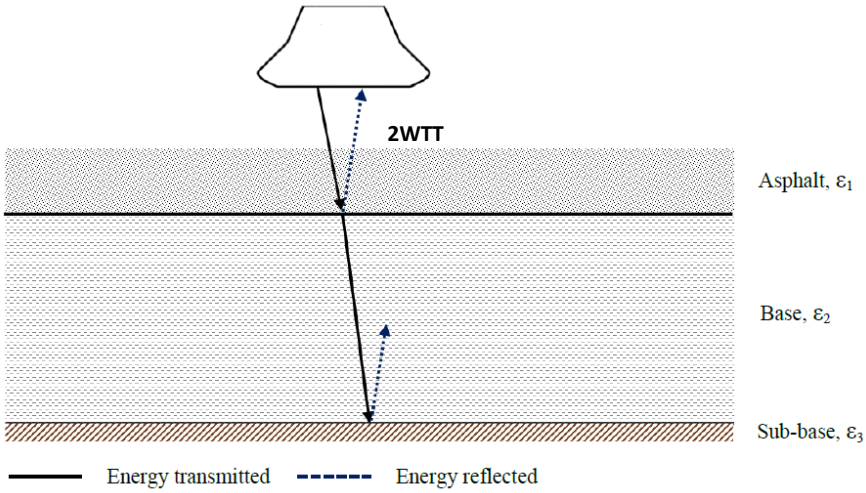

FIGURE 1 GPR PRINCIPLE

GPR is used in a variety of applications, from geological and archaeological investigations to road and structure inspections. Typical road surveys include: layer thickness assessment, utility mapping, detection of underground cavities or structures, asphalt and concrete evaluation (pavement condition, void content, rebar spacing, frost depth), groundwater profiling.

The GPR technique is rapid, accurate and non-destructive, which makes it particularly timesaving and well-suited for many subsurface investigations. However, it has some limitations inherent in the wave propagation theory. The dielectric properties of the targeted structures or layer boundaries must have sufficient contrast with the host environment in order to be detected. Poor results are generally achieved in high-conductive media, such as clay, peat and saline soils,

or in moist conditions. In addition, the selection of the operating frequency directly affects the depth of exploration. A high frequency GPR will have good resolution but a limited depth of penetration. Conversely, at low frequencies greater depths can be probed, but to the detriment of accuracy and clarity. Thus a trade-off between depth and resolution must be found during the feasibility study to achieve the best possible results.

2.2 Calculation of the pavement thickness

The calculation of the pavement thickness is based on the reflection of EM waves when a change in electrical properties occurs. The relative dielectric permittivity controls the velocity at which the EM waves travel through a material. The velocity is given by:

$$\mathrm{v\ (m/s)} = \frac{\mathrm{c}}{\sqrt{\varepsilon_r}} \quad (Eq.1)$$

Where:
v is the velocity of the propagating EM waves in the material
c is the velocity of the propagating EM waves in free space (≈ 3 x 108 m/s)
εr is the relative dielectric permittivity

The layer thickness h is calculated as the product of the two-way travel time (2WTT) Δt of reflected pulses, and the wave velocity v inside the layer:

$$\mathrm{h} = \mathrm{v} \times \frac{\Delta \mathrm{t}}{2} \quad (Eq.2)$$

$$\mathrm{h} = \frac{\mathrm{c} \times \Delta \mathrm{t}}{2\sqrt{\varepsilon_r}} \quad (Eq.3)$$

The calculation of h involves therefore the estimate of εr. The two most common ways to assess εr are:

- *The estimate guess:*

Standard values are available in the literature. They only give a rough estimate of the pavement layer thickness.

- *The reflection amplitudes method:*

When the GPR survey is carried out with a certain type of GPR and antenna (air-coupled horn antenna), one of the most accurate ways to obtain ε_r is to use the reflection amplitudes method.

The dielectric permittivity ε of the asphalt layer is calculated as:

$$\sqrt{\varepsilon} = \frac{1 + \frac{A_0}{A_m}}{1 - \frac{A_0}{A_m}} \quad (Eq. 4)$$

Where:
A_0 is the amplitude of the GPR waveform from the pavement surface
A_m is the amplitude of the GPR waveform from a metal plate (100 % of the emitted energy is reflected)

The reflection amplitudes method allows the continuous estimation of ε, which makes it a very effective and accurate method for layer thickness calculation. For better results it has to be calibrated on several cores, using Eq. 3.

2.3 Calculation of the void content

Once the dielectric permittivity ε has been calculated, the void content of asphalt can be assessed using the following regression model (Saarenketo, 2012):

$$Void\ content\ (\%) = 272.93 \times e^{-1{,}3012.k.\varepsilon} \quad (Eq. 5)$$

Where:
k is the calibration factor (obtained from cores)
ε is the dielectric permittivity

3. FIELD AND LABORATORY TESTS

Field measurements were performed at MnROAD, using a 2 GHz horn antenna GPR system (Figure below, left) and a 200 MHz – 3 GHz step-frequency antenna (right). MnROAD is a pavement test track using various research materials and pavements owned and operated by the Minnesota Department of Transportation, USA.

The tested section is 70 m long and consists of a dense-graded asphalt pavement and a crushed stone base. The positioning of the GPR data was done with metal tape markers. 14 asphalt cores were extracted and sent to the laboratory for density analysis. The GPR measurements were analyzed using the softwares Examiner, RADAN, Pavement QA/QC and Surfer.

FIGURE 2 ANTENNA ARRAY (LEFT) AND GROUND-COUPLED ANTENNA (RIGHT)

4. ANALYSIS

4.1 Asphalt thickness

No calibration core:

When no calibration core is available, a standard value of ε ("educated guess") has to be used for the calculation of the pavement layer thickness. Literature usually recommends a value between 4 and 8 (Saarenketo, 2006).

As can be seen in the figure below, assigning a value of 6 instead of 5 for ε (Δεr = 1) leads to an error of 8,7 % in the layer thickness calculation. It is therefore important to accurately assess ε. The more accurate ε is, the more reliable the calculated thicknesses will be.

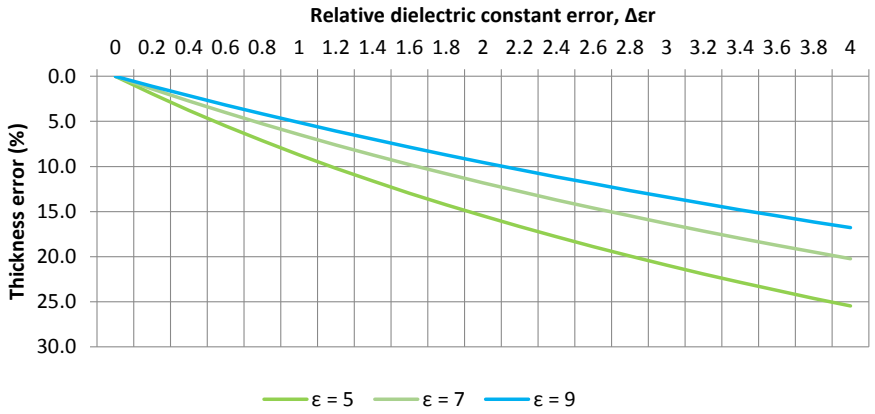

One calibration core:

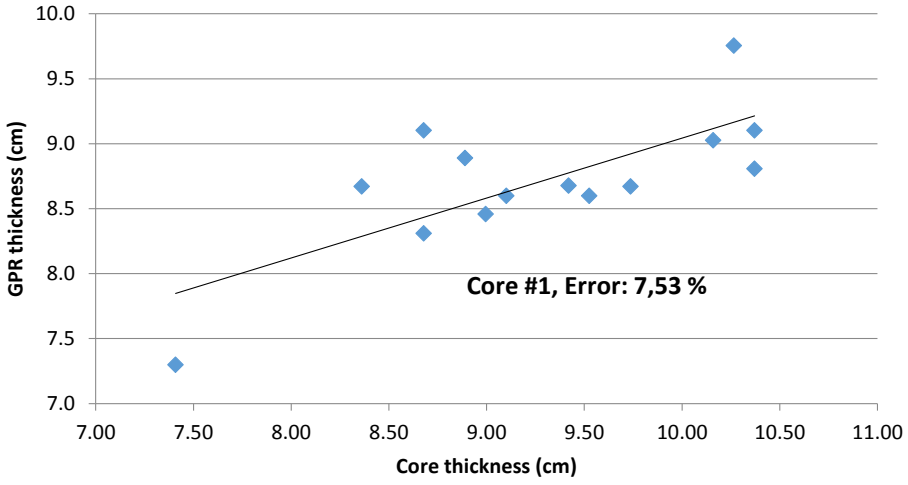

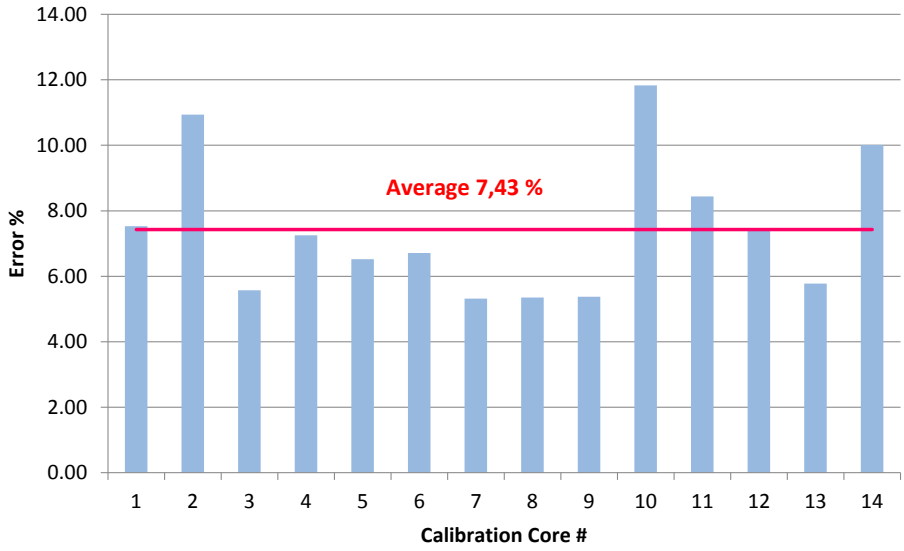

Multiple calibration cores:

It has been investigated whether using multiple cores (2 or more) would significantly increase the overall accuracy of GPR measurements. Again, since the material properties vary along a road section, all core combinations have to be taken into account (Cores 1 & 2, or 1 & 3, or 2 & 3… etc. in the case on a 2-core calibration). All possible combinations (without repetition) have been determined using the binomial coefficient:

$$\frac{n!}{p!\,(n-p)!} = \binom{n}{p}$$

Where:
n is the number of cores to choose from (14)
p is the number of selected cores (from 2 to 11)

How many calibration cores are available (n)?	14	14	14	14	14	14	14	14	14	14	14
How many calibration cores are used (p)?	1	2	3	4	5	6	7	8	9	10	11
Number of combinations	14	91	364	1001	2002	3003	3432	3003	2002	1001	364
Average Error (%)	**7,53**	**6,01**	**5,65**	**5,47**	**5,35**	**5,27**	**5,20**	**5,15**	**5,11**	**5,07**	**5,04**

The table above shows the number of combinations for each case and the calculated average error. As we can see, the accuracy of GPR measurements increases significantly when using 2 or more calibration cores. Above 3 cores, it only improves a little. The curve tends to flatten around 5 % and never goes below that level.

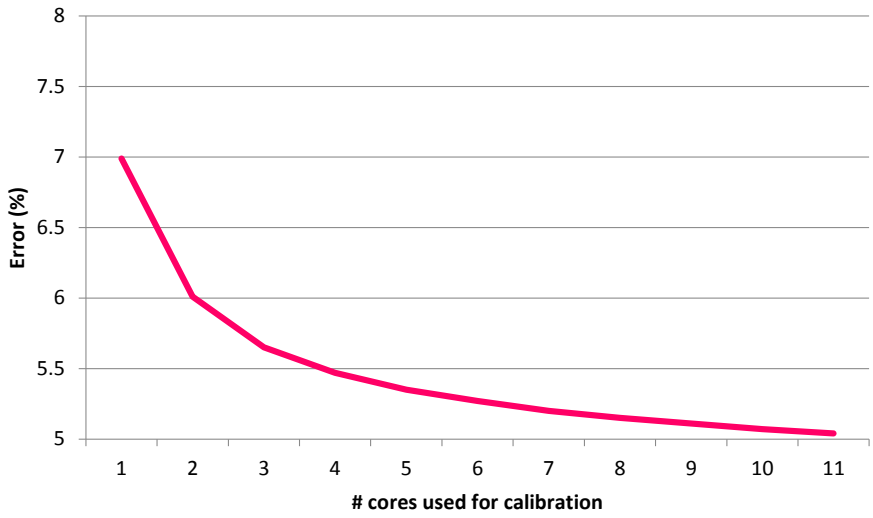

4.2 Void content

The void content of asphalt can be derived from the dielectric permittivity using Eq. 5. Since ε(air) = 1 and ε(asphalt) = 4 – 8 the greater the dielectric value, the greater the density.

The dielectric permittivity values calculated using the reflection amplitude method can be plotted in Surfer. As one can see in the figure below, they are in the range 5,5 – 6,5. They are a bit lower on the left edge, which may indicate that the asphalt material might be slightly less compacted in this area.

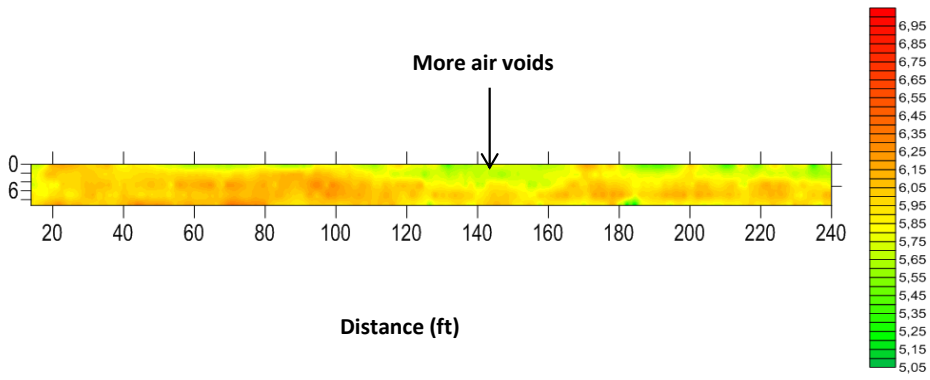

In contrast with pavement layer thicknesses that can roughly be determined with no calibration core (educated guess for ε), the calculation of air voids in asphalt requires at least one sample for the determination of *k.*

k is determined as follows:

$$Void\ content\ (\%) = 272.93 \times e^{-1{,}3012.k.\varepsilon} \qquad (Eq.\ 5)$$

$$Ln\big(Void\ content\ (\%)\big) = Ln(272.93) - 1{,}3012.k.\varepsilon$$

$$k = \frac{Ln(\frac{272.93}{Void\ content})}{1{,}3012 \times \varepsilon} \qquad (Eq.\ 6)$$

The results of the analysis show that a calibration of air voids on 1 core (core #1 or core #2 or core #3…) leads to a measurement error of **17,15 %** on average.

It is a quite high measurement error, that can probably be reduced by using multiple calibration cores instead of one. However, the method is cumbersome and a better way to increase the overall accuracy would be to ensure a better match between the core location and the GPR measurements. Since the density of the asphalt may vary significantly along a road section, an offset of 20 – 50 cm between the core location and the GPR radar pulse may lead to measurements errors.

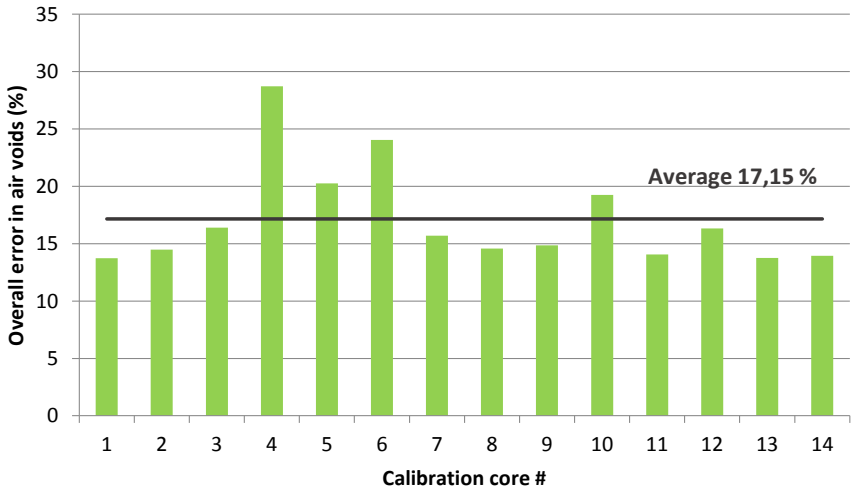

SUMMARY

An accurate measurement of the asphalt thickness and void content is essential in quality assurance of new pavements. As every instrument, GPR needs to be calibrated. The calibration for both pavement thickness determination and void content assessment are made on extracted cores.

- Pavement thickness measurements:

  - The study shows that the accuracy of pavement thickness measurement (same type of pavement all over the section) increases significantly from one core calibration.

  - It reaches an acceptable level for quality assurance purposes from 2 – 3 calibration cores.

  - Above 3 cores, the benefits of calibration are not significant.

  - The maximum achievable accuracy seems to be in this study about **95 %**.

- Void content of asphalt

  - It is possible with certain types of GPR systems to continuously calculate the dielectric permittivity of asphalt pavements.

  - Although the accurate relationship is not currently known, the void content derived directly from the permittivity. The higher the permittivity, the lower the percentage of air voids.

  - A regression model for the calculation of the % air voids from ε has been tested. It gave mixed results, with an average measurement error of 17,15 %. A possibility to increase the overall accuracy could be to calibrate the results on multiple cores.

  - Another likely source of error can be a mismatch between the core locations and, the GPR sampling. This issue can be solved by the use of a reliable and calibrated GPS.

REFERENCE

Saarenketo, T. (2006). *Electrical properties of road materials and subgrade soils and the use of Ground Penetrating Radar in traffic infrastructure surveys*. University of Oulu.

Saarenketo, T. (2012). *Recommendations for guidelines for the use of GPR in asphalt air voids content measurement*.

Appendix B

B TYPICAL VALUES OF RELATIVE PERMITTIVITY

	Experience-based, Scandinavia (Saarenketo 2006)	Measured at 100 MHz (Daniels 2004)
Air	1	1
Water (fresh)	81	81
Seawater		81
Freshwater ice	4	4
Seawater ice		4 – 8
Snow firm		6 - 12
Bedrock		
Average	5 - 7	
Granite dry		5
Granite wet		7
Limestone dry		7
Limestone wet		8
Glacial till	8 – 18	
Concrete		
Average	8 – 10	
Concrete dry		4 – 10
Concrete wet		10 – 20
Road structures (average)		
Asphalt, average	4 – 8	
Asphalt, dry		2 – 4
Asphalt, wet		6 – 12
Average, new/dry	5	
Average, normal	6	
Average, wet/old	7 – 8	
Frozen, normal	5	
Frozen, wet/old	6	
Gravel road structures in average	7 – 9	
Gravel road wearing course	12 – 14	
Crushed base	6 – 8	
Bitumen bound base	6 – 7	
Cement bound base	8 – 10	

	Experience-based, Scandinavia (Saarenketo 2006)	Measured at 100 MHz (Daniels 2004)
Soil		
Silt	16 – 30	
Silty sand	7 – 10	
Sandy, dry		4 – 10
Sandy, wet		10 – 30
Loamy, dry		4 – 10
Loamy, wet		10 – 30
Clayey, dry		4 – 10
Clayey, wet		10 – 30
Peat, natural	60	
Peat, under road	40	
Clay, average	25 - 40	
Clay, dry		2 – 6
Clay, wet		5 – 40
Sand, average	4 – 6	
Sand, dry		2 – 6
Sand, wet		10 – 30
Permafrost		4 – 8